Microvasculature in Microfluidics: matching complexity with compatibility

Duinen, V. van

Microvasculature in microfluidics

Matching complexity with compatibility

Vincent van Duinen

Cover design: Rutger van Aken | Persoonlijk Proefschrift
Thesis lay-out: Vincent van Duinen
Printing: Ridderprint | www.ridderprint.nl

ISBN: 978-94-6375-543-6

Microvasculature in microfluidics:

Matching complexity with compatibility

Proefschrift

ter verkrijging van

de graad van Doctor aan de Universiteit Leiden,

op gezag van Rector Magnificus prof.mr. C.J.J.M. Stolker,

volgens besluit van het College voor Promoties

te verdedigen op woensdag 23 oktober 2019

klokke 10.00 uur

door

Vincent van Duinen

geboren te Amsterdam

in 1988

Promotor:	Prof. Dr. Thomas Hankemeier
Copromotor:	Dr. Ir. P. Vulto
Promotiecommissie:	Prof. Dr. H. Irth (Voorzitter)
	Prof. Dr. J.A. Bouwstra (secretaris)
	Prof. Dr. A.J. van Zonneveld
	Prof. Dr. C.L. Mummery
	Prof. Dr. David J. Beebe
	Prof. Dr. B van de Water

The research described in this thesis was performed at the division Systems Biomedicine and Pharmacology of the Leiden Academic Centre for Drug Research (LACDR), Leiden University (Leiden, The Netherlands).

Table of contents

CHAPTER 1

General introduction and scope

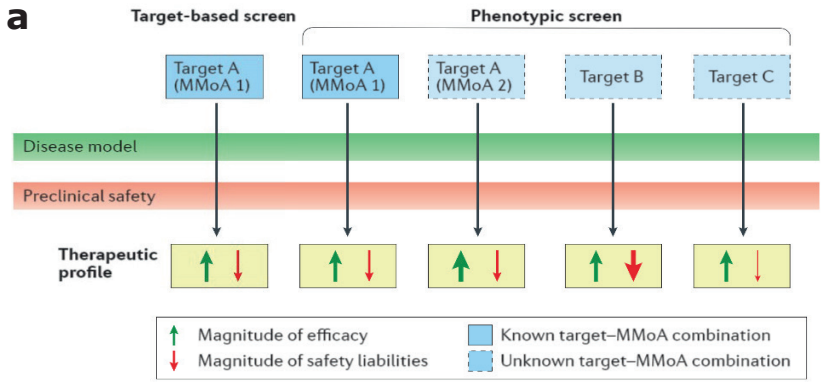
a
Target-based screen
Phenotypic screen
Target A (MMoA 1)
Target A (MMoA 1)
Target A (MMoA 2)
Target B
Target C
Disease model
Preclinical safety
Therapeutic profile
Magnitude of efficacy
Magnitude of safety liabilities
Known target–MMoA combination
Unknown target–MMoA combination

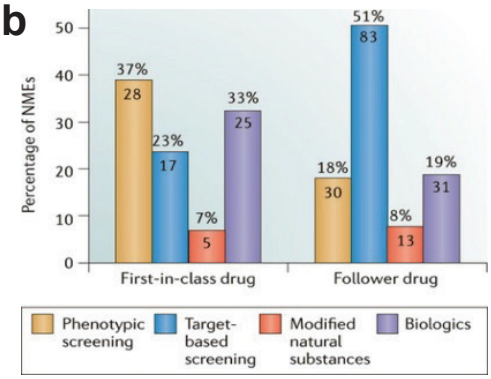
b
Percentage of NMEs
50
40
30
20
10
0
37%
28
23%
17
7%
5
33%
25
18%
30
51%
83
8%
13
19%
31
First-in-class drug
Follower drug
Phenotypic screening
Target-based screening
Modified natural substances
Biologics

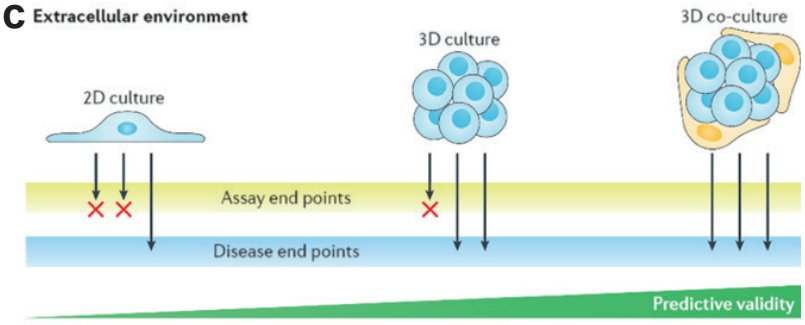
c
Extracellular environment
2D culture
3D culture
3D co-culture
Assay end points
Disease end points
Predictive validity

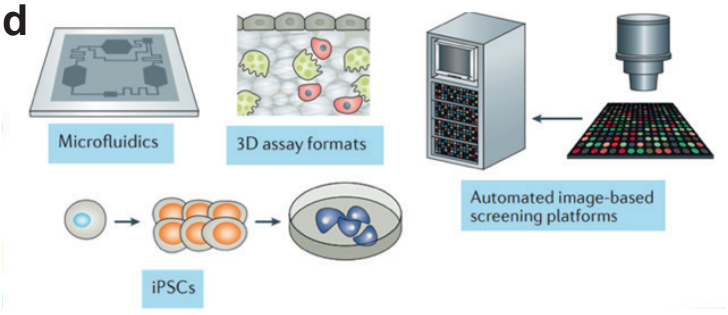
d
Microfluidics
3D assay formats
Automated image-based screening platforms
iPSCs

Drug discovery today

In vitro disease models play a fundamental role in drug research. They enable the systemic identification and validation of disease mechanisms and the discovery of possible drug targets. However, more than often, drug candidates that are identified *in vitro* fail in the later clinical stages of drug development, either due to a lack of efficacy or unforeseen off-target effects[1-3].

In part, this can be contributed to a failure to translate findings from *in vitro* experiments to the more complex *in vivo* environment in humans, and vice versa. For example, in an oversimplified *in vitro* system targets that are present *in vivo* are missing *in vitro*, or off-target effects are not present, leading to a wrong estimation of the therapeutic effect.

Over the last decades, the predominant strategy for the identification of new drug candidates is by high-throughput screening of compounds that modulate a pre-nominated target or pathway that is associated with a disease[4,5]. Initial hits are often generated by targeted screening of a known protein or pathway, using biological or biochemical assays with a specific readout on this effect. Often two dimensional,

◄Figure 1 | Phenotypic versus target-based screening

(a) *Targeted screening focuses on a single molecular mechanisms of action (MMoA) with generally efficacy as outcome. In contrast, a phenotypic screening can involve multiple MMoA's. The therapeutic profile is determined by sum of the efficacy/safety profile for every target.* **(b)** *FDA-approved drugs between 1999 and 2008. The more holistic approach of phenotypic screening has translated into more new molecular entities (NMEs) compared to targeted based screening.* **(c)** *2D cell cultures that lack an extracellular microenvironment have assay end-points that fail to translate into a disease end-point. The more complex the in vitro method is, resulting in a better recapitulation of the complexity of a disease.* **(d)** *By integration of recent advances in cell culture depicted here, the predictive validity can be further increased. Microfluidics enables the development of novel 3D assay formats which better reflect the spatial architecture of tissues, while iPSCs allow standardization and personalization of the cells used in vitro. Images based screening platforms combine high-throughput screening with high-content imaging. Adapted from [4-6].*

high-throughput cellular models are used, based on immortalized cells grown on flat, artificial substrates. Although these methods have contributed to the discovery of many biological insights and pre-selection of compounds, such cellular models often fail to provide a satisfactory representation of a disease. Often diseases affect multiple pathways and targets, which are not replicated in these simplified *in vitro* models. This highlights the importance of *in vitro* models that consider the multifactorial complexity of diseases that is found *in vivo*.

An alternative strategy to discover novel drug candidates *in vitro* is by the use of phenotypic screening. This relies on a switch in phenotype from a diseased state to a healthy state, either in cells, tissues or even whole organs. As the change of phenotype is used to identify biologically active compounds, it relies less on the knowledge of the (often multiple) underlying molecular mechanisms of actions (Fig. 1a). Thus, there is less bias for specific pathways or mechanisms, which yields a higher success rate in the discovery of new, 'first-in-class' drugs[5] (Fig. 1b).

The predictive validity of *in vitro* models relies on the usage of physiologically and clinically relevant disease models that faithfully recapitulate the disease of interest, including as many disease-relevant targets and processes as possible, in order to give a realistic representation of the therapeutic profile. The end-point in assays that use 2D cell culture can often not be translated into disease end-points, as the important cues from the cellular microenvironment are lacking. Increasing the assays complexity by using 3D co-cultures results in a better resemblance of the cellular micro-environment *in vivo*, and it is more likely that the end-point reflects true disease end-points (Fig 1c). It should be mentioned that a good understanding of human diseases processes is considered critical when developing human in-vitro disease models.

Recent advances in cell culture models can be incorporated to further increase the predictive validity (Fig 1d). Using microfluidics, novel 3D assay formats can be designed which better reflect the spatial architecture of tissues. Imaging based screening platforms combine high-throughput screening with high-content imaging, which

enables the automated extraction of large datasets with feature-rich morphological profiles from complex 3D cell culture assays. Finally, with the discovery of induced pluripotent stem cells, it is possible to generate homogenous and nearly unlimited quantities of many different cell types. Also, as iPSCs are amenable to genome-editing and can be patient derived, iPSCs open up unique possibilities in disease modelling.

A current bottleneck is that within *in vitro* modelling, usually an increased complexity results in a decreased throughput. Thus, a balance between throughput and relevance is needed: current efforts should yield cell culture assays that have sufficient throughput for screening purposes, but with enough complexity to capture as many important disease end-points as possible[6]. What are the requirements and trade-offs that need to be considered in order to develop the next generation of cell culture assays for phenotypic drug discovery?

Increasing the physiological relevancy *in vitro*

One of the most critical parameters in increasing the physiological relevancy of cell culture assays is by providing cells a three-dimensional scaffold that mimics the extracellular matrix (ECM) found *in vivo*. Biologically derived hydrogels (e.g. collagen type 1, fibrin) provide cells the necessary cues that are important in cell–cell and cell–ECM interactions[7]. Cells adhere to their ECM using protein complexes called integrins. Adherence to their ECM enable cells to sense the stiffness of their surrounding matrix and change their behavior according to the physical properties of ECMs, such as fiber density or tensile strength. The type of integrins that get activated by binding to the ECM dictates numerous changes in the cellular phenotype[8-11]. For example, if the right ECM is provided, cells are able to polarize into an apical and basal side.

Not only basic cellular functions are regulated by the ECM, such as the proliferation, polarization and differentiation of cells, the interactions with an extracellular matrix also determine more subtle phenotypes of a cell, such as the permeability of cellular monolayers or the collective migration of cells that occurs during embryonic devel-

opment.

Within a 3D extracellular matrix, cells are exposed to short range gradients, as the diffusion of oxygen and nutrients is limited. Also, growth factors that are produced and consumed by cells can bind and interact with the extracellular matrix, which leads to biomolecular gradients that are important in paracrine, juxtracrine and autocrine signaling. Thus, the mechanical and chemical cues presented by the extracellular matrix are crucial for cellular function and behavior.

Cellular microenvironments, however, are more complex than just cells in a 3D scaffold. *In vivo*, organs consist of multiple cell types that are spatially arranged according to a certain architecture. Furthermore, the circulatory system continuously provides cells and tissue with oxygen, nutrients and removal of waste metabolites. 3D culture assays that consist of merely mixing cells and extracellular matrices together typically do not yet capture this tissue complexity that is found in tissues. Furthermore, such 3D culture assays cannot be perfused, and thus important cues are missing. Thus, the physiological relevance of 3D cell culture assays can be improved by engineering and controlling the cellular microenvironment in novel 3D assay formats.

Mimicking cellular microenvironment using microfluidics

Microfluidics is the principle of handling fluids in micrometer-sized channels. Within such small channels, fluids have different physical properties. For example, surface tension becomes a significant force, which can be exploited to spatially define and control fluids[12]. Also, the flow profile in microfluidic channels is laminar: two fluids can flow side-by-side, and the mixing is predominantly molecular diffusion. In contrast, on a larger scale the flow would be turbulent which results in much more rapid mixing due to turbulent diffusion.

The spatial-temporal control over fluids within microfluidic channels enables patterning of cells and scaffolds. Patterning can be achieved by for example geometrical guiding structures such as pillars[13,14] or ridges[15,16], using surface modification[17], molding[18] or 3D printing[19]. By populating these scaffolds with cells, either pre- or

post-patterning, compartmentalized cell culture systems can be created. This enables signaling between cells, either by direct contact or by short-range signaling, and better mimics the spatial organization that is found in tissues *in vivo*.

As the surface area to volume ratio changes dramatically in microfluidic channels, diffusion is a more dominant factor compared to larger channels. These phenomena can be exploited to develop unique cell culture platforms, as this results in more efficient diffusion between the scaffold and cell culture media compared to 2D and large scale 3D cell culture systems. This can increased cell viability and a more efficient removal of waste metabolites.

In a 2 mm layer of stagnant cell culture medium within a e.g. a cell culture flask or well of a titerplate already has significantly different concentrations in oxygen, nutrients an metabolites between the liquid-air surface and at the cell layer[7]. The submillimeter dimensions of cell culture in microfluidics enable quick equilibration between the cell culture media and the cells. The possibility to continuously perfuse a microfluidic cell culture system with culture media allows the continuous supply of nutrients and the removal of waste metabolites, mimicking the functionality of the *in vivo* circulation. Furthermore, flow exerts biomechanical forces by inducing shear stress on the cellular membrane, which activates important signaling pathways within cells.

Within tissues, concentration gradients probably exist for any soluble molecule that is consumed or produced by cells[7]. Cells sense these gradients and respond by for example migrating or invasion in the direction of the source of a signaling molecule. Within microfluidic cell culture systems, the compartmentalization enables gradients to be formed by spatially defining different concentrations of for example growth factors. Furthermore, in combination with continuous perfusion in these microfluidic cell culture systems, these biomolecular gradients are well-defined and stable for multiple hours or days[20].

In conclusion, microfluidic systems enables the control over biological cues that can be used to improve the physiological relevancy[7,21] and allows the development of 3D

cell culture assays that better mimic the cellular microenvironment found in tissues.

Microfluidic models of vascular systems

It is now recognized that microvasculature plays a fundamental role in the onset and progression of the pathophysiology of many diseases[22-26]. Current therapies are mainly focused on restoring the function of the macrovasculature, while for patients with diseases that are associated with microvascular dysfunction, the therapeutic options are severely limited. For example, while it is known that diabetes and hypertension exposes the microvasculature to adverse metabolic and hemodynamic (cardio) vascular risk factors[25], the exact mechanisms and pathways that are involved remain to be elucidated. Thus, an increased understanding of the mechanisms and risk factors that affect the microvasculature is likely to make a significant contribution in the understanding of disease mechanisms and the generation of novel drug targets.

The aforementioned advantages of microfluidic cell culture techniques uniquely match the requirements in vascular biology. Not only are the dimensions of microfluidic channels close to the diameter of that of the microvasculature, the possibility to pattern cells and ECMs brings all sorts of advantages that can be utilized to improve vascular models *in vitro* (as summarized in Fig. 2)

In vivo, microvasculature is surrounded by a soft ECM. This can be mimicked by culturing cells against or within a patterned hydrogel that has similar mechanical and biochemical properties. The mechanical properties of the hydrogels are important in the mechano-transduction between cells and their ECM, as the mechanical cues directly regulate the activity of YAP (Yes-associated protein) and TAZ (transcriptional coactivator with PDZ-binding motif[27]: two transcription factors that play a pivotal role in the VEGF signaling during angiogenesis and the subsequent maturation of angiogenic sprouts *in vivo*[28]. Also, the expression of the family of RNA-binding protein Quaking (QKI) is directly regulated by substrate stiffness in vascular smooth muscle cells[29]. Inhibition of QKI reduces endothelial migration and sprout formation[30].

The biochemical properties, such as the presence of various binding domains that

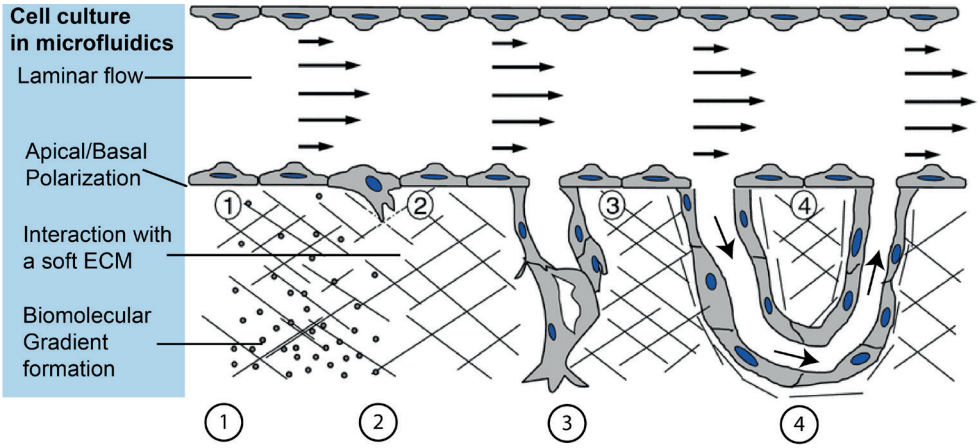

	1	2	3	4
Features of angiogenesis	Single monolayer	Tip cell formation Supression of neighouring cells Junction remodelling	Matrix degradation Directional migration Lumen formation	Anastomosis Flow restoration Junction stabilization Basement membrane
Endothelial phenotype	Quiescent	Pro-angiogenic	Pro-angiogenic	Quiescent

Figure 2 | Endothelial cell culture in microfluidics

Unique features of microfluidic cell culture enables the culture of endothelial cells in a more physiological relevant cellular microenvironment that includes for example laminar flow, gradients and a soft ECM. This allows the study of various endothelial phenotypes that occur during differnet phases of angiogenic sprouting (1-4).

are present in the ECM, regulate the response of endothelial cells through integrins. Some components of the ECM can be either pro-angiogenic or antiangiogenic[31]. For example, fibrin and collagens are present in the provisional matrix during wound healing and promote angiogenesis, while quiescent ECs are surrounded by a basement membrane of laminins that suppress angiogenesis[32].

The compartmentalized nature of microfluidic cell culture enables the formation of accessible and perfusable lumen, thus allows continuous laminar perfusion. Flow exerts shear stress on the cell surface, which is an important biomechanical cue that is involved in many endothelial-specific responses[33]. For example, exposure to laminar shear stress activates the MEK5/ERK5 pathway, leading to the nuclear translocation of KLF-2 and -4. These KLFs trigger cytoskeletal remodeling and play a central role

in the vaso-protective endothelial phenotype: quiescent endothelial cells with an increased junction stability.

Gradients play a crucial role during correct development and patterning during sprouting angiogenesis. *In vivo*, low oxygen levels in tissues trigger the secretion of pro-angiogenic factors such as vascular endothelial growth factors (VEGFs) and fibroblast growth factors (FGFs) into the ECM. Neighboring endothelial cells respond to this by differentiation into more specialized tip- and stalk cells, which invade the oxygen-deprived tissue.

Importantly, the survival of these tip- and stalk cells are dependent on the presence of these pro-angiogenic growth factors. Upon anastomosis with other existing blood vessels, the blood flow is restored and the low oxygen tension is resolved. This stops the production and secretion of growth factors, and the remaining vascular network is allowed to mature by switching from a growth factor dependent state to a quiescent phenotype. This quiescent state is maintained by wall shear stress, which takes over the role of pro-angiogenic growth factors for cell survival. The possibility to apply perfusion in microfluidic cell culture systems enables the study of these phenomena.

Compatible microfluidic systems for phenotypic drug discovery

The demand for increased physiological relevant *in vitro* models of vasculature has resulted in the development of numerous cell culture platforms, as summerized in Fig. 3. Technically, there is sufficient knowledge of how microfluidic techniques can be used to improve 3D cell culture assays. However, within drug discovery, such microfluidic models are still rarely used. Why is this adoption so limited? And what optimizations are required before microfluidic cell culture assays become common practice in drug discovery?

One issue is the availability of microfluidic cell culture platforms. Although there are many available protocols of various microfluidic cell culture devices, many of these microfluidic devices are designed from an engineering perspective[34]. The design

and material choices are made to facilitate the manufacturing, while these materials are not always the most optimal choice for biological compatibility. Furthermore, as many devices need to be microfabricated by the end-user, manufacturing apparatus and technical knowledge is required. Finally, there is usually limited quality control of the final end-product when produced in an academic setting, which introduces variation and negatively affects the reproducibility[35].

Another issue is the limited consensus in the optimal design of microfluidic cell culture platforms and there is a focus on low-throughput, highly specialized applications. For example, to compartmentalize cells and hydrogels, some devices use artificial membranes[9,36,37], while others use casting[38] or direct patterning[39]. Also, some devices use static culture media, while other platforms rely on passive, gravity-driven flow or continuous perfusion using pump setups. Such fundamental differences in culture conditions will arguably influence the representation of a disease. The questions remains in what the crucial parameters are in the translation between *in vivo* and *in vitro*? Answering this fundamental question requires systemic validation of added physiological relevance that is promised by microfluidics.

Finally, to be applicable for pre-clinical drug discovery, microfluidic platforms need to be robust and scalable and easy to implement within the current screening infrastructure. Only then widespread adoption in the phenotypic drug screening pipeline can take place.

2D assays
+ Compatible with high-throughput screening (96- and 384-well plates)
+ Commercially available platforms and consumables
+ Established protocols widely published and validated
- Lacks physiological relevance

3D extracellular matrix-based assays (e.g. Collagen, Matrigel)
+ Mimics native structure of the extracellular matrices
+ 96- and 384-well assay formats available
- Difficult to integrate in an automated screening infrastructure
- High usage and cost of reagents
- High variation (experimental and batch-to-batch)

Organ-on-a-Chip and microfluidic assay systems
+ High physiological relevance when appropriate ECM and cell types are used
+ Integration of physiological relevant cues (perfusion, gradients, contraction)
- Restricted to low-throughput
- Not compatible with standard automation and screening platforms
- Platforms are not commercially available and need to be manufactured by the end users, limiting the adoption across laboratories

Ex-vivo tissue culture assays
+ Intact human tissue with highest physiological relevance
+ Multiple cell types within their native cellular microenvironment
- Low throughput and limited scalability
- Limited supplies of human tissue
- Short lifespan

Figure 3 | Overview of current 2D and 3D in vitro models of vasculature

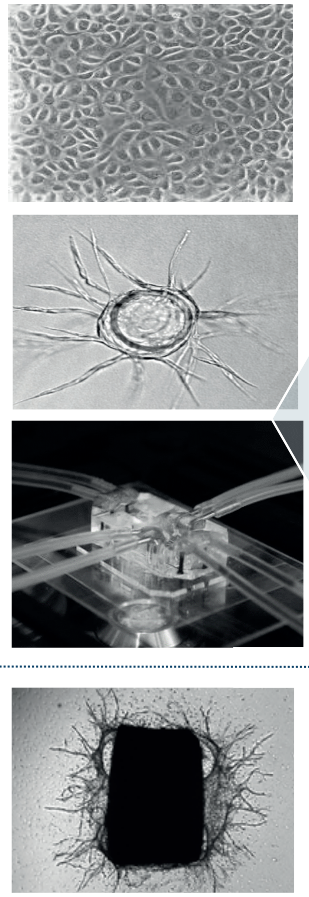

Standardized microfluidic assays

+ Commercially available platforms allow widespread adoption across laboratories
+ Well plate formats for throughput, scalability and compatibility with standard imaging equipment
+ Limited reagent use increases efficiency and reproducibility and reduces influence of batch-to-batch variations
+ Focus on balance between relevance and throughput

Scope of this thesis

The aim of this thesis is to develop microfluidic 3D cell culture assays that balance physiological complexity with compatibility with the high-throughput drug discovery pipeline. As *in vitro* vasculature models benefit most from the added physiological relevance that is provided by microfluidics, this thesis is focused on increasing the physiological relevancy of vasculature models in order to maximize their impact on drug research.

In **chapter 2**, we review the recent advances in the field of microfluidic 3D cell culture. We observed that there is limited innovation in the technical aspects of microfluidic cell culture, as the microfluidic toolset is currently sufficient to increase the physiological relevancy of (3D) cell culture. However, there is still optimization required in terms of biocompatibility and usability. Between 2012 and 2015, most microfluidic 3D cell culture efforts are done in the field of vasculature. We have identified three major advantage to use microfluidics over traditional 3D cell culture, and put the combination of microfluidic and vasculature in perspective. Finally, we concluded that the advantages of microfluidic 3D cell culture are becoming increasingly clear. The main focus should be on the validation of these increased complex culture methods and compare this to existing 3D cell culture assays.

In **chapter 3**, we report a robust, high-throughput method to culture endothelial cells as 96 three-dimensional and perfusable microvessels with *in vivo* relevant permeability. The microvessels are cultured against a patterned collagen-I scaffold. Since selective permeability is one of the hallmarks of healthy vasculature, the aim was to develop microvasculature that is impermeable to high molecular weight compounds (>70 kDa), while being permeable for low molecular weight compounds (<70 kDa). We show a robust, high-throughput screening method to quantify the permeability by using two macromolecular tracers: 20 kDa FITC-Dextran and a 150 kDa TRITC-Dextran. Upon stimulation with various inflammatory stimuli, we observed an increased permeability, which corresponds to a physiological relevant response.

Starting with the microvessels that were developed in chapter 3, we explored in

chapter 4 how these vessels can be induced to form angiogenic sprouts within a patterned collagen-I gel. As gradients play a fundamental role in the onset of angiogenesis, we developed a platform to generate stable biomolecular gradients within the collagen-1 scaffold. We redesigned the microfluidic channel layout so gradients can be formed without the requirement of pumps. Importantly, as the wells act as reservoirs, gradients were stable for multiple days without replenishment. This ensures reproducibility, scalability and ease-of use of the platform.

We optimized the cocktail of angiogenic factors for the formation of perfusable microvascular networks with an evenly distributed network of capillaries with relevant diameters. Depending on the gradient of angiogenic factors, we observe the differentiation of ECs into more specialized subtypes: tip cells that degraded the patterned collagen-1 scaffold, and migrated towards the gradient, and stalk cells that formed a perfusable lumen. This platform was uniquely suited to study the permeability of angiogenic sprouts during and after the formation of a microvascular network, and we showed that anastomosis results in a decrease in permeability, which suggested that in this model, stabilization occurred after anastomosis.

In **chapter 5**, we adapted the method to develop a more standardized angiogenesis assay by using endothelial cells derived from human induced pluripotent stem cells (iPSC). Upon stimulation with an optimized angiogenic cocktail, we observed similar angiogenic sprouting with iPSC-EC compared to primary endothelial cells (HUVEC), including the formation of tip-, stalk cells and phalanx cells. As the iPSC-ECs require fibronectin coating to adhere, the seeding method was optimized to reproducibly seed the cells in a pre-filled microfluidic channel. Finally, we also observed similar decrease in vessels density and permeability after anastomosis.

In **chapter 6**, we validated the angiogenic response of iPSC-ECs using two inhibitors: the clinically available Sunitinib, an angiogenic VEGFR2-inhibitor, 3PO, a PFKB3-inhibitor that targets the glucose metabolism present in tip cells. These results show that, similar to primary cells, the formation of angiogenic sprouts is inhibited and validates the use of iPSC-derived ECs in this angiogenesis model.

Finally, in **chapter 7,** a general conclusion is presented and an outlook is given on how microfluidic assays of microvasculature will develop in the future and what issues still needs to be addressed for its successful integration into drug research.

References

1 Mehta, D., Jackson, R., Paul, G., Shi, J. & Sabbagh, M. Why do trials for Alzheimer's disease drugs keep failing? A discontinued drug perspective for 2010-2015. *Expert Opin Investig Drugs.* **26** (6), 735-739, (2017).

2 Giannuzzi, V. *et al.* Failures to further developing orphan medicinal products after designation granted in Europe: an analysis of marketing authorisation failures and abandoned drugs. *BMJ Open.* **7** (9), e017358, (2017).

3 Petrov, D., Mansfield, C., Moussy, A. & Hermine, O. ALS Clinical Trials Review: 20 Years of Failure. Are We Any Closer to Registering a New Treatment? *Front Aging Neurosci.* **9** 68, (2017).

4 Moffat, J. G., Vincent, F., Lee, J. A., Eder, J. & Prunotto, M. Opportunities and challenges in phenotypic drug discovery: an industry perspective. *Nat Rev Drug Discov.* **16** (8), 531-543, (2017).

5 Swinney, D. C. Phenotypic vs. target-based drug discovery for first-in-class medicines. *Clin Pharmacol Ther.* **93** (4), 299-301, (2013).

6 Horvath, P. *et al.* Screening out irrelevant cell-based models of disease. *Nat Rev Drug Discov.* **15** (11), 751-769, (2016).

7 Griffith, L. G. & Swartz, M. A. Capturing complex 3D tissue physiology *in vitro*. *Nature Reviews Molecular Cell Biology.* **7** (3), 211-224, (2006).

8 McCurley, A. *et al.* Inhibition of alphavbeta5 Integrin Attenuates Vascular Permeability and Protects against Renal Ischemia-Reperfusion Injury. *J Am Soc Nephrol.* **28** (6), 1741-1752, (2017).

9 Polacheck, W. J., German, A. E., Mammoto, A., Ingber, D. E. & Kamm, R. D. Mechanotransduction of fluid stresses governs 3D cell migration. *Proc Natl Acad Sci U S A.* **111** (7), 2447-2452, (2014).

10 Howe, G. A. & Addison, C. L. β1 integrin: An emerging player in the modulation of tumorigenesis and response to therapy. *Cell Adhesion & Migration.* **6** (2), 71-77, (2012).

11 Desgrosellier, J. S. & Cheresh, D. A. Integrins in cancer: biological implications and therapeutic opportunities. *Nature Reviews Cancer.* **10** (1), 9-22, (2010).

12 Beebe, D. J., Mensing, G. A. & Walker, G. M. Physics and applications of microfluidics in biology. *Annu Rev Biomed Eng.* **4** 261-286, (2002).

13 Kim, C., Kasuya, J., Jeon, J., Chung, S. & Kamm, R. D. A quantitative microfluidic angiogenesis screen for studying anti-angiogenic therapeutic drugs. *Lab Chip.* **15** (1), 301-310, (2015).

14 Park, Y. K. *et al. In vitro* Microvessel Growth and Remodeling within a Three-dimensional Microfluidic Environment. *Cell Mol Bioeng.* **7** (1), 15-25, (2014).

15 Trietsch, S. J., Israels, G. D., Joore, J., Hankemeier, T. & Vulto, P. Microfluidic titer plate for stratified 3D cell culture. *Lab Chip.* **13** (18), 3548-3554, (2013).

16 Vulto, P. *et al.* Phaseguides: a paradigm shift in microfluidic priming and emptying. *Lab Chip.* **11** (9), 1596-1602, (2011).

17 Han, S. *et al.* Hydrophobic Patterning-Based 3D Microfluidic Cell Culture As-

say. *Adv Healthc Mater.* **7** (12), e1800122, (2018).

18 Tourovskaia, A., Fauver, M., Kramer, G., Simonson, S. & Neumann, T. Tissue-engineered microenvironment systems for modeling human vasculature. *Exp Biol Med (Maywood).* **239** (9), 1264-1271, (2014).

19 Song, K. H., Highley, C. B., Rouff, A. & Burdick, J. A. Complex 3D-Printed Microchannels within Cell-Degradable Hydrogels. *Advanced Functional Materials.* **28** (31), (2018).

20 Berthier, E. & Beebe, D. J. Gradient generation platforms: new directions for an established microfluidic technology. *Lab Chip.* **14** (17), 3241-3247, (2014).

21 Sackmann, E. K., Fulton, A. L. & Beebe, D. J. The present and future role of microfluidics in biomedical research. *Nature.* **507** (7491), 181-189, (2014).

22 Carmeliet, P. Angiogenesis in life, disease and medicine. *Nature.* **438** (7070), 932-936, (2005).

23 Potente, M., Gerhardt, H. & Carmeliet, P. Basic and therapeutic aspects of angiogenesis. *Cell.* **146** (6), 873-887, (2011).

24 Carmeliet, P. & Jain, R. K. Principles and mechanisms of vessel normalization for cancer and other angiogenic diseases. *Nat Rev Drug Discov.* **10** (6), 417-427, (2011).

25 Goveia, J., Stapor, P. & Carmeliet, P. Principles of targeting endothelial cell metabolism to treat angiogenesis and endothelial cell dysfunction in disease. *EMBO Mol Med.* **6** (9), 1105-1120, (2014).

26 Wong, B. W., Marsch, E., Treps, L., Baes, M. & Carmeliet, P. Endothelial cell metabolism in health and disease: impact of hypoxia. *EMBO J.* **36** (15), 2187-2203, (2017).

27 Dupont, S. *et al.* Role of YAP/TAZ in mechanotransduction. *Nature.* **474** (7350), 179-183, (2011).

28 Kim, J. *et al.* YAP/TAZ regulates sprouting angiogenesis and vascular barrier maturation. *J Clin Invest.* **127** (9), 3441-3461, (2017).

29 van der Veer, E. P. *et al.* Quaking, an RNA-binding protein, is a critical regulator of vascular smooth muscle cell phenotype. *Circ Res.* **113** (9), 1065-1075, (2013).

30 Cochrane, A. *et al.* Quaking Is a Key Regulator of Endothelial Cell Differentiation, Neovascularization, and Angiogenesis. *Stem Cells.* **35** (4), 952-966, (2017).

31 Davis, G. E. & Senger, D. R. Endothelial extracellular matrix: biosynthesis, remodeling, and functions during vascular morphogenesis and neovessel stabilization. *Circ Res.* **97** (11), 1093-1107, (2005).

32 Stratman, A. N., Malotte, K. M., Mahan, R. D., Davis, M. J. & Davis, G. E. Pericyte recruitment during vasculogenic tube assembly stimulates endothelial basement membrane matrix formation. *Blood.* **114** (24), 5091-5101, (2009).

33 Krenning, G., Barauna, V. G., Krieger, J. E., Harmsen, M. C. & Moonen, J. R. Endothelial Plasticity: Shifting Phenotypes through Force Feedback. *Stem Cells Int.* **2016** 9762959, (2016).

34 Junaid, A., Mashaghi, A., Hankemeier, T. & Vulto, P. An end-user perspective

on Organ-on-a-Chip: Assays and usability aspects. *Current Opinion in Biomedical Engineering*. **1** 15-22, (2017).

35 Berthier, E., Young, E. W. & Beebe, D. Engineers are from PDMS-land, Biologists are from Polystyrenia. *Lab Chip*. **12** (7), 1224-1237, (2012).

36 Sip, C. G., Bhattacharjee, N. & Folch, A. Microfluidic transwell inserts for generation of tissue culture-friendly gradients in well plates. *Lab Chip*. **14** (2), 302-314, (2014).

37 Kim, H. J., Huh, D., Hamilton, G. & Ingber, D. E. Human gut-on-a-chip inhabited by microbial flora that experiences intestinal peristalsis-like motions and flow. *Lab Chip*. **12** (12), 2165-2174, (2012).

38 Zheng, Y. *et al. In vitro* microvessels for the study of angiogenesis and thrombosis. *Proc Natl Acad Sci U S A*. **109** (24), 9342-9347, (2012).

39 Erdman, N. *et al.* Microfluidics-based laser cell-micropatterning system. *Biofabrication*. **6** (3), 035025, (2014).

CHAPTER

2

Microfluidic 3D cell culture: from tools to tissue models

V van Duinen, S.J. Trietsch, J. Joore, P. Vulto, T. Hankemeier

Current opinion in biotechnology 35;118-126 (2015)

Abstract

The transition from 2D to 3D culture techniques is an important step in a trend towards more biomimetic tissue models. Microfluidics allows spatial control over fluids in micrometer-sized channels. It is a valuable tool the further increase the physiological relevancy of 3D cell culture by enabling spatially controlled co-cultures, perfusion flow and spatial control over of signaling gradients. This paper reviews most important developments in microfluidic 3D culture progress since 2012. Most efforts were exerted in the field of vasculature, both as a tissue on its own and as part of cancer models. We observe that the focus is shifting from tool building to implementation of specific tissue models. The next big challenge for the field is the full validation of these models and ultimately to become implemented in the drug development pipelines of the pharmaceutical industry.

Introduction

Two-dimensional cell culture techniques, in which cells are grown on a flat substrate such as petri-dishes or microtiter plate wells, are still common laboratory practice. However, over the last two decades, awareness of the relevance of the cellular micro-environment (e.g. the extracellular matrix and interstitial fluids) increased. This new cell culture paradigm, referred to as 3D cell culture, is rapidly gaining popularity. For example, embedment of cells in an extracellular matrix is associated with more relevant physiological behavior, such as witnessed by apical-basal polarization[1], lumen formation[2], reduced proliferation and increased differentiation[3] and numerous changes in RNA and protein expression[4]. Furthermore, cells cultured in 3D show important hallmarks of tissues in vivo, such as for example bile duct formation in liver spheroids[5] and milk protein secretion by mammary epithelial cells[4].

The transition from 2D to 3D culture techniques is an important step in a trend towards ever more physiologically relevant tissue models. 3D culture techniques typically do not yet capture the multicellular complexity of tissues, lack vasculature, do not offer precise control over gradients and undergo medium exchange at discrete time points instead of in a continuous manner.

Microfluidic techniques allow spatial control over fluids in micrometer-sized channels that can be explored to extend the physiological relevance of 3D culture models. Early examples demonstrate spatial patterning of adhesion molecules[6] and hydrogels[7,8]. We identify three important drivers for the use of microfluidic techniques in 3D cell culture:

1. The integration of perfusion flow.
2. The ability of co-culturing cells in a spatially controlled manner
3. Generation of and control over signaling gradients.

Mechanobiological aspects, such as active stretch and tension, is another functional aspect that can be added using microfluidics. Although interesting, it has received minor attention in combination with 3D cell culture, and will therefore not be dis-

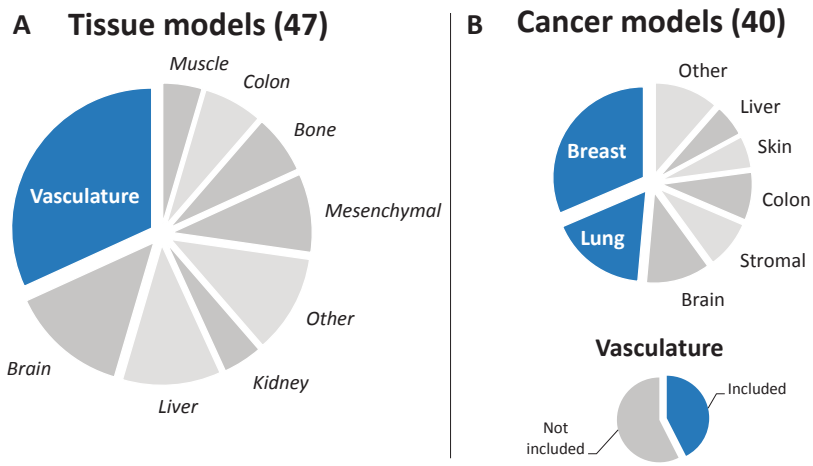

Figure 1 | Overview of the modelled organs of 87 articles which combine 3D cell culture with microfluidics since 2012

(a) *The distribution of different organ and tissue models addressed by microfluidic 3D cell culture. Vasculature was the most modelled tissue, followed by brain and liver.* **(b)** *The distribution of the recently developed cancer models. Breast and lung tumour models compromise half of the developed models. Almost half of the cancer models include vasculature.*

cussed in detail. The interested reader is referred to a recent review by Polacheck et al[9].

In this review, we discuss the most dominant and important recent examples of how microfluidic tools were applied to improve 3D cell culture models. Efforts over the last two years will be categorized and discussed in the context of abovementioned drivers. We particularly emphasize the contribution of microfluidics to the unmet needs in 3D cell culture, as well as the role of these models in the drug development pipeline. For reviews regarding manufacturing of microfluidic devices we refer to other publications[10,11]. We observe that the focus is shifting from tool building to more in-depth focus on the development of specific models. The full validation of these models and the symbiosis with recent developments in stem cell niches and induced pluripotent stem cells (iPSc) will determine the trend for the coming years.

Overview

We inventorized 87 papers that contained the keywords: '[microfluidic OR microengineered] AND 3D cell culture' which appeared on Pubmed since 2012. The papers were categorized according to the tissue and organ model addressed and depicted in Figure 1a. Cancer is a particularly dominant field in microfluidic 3D cell culture, and therefore depicted separately in Figure 1b.

As is shown in Figure 1a, most tissue modelling efforts were focused on vascularity, followed by brain and liver tissue models. The striking dominance of efforts in vascular modelling might be explained by the fact that microfluidics is the only platform capable of perfusing such vessels, thereby inducing the vitally important flow and accompanying shear stresses. This, in addition to the co-culture context and relevance of gradients in for instance angiogenesis assays, makes that vasculature models benefit most from the added value of microfluidics[12]. The attention for brain models fits in a wider trend towards attention for stem cell-derived neuronal models for diseases such as Alzheimer and Parkinson. This follows the more generic increase in popularity of induced pluripotent stem cell techniques and progress in controlling the stem cell niche of differentiated tissues.

Cancer is a complex heterogeneous disease and cancer in vitro models are driven by the demand for phenotypic screening models. This fits in a trend towards more systemic approaches to therapy discovery and selection, as well as in the trend towards tailoring therapies to individual patient's characteristics, so-called personalized medicine. Breast and lung cancer models comprise half of the developed cancer models (see Figure 1b), correlating with their high incidence in humans. Vasculature is involved in many parts of the metastatic cascade, the spread of cancer cells. Interestingly, many of the recent developed microfluidic 3D cancer models include a vascular component, as shown in the subgraph of Figure 1b. These models include processes such as angiogenesis, migration and intravastion and extravastion, and will be discussed later.

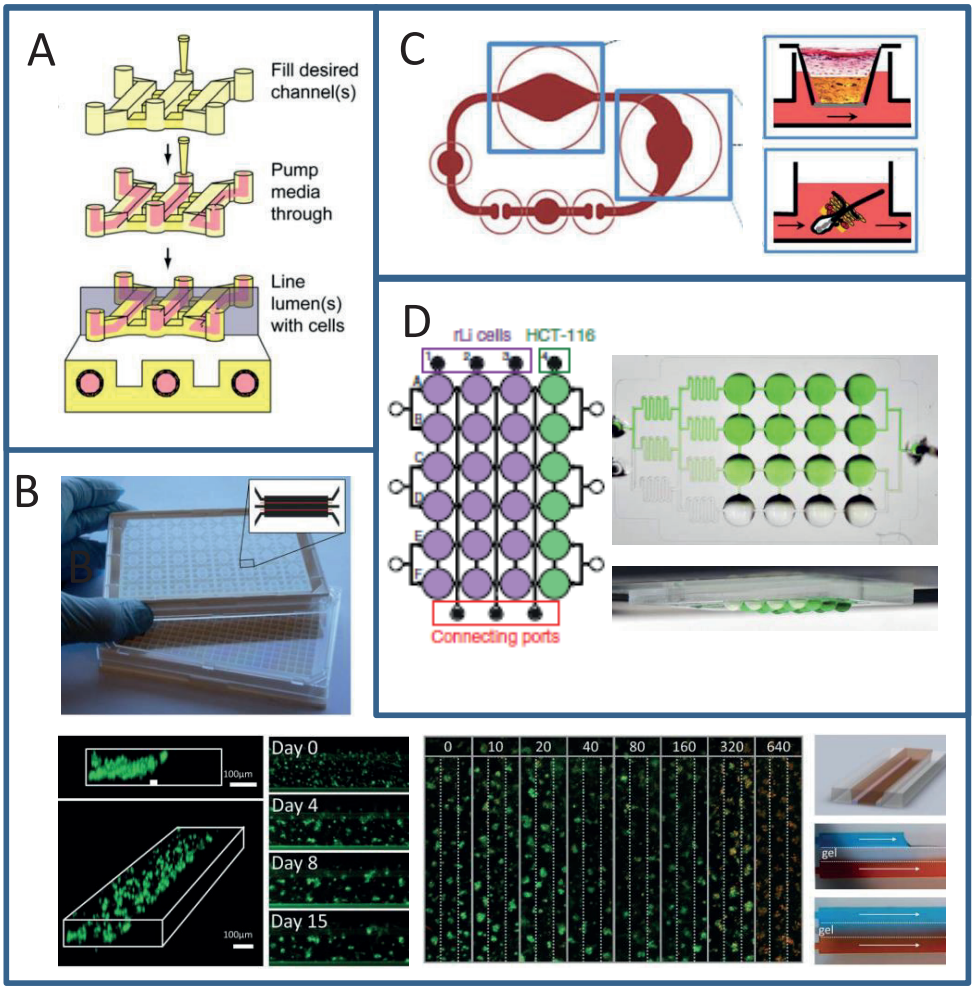

Figure 2 | Microfluidic techniques for 3D cell culture

(a) *Lumen and cell patterning inside a hydrogel. First, the hydrogel (yellow) is loaded inside the microfluidic channel. Then, a cell suspension is introduced, which patterns a lumen inside, exploiting the microfluidic properties and differences in viscosity and pressure.* **(b)** *A whole tissue perfusion system developed by Wagner et al.[27] tissues are isolated and cultured on membrane inserts. Microfluidic channels interconnect the tissue chambers, allowing continuous perfusion and paracrine cell signaling.* **(c)** *Hanging droplet system developed by Frey et al. [29]. This picture demonstrated the hanging droplet array in combination with a gradient generator.* **(d)** *96 microfluidic culture chambers integrated underneath a microtiter plate. Extracellular matrix gels are selectively patterned in the chamber by phaseguides obtain a layered profile.*

Microfluidic tools for spatially controlled cell culture

Spatial control is at the basis of many principles found in microfluidic 3D cell culture. It allows patterning of cells and extracellular microenvironment, to create stratified (co-)cultures with basal–apical access, gradient formation and medium perfusion.

In classical culture techniques, the spatial control is usually achieved by a membrane, such as in Boyden chambers[13], to support surface-attached cell growth, and separation of the culture reactor in two compartments. Although typically associated with 2D cell culture, membranes are also widely used in microfluidic chips[14]. A recent trend in microfluidic systems is to use hydrogels to offer cells a more physiologically relevant, three dimensional matrix[15,16]. Hydrogels enable a more relevant environment in which cell can cluster together, without need for surface adhesion. Selective patterning of hydrogels enables co-culture of cells without the need for artificial membranes.

Spatial control over hydrogels is achieved using guiding structures such as ridges, pillars or posts[17-19]. Alternatively, hydrogels can be molded into the right geometry[20,21]. Bischel et al. show an interesting technique to pattern cells inside a hydrogel, requiring just a few pipetting steps. The hydrogel is introduced into the microfluidic channel. Due to the fluidic properties and differences in viscosity and pressure, a liquid can create a lumen inside the hydrogel. A vessel is formed by introducing a cell suspension, which adheres to the hydrogel[22] (see Figure 2a).

In the surge towards high throughput, standardized microfluidic platforms, Trietsch et al. developed a microfluidic 3D co-culture plate with 96 individually addressable chambers. In this plate, hydrogels are patterned by phaseguides. Perfusion flow was maintained by passive levelling between two reservoirs, thereby eliminating the need for external pumps. The microfluidic channel dimensions were optimized to enable screening using a standard fluorescent microscopy. This was demonstrated by generating a IC50 curve of the toxicity of Rifampicin to 3D liver spheroids (Figure 2b)[23].

Cells can also be spatially controlled without hydrogels, using microchambers or

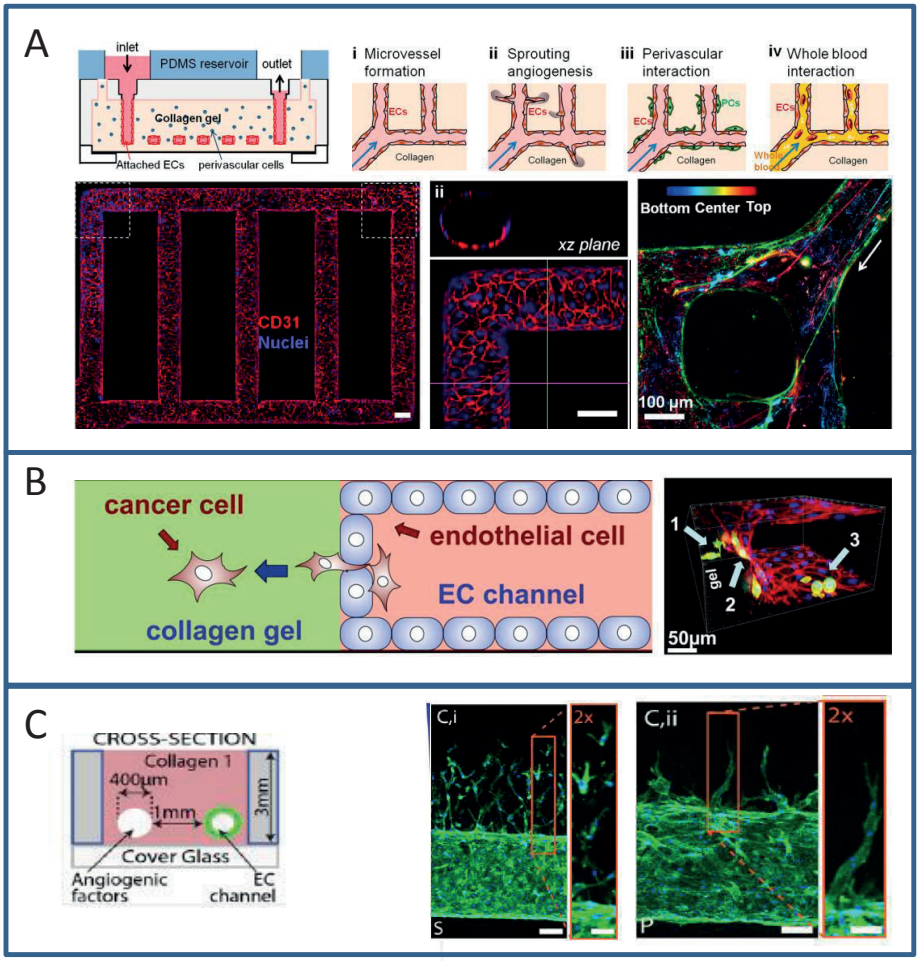

Figure 3 | Vasculature tissue- and cancer models

(a) *Vasculature in vitro model developed by Zheng et al. [17]. A grid layout is patterned in collagen gel and HUVECs are seeded inside. The vasculature shows formation VWF after perfusion with whole blood and stimulation with phorbol-12-myristate-13-acetate (PMA)* **(b)** *A microfluidic in vitro model for extravasation, using a co-culture of HUVEC cells and a breast cancer cell line. The breast cancer cells inside the lumen (indicated with 3) extravasate through the endothelial barrier (indicated with 2) into the matrix (indicated with 1)[49].* **(c)** *Microfluidic angiogenesis model, using a two channel design with lumen inside a collagen gel. HUVEC cells are seeded and form a vessel, which showed migration (Ci) as well as sprouting (Cii) of the endothelial cells after stimulation with different pro-angiogenic factors.[18]*

droplets, in which suspended cells settle and cluster to form spheroids[24-27]. Wang et al. show an interesting microfluidic device which captures colon spheroids using an microfluidic cell strainer. The captured colon spheroids are then embedded in a hydrogel to provide an extracellular matrix which is crucial for spheroid growth[28].

Co-culture

The ability to spatially control cells paves the way for combining multiple cell types in a way that more faithfully represents the organization of tissues and organs. Using hydrogels, cells can be patterned to mimic the spatial organization found in vivo, which is useful to mimic for example the interaction between stromal cells with various tissues. Furthermore, the formation of monolayers against hydrogels allows the study of trans-endothelial migration of (cancer) cells. Microfluidics can also be used to (co-)culture whole tissues and to interconnect them through microfluidic channels for media circulation. For example, Ataç et al. show a co-culture of hair follicles with skin tissue slices in a microfluidic Boyden chamber-like system (Figure 2c)[29,30]. Vasculature can be included as well by seeding endothelial cells inside the interconnecting channels[31].

A hydrogel-free co-culture environment can be created using a microfluidic hanging drop system. Frey et al. demonstrate a continuously perfused array containing both liver and colorectal cancer (CRC) spheroids. This was used to study drug metabolism and toxicity: the liver spheroids metabolize a chemotherapeutic compound, thus exposing the CRC spheroids to the metabolized drug (see Figure 2d)[32].

Gradients

In vivo, soluble (bio)molecular gradients are found in many different biological phenomena, such as angiogenesis, invasion and migration. Microfluidic devices have been developed to study angiogenesis and (anti)angiogenic factors[19,22,33,34], as well as tumor invasion assays[35,36].

Since microfluidics enables spatial control over fluids, the gradients can be precisely

controlled. For example, by patterning a hydrogel between to fluids, stable and predictable linear gradients are formed. By altering the channel geometry and applied flow rates, more complex gradient patterns are possible[37].

Han et al. studied trans-endothelial migration of neutrophils under influence of a gradient of two chemo-attractants, elegantly demonstrating the power of compartmentalization, spatial control and gradient formation in microfluidic 3D cell culture. They show that the neutrophils respond differently to the two different chemo-attractants and correlate ECM stiffness with migration speed[38].

To integrate these type of assays into the high throughput drug-screening pipeline, Trietsch et al. demonstrate gradient formation within their microfluidic titer plate format[23]. A double perfusion flow was used to generate a gradient over a compartmentalized hydrogel (see Figure 2b). This allows high throughput migration assays, gradient formation in combination with stratified co-cultures.

Instead of using soluble molecules, cells can be used to create gradients as well, resulting in heterogeneous cell densities within a hydrogel. Mahadik et al. show a microfluidic device which creates opposing gradients of two cell types[39]. This will be a useful tool to determine for example the optimal cell ratio of niche cells and stem cells.

Perfusion

Perfusion of 3D cell culture is almost exclusively reserved for microfluidic techniques, since the compartmentalized nature of microfluidics allows to perfuse media adjacent to or through a 3D cell culture. Benefits associated with perfusion flow include stable nutrient supply, waste metabolites removal and control of oxygen tension. Perfusion is one of the crucial aspects in vasculature, as it provides shear stress, which affects the cellular morphology and gene expression[40,41].

Vasculature

In the context of 3D cell culture, vasculature models benefit most from the added

value of these microfluidics tools including spatial control, co-culture, gradients and perfusion. Vascular models are typically grown by seeding endothelial cells in or against a hydrogel[19,20,34,37,42,43]. Zheng et al. created a perfusable vascular network in microchannels that were molded into collagen (see Figure 2e)[20]. As a result, endothelial cells are fully surrounded by a natural collagen matrix. Under perfusion with whole blood, authors showed that upon stimulation with phorbol-12-myristate-13-acetate (PMA), long fibers of Von-Willebrand factor (VWF) are secreted. Webs of VWF-fibers form at channel intersections, which were demonstrated to trap platelets more effectively.

Tourovskaia et al. used a similar approach for culturing brain vasculature together with stromal and neuronal cells in an attempt to create a model for the blood brain barrier. Pericytes and astrocytes were mixed with collagen that was injected around needles inserted in a chip. After polymerization, the needles were removed leaving a lumen that was subsequently seeded with brain endothelial cells[44], thereby creating a co-culture of the key cell types that play a role in the blood brain barrier.

Also endothelial–epithelial vessels can be created, as demonstrated by a kidney-endothelial double tubules. A collagen microfluidic structure was used to pattern a tube of Madin-Darby canine kidney (MDCK) cells, next to a tube of human umbilical vein endothelial cells (HUVEC)[45]. Huang et al. also show a perfusable, stratified MDCK co-culture with adipose derived stem cells[46], which enhanced cilia formation and increased expression of ion transporters of the MDCK cells.

The predictability of microfluidic flows can be used to control the interstitial flow in the cellular microenvironment, as demonstrated by Hsiang Hsu et al. They show a microfluidic device with endothelial cells and fibroblasts embedded in hydrogel. Medium is perfused through the gel from small inlets resulting in spatially defined interstitial flow patterns. The interstitial flow provides mechanical cues that induce vasculogenesis, resulting in in vivo like vascular architecture (Figure 3b)[47].

The mechanical cues however can also be transduced by the microfluidic channel geometry, as suggested by a study of the response of endothelial cells on various

curvatures[48]. Within a microfluidic device, HUVEC and brain microvascular endothelial cells (HBMVEC) were grown around small glass rods with a diameter of 10 µm, mimicking the curvature found in microcapillaries. Under continuous flow, HUVECs and brain microvascular endothelial cells (HBMVEC) responded differently. At high curvature, brain endothelial cells resist elongation while HUVECs aligned in the flow direction, suggesting that this phenotype plays a role in vivo: by minimizing the elongation, the tight junction length is decreased thereby minimizing paracellular transport, one of the hallmarks of the blood brain barrier.

Cancer models

The metastatic cascade, the way cancer cells spread, is closely linked to the vascular system. Many parts within the metastatic cascade can be studied by co-culturing perfusable endothelial vessels with cancer cells. Using microfluidic 3D cell culture, effects such as angiogenesis[20,22,33], migration[49,50], intravasation[51] and extravasation [18,19,44,52] have been studied, and will be discussed in more detail.

Figure 3c illustrates an extravasation setup in which endothelial cells are seeded against a compartmentalized hydrogel. After two days, breast cancer cells (MBA-MD-231) were perfused through the lumen. The breast cancer cells extravasated into the gel and increased the endothelial permeability[52]. Bersini et al. modified this setup by seeding human mesenchymal cells (hMSC) into the gel, to create a more specific niche for the extravasating cells and show a significant increase in extravasation compared with the previous setup. Furthermore, the authors show that a gradient of cytokine CXCL5 show similar extravasation compared with the hMSC co-culture. Blocking the CXCL2 receptor, which has a ligand for CXCL5, reduced extravasation[18].

An important driver in tumor migration is interstitial flow[53,54]. A microfluidic 3D interstitial flow chamber was used to study the migration behavior of MDA-MB-231 breast cancer cells and glioma cells[55].

Many publications show gradient formation of angiogenic factors in combination with perfusable vasculature to study angiogenesis[19-21,33-36]. Nguyen et al. study in-

vasion and sprouting of HUVECs which are exposed to a gradient of various cocktails of pro-angiogenic factors. Interestingly, they found that a gradient of vascular endothelial growth factor (VEGF) alone was not sufficient to trigger angiogenesis. It was found that a gradient of spingosine-1-phosphate (S) triggered single cell migration and phorbol 12-myristate 13-acetate (P) triggered collective cell migration (see Figure 3d). Mixtures of multiple pro-angiogenic factors triggered multicellular sprouting; a hallmark of angiogenesis *in vivo*. This demonstrates the potential for elucidating molecular mechanism of angiogenesis using microfluidic devices.

Discussion

Above examples demonstrate the potential of microfluidic techniques to improve the physiological relevance of 3D cell culture models. We discussed functional additions such as stratified co-cultures, gradient formation, vessel formation and medium perfusion. In addition to the physiological relevance, there are incentives such as improved reproducibility, cost effectiveness and/or ease of handling that may drive the implementation of microfluidics. For example, the reduced dimensions offer advantages such as reduced consumption of expensive cell material, hydrogels and screening reagents. Well defined heights of microfluidic channels dramatically improve imaging quality and speed. Z-stacking with confocal imaging equipment might for many assays not be necessary anymore, as co-culture and migration assays are patterned in the horizontal plane and most cells lie within the same focal plane. Precise metering of liquids with microfluidic techniques enables better quantification of assays.

A model system is only as good as the cells that are used to build it. Human cells are a must for enhanced predictive models. Primary material is physiologically most relevant, but suffers from complex logistics, batch-to-batch variation and often limited life span in vitro. Cell lines overcome these problems, but are not always considered good representatives for the in vivo situation. iPSc and organoid techniques have rapidly increased in popularity. Organoids are derived from primary stem cells. Stem cells expressing the LGR5 receptor have been identified which have been shown to

maintain stemness in vitro and differentiate into fully functional intestine[56], stomach[57] and liver[58]. The iPSC techniques allow reprogramming of fibroblasts into stem cells that can be differentiated into various tissues, such as neurons[59], cardiomyocytes[60] and several blood lineage cells[61]. Both cell sources allow to recapitulate various inherited diseases *in vitro*, and to study genotypic differences.

Microfluidic 3D culture models need to be fully validated before they can be applied by a wide range of users in academia and pharmaceutical industry. However, validation is a challenge in its own, and still an issue for many in vitro models[62]. It is widely expected that 3D culture models based on human derived cells are better predictive of clinical outcome than animal tests due to their human origin. Animal tests are thus not suited as a reference model for validation. Retrospective validation based on clinical results for, for example, successful and failed compounds with regards to toxicology, should be used as reference points for validation. However, these data and the relevant biological materials are in many cases not publicly available. An alternative validation strategy is to compare biochemical changes between an in vitro model system and clinical studies, such as for example gene expression profiles, enzymatic activities and metabolism. Clinical biomarkers can guide this validation and improve the comparability between organ models and the clinical reference point. To identify and assess such biomarkers, sensitive analytical methods are needed such as sequencing, microarray and/or mass spectrometry techniques. A particular challenge here is the sensitivity of analytical systems as only small amounts of medium and cells are available from microfluidic cell cultures. We expect important developments in the near future in which microfluidics and Organ-on-a-Chip systems are coupled with mass spectrometry analysis[63].

In our opinion, the various microfluidic designs of available model systems are no longer the bottleneck to the use of microfluidic 3D cell cultures in a wide range of academic and industrial applications. Although complications such as material incompatibility to hydrophobic compounds, as for instance the case for PDMS systems, still persist and many chips still lack a user-friendly interfacing [11], others have

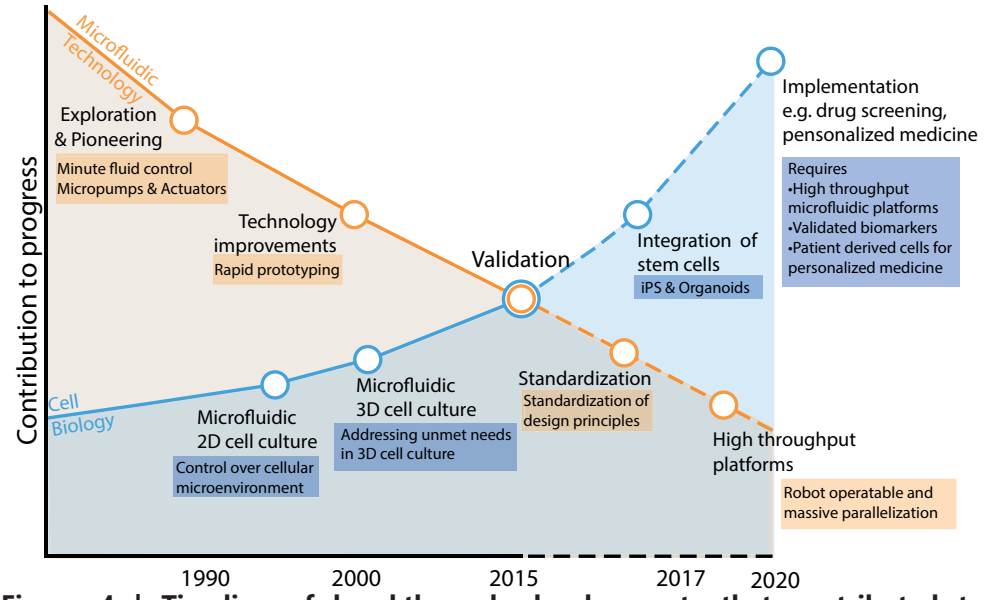

Figure 4 | Timeline of breakthrough developments that contributed to microfluidic 3D cell culture

As the microfluidic tools are in place, we are currently at the validation phase, a bottleneck that needs to be addressed before the field can advance and replace current in vitro models.

addressed these issues in a convincing manner. As microfluidic technology matures, the focus will shift towards biological development and validation of physiologically relevant models (Figure 4).

The trend for the coming years will be to use microfluidic 3D cell culture in combination with the recent advances in stem cell biology, such as iPSC[64] and organoid technology. This will allow to take into account differences between patients in various applications: first, novel diagnostic tests to predict treatment outcome for an individual patient; second, supporting clinical trial design; or third, taking the individual differences already into account during drug discovery and developments, both in respect to efficacy and toxicity. Thus, ultimately, we expect that microfluidic humanized 3D cell cultures will play an important role in the development of personalized medicine.

References

1 Schoenenberger, C. A., Zuk, A., Zinkl, G. M., Kendall, D. & Matlin, K. S. Integrin expression and localization in normal MDCK cells and transformed MDCK cells lacking apical polarity. *J Cell Sci.* **107 (Pt 2)** 527-541, (1994).

2 Debnath, J., Muthuswamy, S. K. & Brugge, J. S. Morphogenesis and oncogenesis of MCF-10A mammary epithelial acini grown in three-dimensional basement membrane cultures. *Methods.* **30** (3), 256-268, (2003).

3 Weaver, V. M. *et al.* Reversion of the malignant phenotype of human breast cells in three-dimensional culture and in vivo by integrin blocking antibodies. *The Journal of cell biology.* **137** (1), 231-245, (1997).

4 Lin, C. Q. & Bissell, M. J. Multi-faceted regulation of cell differentiation by extracellular matrix. *FASEB J.* **7** (9), 737-743, (1993).

5 Ramaiahgari, S. C. *et al.* A 3D in vitro model of differentiated HepG2 cell spheroids with improved liver-like properties for repeated dose high-throughput toxicity studies. *Arch Toxicol.* **88** (5), 1083-1095, (2014).

6 Chen, C. S., Mrksich, M., Huang, S., Whitesides, G. M. & Ingber, D. E. Geometric control of cell life and death. *Science.* **276** (5317), 1425-1428, (1997).

7 Koh, W. G. & Pishko, M. V. Fabrication of cell-containing hydrogel microstructures inside microfluidic devices that can be used as cell-based biosensors. *Anal Bioanal Chem.* **385** (8), 1389-1397, (2006).

8 Tan, W. & Desai, T. A. Microscale multilayer cocultures for biomimetic blood vessels. *J Biomed Mater Res A.* **72** (2), 146-160, (2005).

9 Polacheck, W. J., Li, R., Uzel, S. G. & Kamm, R. D. Microfluidic platforms for mechanobiology. *Lab Chip.* **13** (12), 2252-2267, (2013).

10 Alrifaiy, A., Lindahl, O. A. & Ramser, K. Polymer-Based Microfluidic Devices for Pharmacy, Biology and Tissue Engineering. *Polymers.* **4** (4), 1349-1398, (2012).

11 Berthier, E., Young, E. W. & Beebe, D. Engineers are from PDMS-land, Biologists are from Polystyrenia. *Lab Chip.* **12** (7), 1224-1237, (2012).

12 Wong, K. H., Chan, J. M., Kamm, R. D. & Tien, J. Microfluidic models of vascular functions. *Annu Rev Biomed Eng.* **14** 205-230, (2012).

13 Boyden, S. The Chemotactic Effect of Mixtures of Antibody and Antigen on Polymorphonuclear Leucocytes. *Journal of Experimental Medicine.* **115** (3), 453-466, (1962).

14 Kim, H. J., Huh, D., Hamilton, G. & Ingber, D. E. Human gut-on-a-chip inhabited by microbial flora that experiences intestinal peristalsis-like motions and flow. *Lab Chip.* **12** (12), 2165-2174, (2012).

15 Chung, B. G., Lee, K. H., Khademhosseini, A. & Lee, S. H. Microfluidic fabrication of microengineered hydrogels and their application in tissue engineering. *Lab Chip.* **12** (1), 45-59, (2012).

16 Huang, G. Y. *et al.* Microfluidic hydrogels for tissue engineering. *Biofabrication.* **3** (1), 012001, (2011).

17 Chung, S. *et al.* Cell migration into scaffolds under co-culture conditions in a microfluidic platform. *Lab Chip.* **9** (2), 269-275, (2008).

18 Bersini, S. *et al.* A microfluidic 3D in vitro model for specificity of breast cancer metastasis to bone. *Biomaterials.* **35** (8), 2454-2461, (2014).

19 Kim, S., Lee, H., Chung, M. & Jeon, N. L. Engineering of functional, perfusable 3D microvascular networks on a chip. *Lab Chip.* **13** (8), 1489-1500, (2013).

20 Zheng, Y. *et al.* In vitro microvessels for the study of angiogenesis and thrombosis. *Proc Natl Acad Sci U S A.* **109** (24), 9342-9347, (2012).

21 Nguyen, D. H. *et al.* Biomimetic model to reconstitute angiogenic sprouting morphogenesis in vitro. *Proc Natl Acad Sci U S A.* **110** (17), 6712-6717, (2013).

22 Bischel, L. L., Lee, S. H. & Beebe, D. J. A practical method for patterning lumens through ECM hydrogels via viscous finger patterning. *J Lab Autom.* **17** (2), 96-103, (2012).

23 Trietsch, S. J., Israels, G. D., Joore, J., Hankemeier, T. & Vulto, P. Microfluidic titer plate for stratified 3D cell culture. *Lab Chip.* **13** (18), 3548-3554, (2013).

24 Kwapiszewska, K., Michalczuk, A., Rybka, M., Kwapiszewski, R. & Brzozka, Z. A microfluidic-based platform for tumour spheroid culture, monitoring and drug screening. *Lab Chip.* **14** (12), 2096-2104, (2014).

25 Kuo, C. T. *et al.* A spatiotemporally defined in vitro microenvironment for controllable signal delivery and drug screening. *Analyst.* **139** (19), 4846-4854, (2014).

26 Krause, S., Maffini, M. V., Soto, A. M. & Sonnenschein, C. A novel 3D in vitro culture model to study stromal-epithelial interactions in the mammary gland. *Tissue Eng Part C Methods.* **14** (3), 261-271, (2008).

27 Ziolkowska, K. *et al.* Long-term three-dimensional cell culture and anticancer drug activity evaluation in a microfluidic chip. *Biosens Bioelectron.* **40** (1), 68-74, (2013).

28 Wang, Y., Ahmad, A. A., Sims, C. E., Magness, S. T. & Allbritton, N. L. In vitro generation of colonic epithelium from primary cells guided by microstructures. *Lab Chip.* **14** (9), 1622-1631, (2014).

29 Wagner, I. *et al.* A dynamic multi-organ-chip for long-term cultivation and substance testing proven by 3D human liver and skin tissue co-culture. *Lab Chip.* **13** (18), 3538-3547, (2013).

30 Atac, B. *et al.* Skin and hair on-a-chip: in vitro skin models versus ex vivo tissue maintenance with dynamic perfusion. *Lab Chip.* **13** (18), 3555-3561, (2013).

31 Schimek, K. *et al.* Integrating biological vasculature into a multi-organ-chip microsystem. *Lab Chip.* **13** (18), 3588-3598, (2013).

32 Frey, O., Misun, P. M., Fluri, D. A., Hengstler, J. G. & Hierlemann, A. Reconfigurable microfluidic hanging drop network for multi-tissue interaction and analysis. *Nat Commun.* **5** 4250, (2014).

33 Verbridge, S. S. *et al.* Physicochemical regulation of endothelial sprouting in a 3D microfluidic angiogenesis model. *J Biomed Mater Res A.* **101** (10), 2948-2956, (2013).

34 Lee, H., Kim, S., Chung, M., Kim, J. H. & Jeon, N. L. A bioengineered array of 3D microvessels for vascular permeability assay. *Microvasc Res.* **91** 90-98, (2014).

35 Wood, L. B., Ge, R., Kamm, R. D. & Asada, H. H. Nascent vessel elongation rate is inversely related to diameter in in vitro angiogenesis. *Integr Biol (Camb).* **4** (9), 1081-1089, (2012).

36 Fang, C., Avis, I., Salomon, D. & Cuttitta, F. Novel Phenotypic Fluorescent Three-Dimensional Platforms for High-throughput Drug Screening and Personalized Chemotherapy. *J Cancer.* **4** (5), 402-415, (2013).

37 Baker, B. M., Trappmann, B., Stapleton, S. C., Toro, E. & Chen, C. S. Microfluidics embedded within extracellular matrix to define vascular architectures and pattern diffusive gradients. *Lab Chip.* **13** (16), 3246-3252, (2013).

38 Han, S. *et al.* A versatile assay for monitoring in vivo-like transendothelial migration of neutrophils. *Lab Chip.* **12** (20), 3861-3865, (2012).

39 Mahadik, B. P., Wheeler, T. D., Skertich, L. J., Kenis, P. J. & Harley, B. A. Microfluidic generation of gradient hydrogels to modulate hematopoietic stem cell culture environment. *Adv Healthc Mater.* **3** (3), 449-458, (2014).

40 Polacheck, W. J., German, A. E., Mammoto, A., Ingber, D. E. & Kamm, R. D. Mechanotransduction of fluid stresses governs 3D cell migration. *Proc Natl Acad Sci U S A.* **111** (7), 2447-2452, (2014).

41 Altmann, B. *et al.* Differences in morphogenesis of 3D cultured primary human osteoblasts under static and microfluidic growth conditions. *Biomaterials.* **35** (10), 3208-3219, (2014).

42 Wang, X. Y. *et al.* Engineering interconnected 3D vascular networks in hydrogels using molded sodium alginate lattice as the sacrificial template. *Lab Chip.* **14** (15), 2709-2716, (2014).

43 Park, Y. K. *et al.* In Vitro Microvessel Growth and Remodeling within a Three-dimensional Microfluidic Environment. *Cell Mol Bioeng.* **7** (1), 15-25, (2014).

44 Tourovskaia, A., Fauver, M., Kramer, G., Simonson, S. & Neumann, T. Tissue-engineered microenvironment systems for modeling human vasculature. *Exp Biol Med (Maywood).* **239** (9), 1264-1271, (2014).

45 Mu, X., Zheng, W., Xiao, L., Zhang, W. & Jiang, X. Engineering a 3D vascular network in hydrogel for mimicking a nephron. *Lab Chip.* **13** (8), 1612-1618, (2013).

46 Huang, H. C. *et al.* Enhancement of renal epithelial cell functions through microfluidic-based coculture with adipose-derived stem cells. *Tissue Eng Part A.* **19** (17-18), 2024-2034, (2013).

47 Hsu, Y. H., Moya, M. L., Hughes, C. C., George, S. C. & Lee, A. P. A microfluidic platform for generating large-scale nearly identical human microphysiological vascularized tissue arrays. *Lab Chip.* **13** (15), 2990-2998, (2013).

48 Ye, M. *et al.* Brain microvascular endothelial cells resist elongation due to curvature and shear stress. *Sci Rep.* **4** 4681, (2014).

49 Hockemeyer, K. *et al.* Engineered three-dimensional microfluidic device for interrogating cell-cell interactions in the tumor microenvironment. *Biomicrofluidics.* **8** (4), 044105, (2014).

50 Haessler, U., Teo, J. C., Foretay, D., Renaud, P. & Swartz, M. A. Migration dynamics of breast cancer cells in a tunable 3D interstitial flow chamber. *Integr Biol (Camb).* **4** (4), 401-409, (2012).

51 Zervantonakis, I. K. *et al.* Three-dimensional microfluidic model for tumor cell intravasation and endothelial barrier function. *Proc Natl Acad Sci U S A.* **109** (34), 13515-13520, (2012).

52 Jeon, J. S., Zervantonakis, I. K., Chung, S., Kamm, R. D. & Charest, J. L. In Vitro Model of Tumor Cell Extravasation. *PLoS One.* **8** (2), (2013).

53 Swartz, M. A. & Lund, A. W. Lymphatic and interstitial flow in the tumour microenvironment: linking mechanobiology with immunity. *Nat Rev Cancer.* **12** (3), 210-219, (2012).

54 Wiig, H. & Swartz, M. A. Interstitial fluid and lymph formation and transport: physiological regulation and roles in inflammation and cancer. *Physiol Rev.* **92** (3), 1005-1060, (2012).

55 Munson, J. M., Bellamkonda, R. V. & Swartz, M. A. Interstitial flow in a 3D microenvironment increases glioma invasion by a CXCR4-dependent mechanism. *Cancer Res.* **73** (5), 1536-1546, (2013).

56 Sato, T. & Clevers, H. Growing self-organizing mini-guts from a single intestinal stem cell: mechanism and applications. *Science.* **340** (6137), 1190-1194, (2013).

57 Barker, N. *et al.* Lgr5(+ve) stem cells drive self-renewal in the stomach and build long-lived gastric units in vitro. *Cell Stem Cell.* **6** (1), 25-36, (2010).

58 Huch, M. *et al.* In vitro expansion of single Lgr5+ liver stem cells induced by Wnt-driven regeneration. *Nature.* **494** (7436), 247-250, (2013).

59 Caiazzo, M. *et al.* Direct generation of functional dopaminergic neurons from mouse and human fibroblasts. *Nature.* **476** (7359), 224-227, (2011).

60 Ieda, M. *et al.* Direct reprogramming of fibroblasts into functional cardiomyocytes by defined factors. *Cell.* **142** (3), 375-386, (2010).

61 Ellis, J. & Bhatia, M. iPSC technology: platform for drug discovery. Point. *Clin Pharmacol Ther.* **89** (5), 639-641, (2011).

62 Astashkina, A. & Grainger, D. W. Critical analysis of 3-D organoid in vitro cell culture models for high-throughput drug candidate toxicity assessments. *Adv Drug Deliv Rev.* **69-70** 1-18, (2014).

63 Oedit, A., Vulto, P., Ramautar, R., Lindenburg, P. W. & Hankemeier, T. Lab-on-a-Chip hyphenation with mass spectrometry: strategies for bioanalytical applications. *Curr Opin Biotechnol.* **31** 79-85, (2015).

64 Moreno, E. L. *et al.* Differentiation of neuroepithelial stem cells into functional dopaminergic neurons in 3D microfluidic cell culture. *Lab Chip.* **15** (11), 2419-2428, (2015).

CHAPTER

3

96 perfusable blood vessels to study vascular permeability in vitro

V van Duinen, A Heuvel, SJ Trietsch, HL Lanz, JM Gils,
AJ van Zonneveld, P Vulto, T Hankemeier

Scientific reports, 7; 18071 (2017)

Abstract

Current *in vitro* models to test the barrier function of vasculature are based on flat, two-dimensional monolayers. These monolayers do not have the tubular morphology of vasculature found *in vivo* and lack important environmental cues from the cellular microenvironment, such as interaction with an extracellular matrix (ECM) and exposure to flow. To increase the physiological relevance of *in vitro* models of the vasculature, it is crucial to implement these cues and better mimic the native three-dimensional vascular architecture.

We established a robust, high-throughput method to culture endothelial cells as 96 three-dimensional and perfusable microvessels and developed a quantitative, real-time permeability assay to assess their barrier function. Culture conditions were optimized for microvessel formation in 7 days and that were viable for over 60 days. The microvessels exhibited a permeability to 20 kDa dextran, but not to 150 kDa dextran, which mimics the functionality of vasculature *in vivo*. Also, a dose-dependent effect of VEGF, TNFα and several cytokines confirmed a physiologically relevant response.

The throughput and robustness of this method and assay will allow end-users in vascular biology to make the transition from two-dimensional to three-dimensional culture methods to study vasculature.

Introduction

Disruption of the vascular barrier plays a central role in the onset and progression of diseases, including chronic kidney disease[1], (vascular) dementia [2,3], Alzheimer's [4,5] and atherosclerosis [6-8]. Preventing the disruption or restoring the barrier is thus an attractive target for drug discovery. However, for in-depth analysis and validation of new drug candidates, we still rely on *in vitro* models, which are based on flat monolayers of endothelial cells. These monolayers do not have the complete anatomic architecture of the vasculature, as cells are growing on flat, artificial substrates. Also, important cues in the cellular microenvironment are missing, including interaction with an extracellular matrix (ECM) and exposure to flow. It is crucial to mimic these cues and the three-dimensional morphology found *in vivo* in order to increase the physiological relevance *in vitro*[9].

Models that use of microfluidics techniques have recently emerged to increase the physiological relevance *in vitro*, as it allows patterning of cells and hydrogels and ECMs, application of perfusion and spatial control over signaling gradients. Recent reports show microfluidic devices to culture of endothelial cells as perfusable microvessels [10-17]. However, as these devices are early prototypes, we identified three main drawbacks that hinder optimization and adoption of microfluidic methods to culture vasculature[18]. First, there is limited consensus in design and used materials, and many devices are designed from an engineering perspective[19]. This makes direct comparisons between results obtained in these devices difficult, and limits widespread adoption and efficient experimental design. Second, many of silicone-based devices require pre-fabrication before use[10,20] and require molds (e.g. needles [12,21] or stamps [10]) to pattern hydrogels. Finally, these devices typically allow for single or low amounts of data points per device and cannot be handled in a high-throughput setting. This hinders optimization of culture conditions and testing of multiple experimental conditions, which renders screening of compounds virtually impossible. As a result, despite the widespread interest in microfluidic cell culture techniques to culture vasculature[22,23], there are yet no standardized and validated microfluidic

assays to study vascular permeability.

Here, we describe a method to culture endothelial cells as 96 individually addressable, three-dimensional microvessels in a standardized microfluidic platform. This platform is based on a microtiter plate format[24] that was shown compatible with culture of a wide variety of cell types, including neurons[25,26], intestine[27] and liver[28]. To mimic the morphology and microenvironment of vasculature *in vivo,* the microvessels are cultured against a 3D scaffold of polymerized collagen-1 and are continuously perfused using a rocker platform. To assess the barrier function, we developed a real-time permeability assay that quantifies the diffusion of 20 kDa and 150 kDa fluorescent dextrans over the vessel wall. This assay was used to optimize the culture conditions for robust and long-term culture of microvessels. Furthermore, we investigated the dose-dependent effect of VEGF, TNFα and several cytokines to study the effect on the permeability of the microvessels.

Methods

Cell Culture

HUVEC-VeraVec human endothelial cells (Angiocrine Biosciences, hVera101) were cultured in T75 flasks (Nunc Easyflask, Sigma F7552) with endothelial Cell Growth Medium MV2 (Promocell, C-22022) and used at P3 till P5. Media was replaced three times a week. Cells tested negative for mycoplasma. MV2 endothelial cell Growth Medium (Promocell, C-22022) and Pericyte Growth Medium SR Formulation (Angioproteomie, cAP-09B) were supplemented with 1% pen/strep (Sigma, P4333). M199 medium (Sigma, M4530) was supplemented with 50 µg/mL endothelial cell supplement (Biomedical Technologies, BT-203), 20% Fetal Bovine Serum (Gibco, 16140-071), 1% Antibiotic-Antimycotic solution (Invitrogen, 15240-062), 10 mmol/L HEPES buffer (Invitrogen. 5630-080), 50 µg/mL heparin (Sigma, H3149-100KU) and 2 mmol/L GlutaMAX (Life Technologies, 35050061). All cell culture was performed in a humidified incubator at 37°C and 5% CO_2.

The OrganoPlate (Mimetas, 9603-400B) was used for all microfluidic cell culture. Be-

fore cell seeding, each observation window was filled with 50 µL HBSS for optical clarity and to prevent gel dehydration. In all experiments collagen type I (R&D systems, 3447-020-01) was used as matrix for the cells to adhere on. A stock solution of 5 mg/mL rat tail collagen type I was neutralized with 10% 37g/L Na_2CO_3 (Sigma, S5761) and 10% 1 M HEPES buffer (Gibco, 15630-056) to obtain a concentration of 4 mg/mL. The neutralized collagen was kept on ice until and used within 30 min. Using a repeater pipette, 2 µL of the neutralized collagen was added into the inlet of each gel channel. To polymerize the collagen, the device was incubated for 30 minutes at 37°C, 5% CO_2. After incubation, the device was removed from the incubator and kept sterile at room temperature right before cell loading. Endothelial cells were dissociated, pelleted and resuspended in MV2 medium in a concentration of $2{\cdot}10^7$ cells/mL. 2 µL of the cell suspension was dispensed into the perfusion inlet well and the device was placed on its side and incubated for 15 min at 37°C, 5% CO_2. After incubation, 25 µL of medium is added in the perfusion inlet well to prevent dehydration of the cell suspension. The plate was placed back in the incubator on its side to allow cells to adhere for at least 45 minutes. After the cells attached to the gel, the plates were rotated back into an upright position and 75 µL of medium was added to the medium outlet. The device was placed on an interval rocker platform for continuous perfusion. (Perfusion rocker, MIMETAS). The rocker was set at a 7 degree inclination and 8 minutes cycle time. Medium was refreshed three times a week and right after each permeability assay.

Visualization and quantification of permeability

The macromolecular flux of a mixture of two fluorescent labeled dextrans (20 kDa FITC (Sigma, FD20S) and 150 kDa TRITC (Sigma, 48946) was used to quantify and visualize the permeability of the microvessels. The molecular weight of both fluorescence labels is insignificant compared to the molecular weight of the dextrans, thus the fluorescence label does not play a role in the diffusion speed[29] and the determination of the permeability.

For visualization of the images, the intensities are normalized to the highest intensity

in the perfusion channel. To these normalized images, a lookup table is applied to map the color scale, with the highest value of the lookup table set at ¼ of the maximum intensity (0.125 mg/mL). The background intensity (0 mg/mL) is determined by median of the intensity in the gel at t=0 min and we used this value as lowest value for the lookup table.

For quantification, all images were aligned based on the fluorescent image at t=0 min. The part containing the microfluidics was cropped and the regions of interest (ROIs) for the perfusion channel and gel channel were manually defined by drawing a ROI for the complete acquired area of the gel channel just below the phaseguide and the ROI of perfusion channel is always selected in the middle along the total length and half the width of the acquired part of the perfusion channel.

The fluorescent intensities of the gel channel and the perfusion channel were quantified using FIJI[30]. The apparent permeability (Papp) in cm/s was derived from formula 1[31]:

$$P_{app}\ (cm/s) = \frac{dQ}{dt} \cdot \frac{1}{A \cdot C_{donor}} \qquad (1)$$

where dQ/dt is the flux, A is the surface area in cm^2 and C_{donor} is the initial fluorescent dextran concentration in the apical side. We assumed a linear relationship between fluorescent intensity and concentration and a starting concentration of zero in the gel. C_{donor} is equal to the intensity in the perfusion channel ($I_{perfusion}$) at the start of the assay. However, as $I_{perfusion}$ changes throughout the experiment due to bleaching or diffusion into the gel, the formula was improved by normalizing the intensity in the gel (I_{gel}) to the intensity in the perfusion channel ($I_{perfusion}$)[32], yielding formula 2:

$$P_{app}\ (cm/s) = \frac{d\left(\frac{I_{gel}}{I_{perfusion}}\right)}{dt} \cdot V_{gel} \cdot \frac{1}{A} \qquad (2)$$

where I_{gel} /$I_{perfusion}$ is the ratio between the intensity in the gel and perfusion channel, V_{gel} the volume of the gel ($4{,}54 \cdot 10^{-4}$ cm^3), A the surface area of the microvessel that is in contact with the gel in cm^2 ($1{,}21 \cdot 10^{-2}$ cm^2). The ratio (I_{gel}/$I_{perfusion}$) was calculated for each individual timepoint. A linear regression was fitted through these ratios to

calculate the slope. The slope was multiplied with V_{gel} to obtain the flux over time and divided by A to obtain the apparent permeability.

The apparent permeability includes both the resistance of the cell barrier as well as the resistance in the gel, and the permeability of the microvessel can be derived from the formula:

$$\frac{1}{P_{app}} = \frac{1}{P_{microvessel}} + \frac{1}{P_{gel}} \quad (3)$$

where is the permeability of the microvessel and the permeability of the collagen. However, the diffusion rate of low molecular weight compounds (a hydrodynamic radius below < 8 nm.) in 4 mg/ml collagen does not significantly differ from the diffusion rates in an aqueous solution[33,34]. This suggests that the permeability of the gel does not significantly contribute to apparent permeability. We verified this experimentally and found that the permeability is around 20 times higher compared to the permeability when a confluent microvessel is present. Thus, we conclude that the influence of the gel can be neglected.

Media optimization

Both dextrans (25 mg/mL) were mixed and diluted in the appropriate cell culture media to a concentration of 0.5 mg/mL. At the start of the permeability assay, 20 µL of media was added in the gel inlet well, media containing both dextrans was added to both perfusion inlet (40 µL) and the perfusion outlet (30 µL). After addition of the dextran mixture, the device was placed directly inside a conditioned high content imaging system (Molecular Devices, ImageXpress Micro XLS). Fluorescent images were acquired every 3 for 30 minutes. The exposure time was adjusted so the fluorescent intensity in the perfusion channel was below saturation of the detector. After the image acquisition, the plate was removed the media was refreshed to use the plate for additional assays.

Compound exposure

The microvessels were cultured in MV2 medium for at least 7 days to obtain a proper barrier function. Prior to compound exposure, the microvessels were growth factor starved overnight using basal MV2 supplemented with 0.5% FBS. The compounds used for permeability studies (murine VEGF-165 (PeproTech 450-32), Retinoic Acid (Sigma R2625), Tumor Necrosis Factor α (TNFα) (Sigma T0157), IL8 (ImmunoTools 11349084) and IL1β (ImmunoTools 11343538)) were all aliquoted and stored according to manufacturer's protocol and diluted in growth factor free MV2 basal medium (Promocell C22221, Germany), supplemented with 0.5% FBS. All compounds were assessed at three concentrations[35]: 1, 10 and 100 ng/mL for IL8, INFγ, RA and TNFα; 10, 100 and 200 ng/mL for VEGF and 0.2, 2 and 20 ng/mL for IL1β. Unless stated otherwise, microvessels were exposed to compounds for 24 hours before doing permeability assays. The permeability assay was performed by diluting 20 kDa FITC- and 150 kDa TRITC-dextran in growth factor free MV2 basal medium to a concentration of 0.5mg/mL, with 20 µL of media in the gel inlet well, 40 µL of media containing both dextrans to the perfusion inlet and 30 µL of media to the perfusion outlet well. the Fluorescent images were acquired every 3 for 30 minutes, directly after addition of the dextran mixture. After the image acquisition, the plate was removed and media was either refreshed or the microvessels were fixed. Growth factor starved microvessels were refreshed with media containing 5% serum and growth factors to allow them to recover for additional experiments.

Immunocytofluorescent staining

During all steps of the immunocytofluorescent staining, the device is placed under an angle at all times to create flow, except during staining with primary antibody. Every solution was used in quantities of 100 µL per chip (50 µL in the perfusion inlet, 50 µL in the perfusion outlet) unless specified otherwise. Cells were fixed using freshly prepared 3.7% formaldehyde (Sigma 252549) in PBS. 50 µL of the fixative was added to both the perfusion inlet and outlet for 15 minutes at room temperature (RT), followed by a wash step with 4% FBS in PBS for 5 minutes. After fixation, the

cells were permeabilized using 0.3% Trition-X (Sigma T8787) in PBS. After washing, the microvessels were blocked for 45 min using blocking solution (2% FBS, 0.1% Tween20 (Sigma P9169), 2% BSA (Sigma A2153) in PBS). The adherence junctions were visualized using VE-Cadherin (Abcam, 33168, 1:1000 in blocking solution, 30 µL in perfusion inlet, 20 µL perfusion outlet) which was incubated for 1 hr. at RT followed by 30 min. incubation with Alexa Fluor 488 (ThermoFisher Scientific, A11008, 1:250 in blocking solution). To continuously perfuse the chips with primary antibody, the device was placed on a rocker platform. After incubation with the secondary antibody, the device is washed once with washing solution, followed by nuclei staining (NucBlue Fixed cell staining, Life technologies, R37606), and the cytoskeletal marker F-actin staining ActinRed 555 ReadyProbes (ThermoFisher Scientific, R37112) in PBS and imaged using a high content confocal microscope (Molecular Devices, ImageXpress Micro Confocal) at 10x magnification.

Statistical test

Welch Two Sample t-tests are used to compare treated microvessels with control. Graphs are plotted as mean (SD). Asterisks indicate a significant difference compared to control ($P \leq 0.05$). In sample sizes of $n>9$, Tukey's test is used to remove outliers.

Results

Microvessel formation and media optimization

The platform is based on a standardized microfluidic cell culture platform based on the footprint of a 384 well microtiter plate. It contains 96 microfluidic devices integrated in the bottom, and each single microfluidic device is positioned underneath 4 adjacent wells (Fig. 1a). Each microfluidic device consists of two channels that meet in the center, underneath the third well (Fig. 1b). The channels are separated by a phaseguide, a small ridge that act as a pressure barrier. This enables patterning of cells and the ECM without the use of artificial membranes[36].

The method to grow microvessels within the microfluidic channels is illustrated in Fig. 1c. First, collagen-1 was seeded into the gel channel (step 1). A droplet of gel on top of the inlet fills the gel channel by capillary force. The phaseguide prevents overflow into the adjacent perfusion channel. After gel loading and polymerization, an endothelial cell suspension was added to the adjacent perfusion channel (step 2). To promote cell adhesion to the collagen-1, the microtiter plate was placed on its side. After the cells adhered to the collagen-1, perfusion was applied by placing the device on a rocker platform (step 3). The rocker platform inverts the angle of inclination (7 degrees) every 8 minutes (Fig. 1d). After 3 days in culture, a confluent microvessel is formed against the collagen-1 (Fig. 1f). When the microvessels are formed, the apical side of the vessel (the lumen) can be accessed through the perfusion channel, while the basal side of the tube is in contact with the collagen-1. Importantly, the presence of a perfusion flow was observed to be crucial for the formation of the microvessels. In the absence of flow, the endothelial cells did not form a confluent monolayer on the bottom of the perfusion channel. Furthermore, after 7 days of culture the microvessels contracted and non-viable cells were visible (Supplementary Fig. 1).

The 3D reconstruction of a microvessel stained for F-Actin and nuclei shows the 3D architecture of the vessel (Fig. 1g) and shows a complete and confluent monolayer and a clear tubular morphology with a perfusable lumen. The curved part adheres to

►Figure 1 | Microfluidic platform for robust culture of perfusable microvessels.

(a) *The microfluidic microtiter plate used for perfusable microvessel culture, based on a 384 wells plate interface on top and 96 microfluidic devices integrated in the bottom.* **(b)** *Each microfluidic device consists of two channels: an 'perfusion' channel (1) and a 'gel' channel (2) separated by a phaseguide (*). Every microfluidic structure is positioned underneath 4 adjacent wells. Every first well (3) is positioned on top of the inlet of the gel channel, while every second (4) and fourth well (6) are above respectively the perfusion channel inlet and outlet. Every third well (5) is used for imaging and observation of the experiment. Note that this well does not have an in- or outlet and is therefore not in contact with the microfluidics. Phaseguide, top and bottom substrates are not to scale* **(c)** *Method for seeding microvasculature. Collagen-1 gel is seeded as extracellular matrix (ECM) and polymerized (step 1). After polymerization, the cells suspension is seeded in the perfusion channel (step 2). The device is placed on its side to allow the cells the settle and adhere to the collagen-1. After adhesion of the cells, perfusion is started by placing the device on a rocker platform (step 3). In 48 hours the cells grow as a confluent monolayer against the collagen gel and channel walls, resulting in a microvessel with a perfusable lumen (step 4).* **(d)** *A rocker platform is used to induce gravity driven, continuous, bi-directional flow. The device is placed at a 7 degree angle which is inverted every 8 minutes.* **(e)** *4x Phase contrast image when imaged below an observation window. Scale bar: 200 µm.* **(f)** *48 hr after cell seeding, a confluent vessel of endothelial cells is formed and an apical side (lumen) and basal side (part of microvessel that adheres to collagen-1) can be distinguished. Scale bar: 200 µm* **(g)** *3D reconstruction of a DAPI/F-actin stained microvessel*

►Figure 2 | Method for real-time quantification and visualization of the permeability.

(a) *Fluorescent dextran solution is added to the perfusion inlet well. This enters the perfusion channel and completely fills the lumen of the vessel. Without a cells or in case high permeability, the dextran equilibrates between the perfusion and the gel channel.* **(b)** *For every well, images were acquired every 3 minutes for a total of 30 minutes, resulting in 2112 images per permeability assay. Images are loaded into FIJI and aligned (step 1). Next, the region of interests (ROIs) are defined (step 2) to quantify the permeability to 20 kDa FITC-dextran and 150 kDa TRITC-dextran. For visualization of the permeability, the fluorescent intensity was normalized to the highest value in the perfusion channel and a lookup table was applied to a concentration range between 0 and 0.125 mg/ml dextran. Scale bars: 200 µm.*

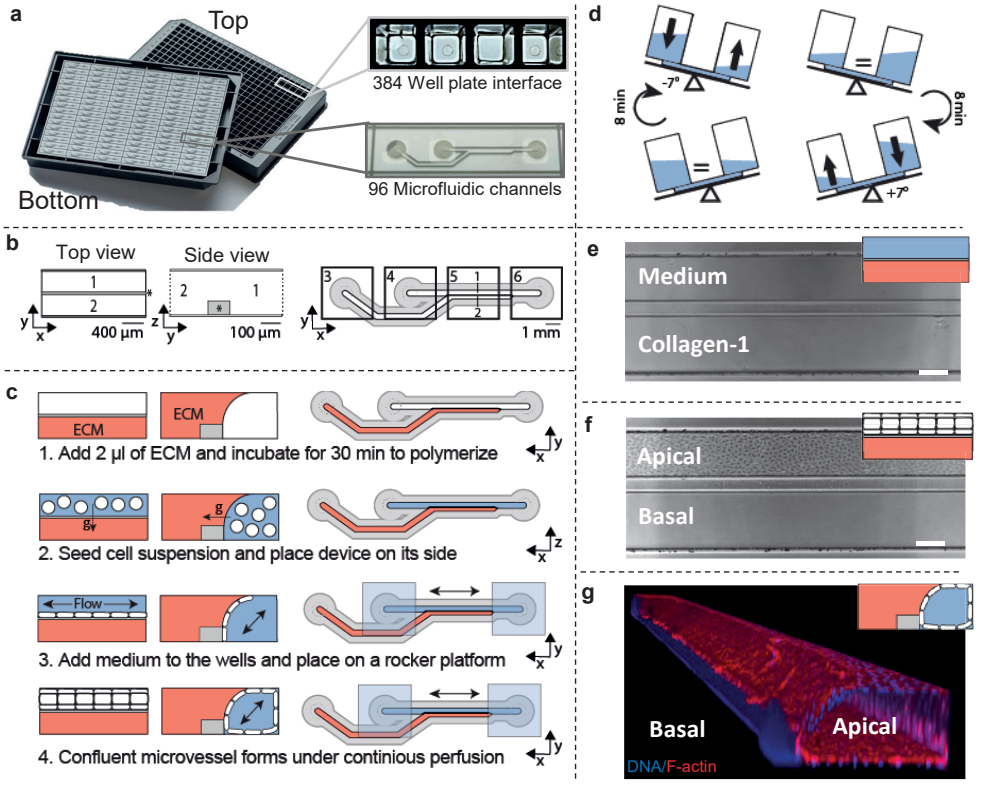
a
Top
Bottom
384 Well plate interface
96 Microfluidic channels
b
Top view
Side view
400 µm
100 µm
1 mm
c
ECM
ECM
1. Add 2 µl of ECM and incubate for 30 min to polymerize
2. Seed cell suspension and place device on its side
Flow
3. Add medium to the wells and place on a rocker platform
4. Confluent microvessel forms under continious perfusion
d
-7°
+7°
8 min
8 min
e
Medium
Collagen-1
f
Apical
Basal
g
Basal
Apical
DNA/F-actin

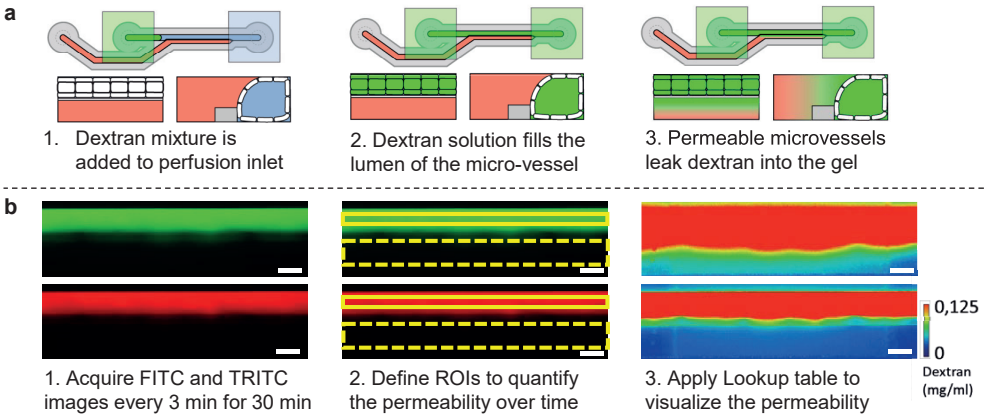
a
1. Dextran mixture is added to perfusion inlet
2. Dextran solution fills the lumen of the micro-vessel
3. Permeable microvessels leak dextran into the gel
b
1. Acquire FITC and TRITC images every 3 min for 30 min
2. Define ROIs to quantify the permeability over time
3. Apply Lookup table to visualize the permeability
0,125
0
Dextran (mg/ml)

the collagen-1 gel. After 7 days, the morphology of the vessel stabilizes, and can be maintained for at least 60 days. After 60 days, the morphology of the microvessels could not be distinguished from 1-week old cultures. After 60 days, the microvessels were still viable but showed invasion into the adjacent collagen gel

Permeability of the microvessels under exposure to different culture media

Diffusion of dextran into the adjacent collagen gel provides a measure for the permeability of the microvessels. *In vivo*, macromolecules above the molecular weight (MW) of albumin (MW>70 kDa) are retained in the lumen, while microvessels are permeable to macromolecules smaller then albumin (MW<70 kDa)[37]. This behavior was simulated by testing the permeability for two different MW dextrans: FITC-Dextran of 20 kDa and TRITC-Dextran of 150 kDa. A mixture of both fluorescent dextrans was added to each perfusion inlet well. This mixture fills into the lumen of the microvessels by passive leveling (Fig. 2a). In the case of a fully impermeable microvessel, the high molecular weight dextran should be retained within the lumen, while for a permeable barrier the dextran diffuses into the gel. Fluorescent images were acquired for 30 minutes with 3 min. interval, yielding a total of 2112 images per permeability assay (Fig. 2b). For quantification, all images were aligned and regions of interest (ROIs) are manually defined. The mean intensity within each ROI is used to calculate the ratio of the fluorescent intensity between the gel and perfusion compartments per time point. The intensity was normalized to the maximum intensity in the perfusion channel and visualized by applying a lookup table (LUT). At the start of the assay (t=0min) all dextran is confined to the lumen of the microvessels (Fig. 3a). Differences in permeability are clearly observed at the end of the assay (t=30 min, Fig. 3b) by the amount of dextran that diffused into the gel.

The permeability of the microvessels was quantified and visualized for three different media compositions: M199, MV2 and Pericyte (PC) medium. After 2 days of culture, 20 kDa dextran diffused into the gel within 30 minutes under all conditions, which indicated that the barrier formation was sub-optimal at this time point (Fig. 3c+d). During the following days, the permeability to 20 kDa and 150 kDa decreased for all

media conditions (Fig. 3c+d). Microvessels cultured in MV2 or PC medium are impermeable for 150 kDa dextran after 7 days, while M199 medium still shows leakage of 150 kDa dextran. Importantly, while MV2 and PC grown vessels appear impermeable for 150 kDa dextran, a slight leakage of 20 kDa was still observed. These results suggest that MV2 medium is the optimal choice to study the barrier integrity of the microvessels in this platform and that the microvessels are comparable to microvessels *in vivo*, where microvessels are permeable to compounds with a MW below 70kDa.

Effect of VEGF on vascular leakage

Vascular endothelial growth factor (VEGF) is an important and well known modulator of vascular permeability *in vitro* [38] and *in vivo* [39]. We investigated the effect of VEGF on the microvessels after 4hrs and 24hrs of exposure. First, the microvessels were cultured for 7 days before removing the growth factors to obtain a proper barrier function. Prior to exposure, the microvessels were growth factor and serum starved overnight. After exposure to VEGF the permeability was quantified by adding the dextran mixture to the lumen of the vessel (Fig. 4a). Although a trend is observed, the permeability that was measured after 4 hours of exposure did not significantly increase. However, after 24 hours the permeability changed significantly. Interestingly, VEGF showed a dose dependent inversion of the effect: 10 ng/mL VEGF showed a significant decrease in permeability compared to control, whereas the highest concentration of 100 ng/mL significantly increased permeability. Another 24-hour exposure including 30 and 50 ng/mL VEGF resulted in a similar response: a significant decrease in permeability at 10 ng/mL VEGF and a significant increase in permeability at 100 ng/mL VEGF (Fig. 4b). To study reversibility of this increased permeability, all media was replaced with MV2 growth media which contained 5% FBS and the complete set of growth factors. It was observed that the permeability of microvessels exposed to 100 ng/mL VEGF returns to control levels after being cultured for 24 hours on MV2 growth media (Fig. 4c). These results show that VEGF modulates the permeability and that this effect is rescued by returning to standard culture conditions.

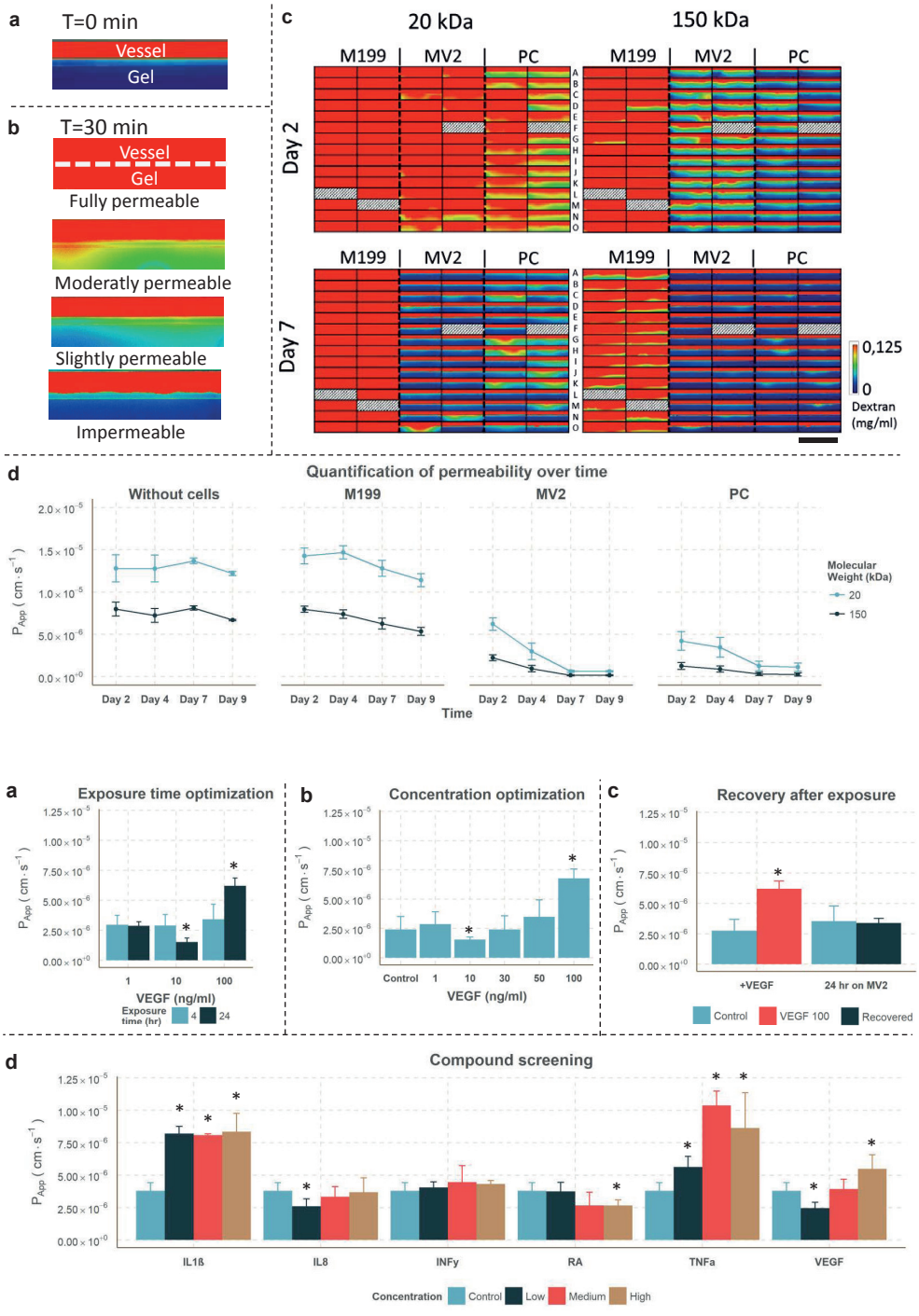
a
T=0 min
Vessel
Gel
b
T=30 min
Vessel
Gel
Fully permeable
Moderatly permeable
Slightly permeable
Impermeable
c
20 kDa
150 kDa
M199
MV2
PC
Day 2
Day 7
0,125
0
Dextran (mg/ml)
d
Quantification of permeability over time
Without cells
M199
MV2
PC
Day 2 Day 4 Day 7 Day 9
Time
Molecular Weight (kDa)
20
150
a
Exposure time optimization
VEGF (ng/ml)
Exposure time (hr)
b
Concentration optimization
Control
c
Recovery after exposure
+VEGF
24 hr on MV2
Control
VEGF 100
Recovered
d
Compound screening
IL1ß
IL8
INFy
RA
TNFa
VEGF
Concentration
Control
Low
Medium
High

◄Figure 3 | Media optimization on microvessels using the permeability assay

(a) *At the start of the assay (t=0 min), the fluorescent dextrans are contained within the microvessel. Scale bar: 200 µm.* **(b)** *After 30 min, the differences in permeability are clearly visible: the dextran fills the gel in case of a completely permeable microvessel, while an impermeable vessel retains the dextran within the lumen of the vessel. The dotted line indicates the position of the cell barrier. Scale bar: 200 µm.* **(c)** *Visualization of dextran diffusion after 30 minutes for an array of 86 microvessels with three different culture conditions (M199 medium=M199, MV2 medium=MV2, Pericyte medium=PC). Excluded vessels due improper barrier formation or gel seeding are indicated with a diagonal hatch pattern. Scale bar: 2 mm.* **(d)** *Quantification of the permeability over different days for M199 (n=28), MV2 (n=29) and PC (n=29). Data is presented as mean±SD.*

◄Figure 4 | Permeability to 20 kDa dextran after exposures

(a) *Quantification of the permeability to 20 kDa FITC-dextran after 4 or 24 hr exposure to different VEGF concentrations (n≥5).* **(b)** *Concentration optimization experiment after 24 hr exposure to VEGF, including 30 ng/ml and 50 ng/ml (Conditions n≥11, gel n=6)* **(c)** *Recovery of VEGF stimulated microvessels, where VEGF was removed (n=5) and replaced with MV2 growth media. 24 hours later the permeability of the recovered microvessels was not significant different to unexposed microvessels (n=62).* **(d)** *Permeability after 24 hr exposure to IL1ß, IL8, INFγ, RA, TNFα and VEGF in 3 different concentrations. All data is presented as mean±SD. Asterisks indicate a P-value ≤ 0.05.*

Compound screening for induced vascular leakage

Besides VEGF, more cytokines that have a known influence on the endothelial permeability. A range of cytokines which are involved in inflammation have been assessed, including Interleukin 1 beta (IL1β), Interleukin 8 (IL8), Interferon gamma (INFγ), Tumor Necrosis Factor alpha (TNFα). Retinoic acid (RA) was included since it decreases the permeability of endothelium[40] by upregulating tight junction markers, which are expressed in the blood-brain-barrier[41]. VEGF was added as positive control. All compounds were assessed for three concentrations[35]: 1, 10 and 100 ng/mL for IL8, INFγ, RA and TNFα; 10, 100 and 200 ng/mL for VEGF and 0.2, 2 and 20 ng/mL for IL1β.

IL1β and TNFα treatment resulted in a significantly increased permeability. RA significantly reduced the permeability at high concentrations (Fig. 4d), similar to the effect of 10 ng/mL VEGF. INFγ did not induce a significant change in permeability. These results show that the microvessels have a dose dependent response to cytokines that are known to change the permeability *in vitro* as well as *in vivo*.

The microvessels exposed to TNFα and VEGF were fixed and stained for DNA (Hoechst), VE-cadherin (antibody) and F-actin (phalloidin) (Fig. 5). The vessels treated with TNFα show a decreased expression of VE-cadherin and decreased alignment of the actin fibers. At the two highest doses, large perforations in the monolayer could be distinguished, which correlates nicely with the permeability values. TNFα-treated microvessels show actin stress fibers in the direction of the elongated cell axis in combination with a reduction of VE-cadherin expression. In contrast, microvessels exposed to VEGF do show an increased permeability, but the expression of VE-cadherin is not affected. This shows that in this platform, the permeability assay and immunocytofluorescent staining can be easily combined to get a more comprehensive overview of the mechanism of action.

Discussion

Microfluidics has a clear potential to add physiological relevant cues to vasculature *in vitro* (e.g. perfusion, adherence to an ECM)[22,42], and there are various examples of

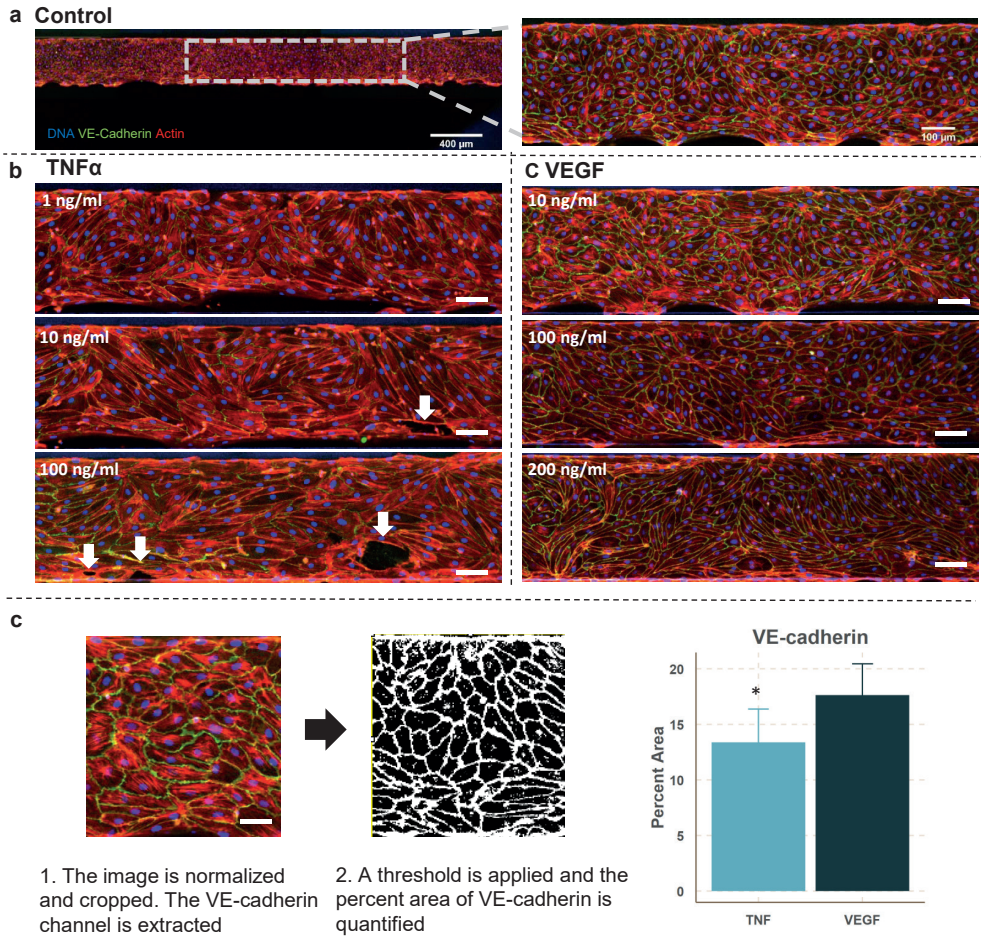

Figure 5 | Stained microvessels after 24 hr exposure to TNFα. or VEGF

(a) *The microvessels are stained for VE-cadherin (green), F-actin (red and the nuclei (blue) and the bottom of every microvessel was imaged using confocal microscopy, with a close-up to highlight the typical cobblestone appearance with uniform expression of VE-cadherin around the cell borders.* **(b)** *Stained microvessels after exposure to different concentrations of TNFα. All microvessels show a decreased expression of VE-cadherin and induction of actin stress fibers compared to control. Arrows indicate the large perforations in the microvessels. Scale bars are 100 µm.* **(c)** *Stained microvessels after exposure to different concentrations of VEGF. Scale bar is 100 µm.* **(d)** *Difference in VE-Cadherin between TNFα exposed and VEGF exposed microvessels. Data is presented as mean±SD*

the culture of 3D, perfusable microvessels in microfluidic platforms. However, unlike other microfluidic platforms which demonstrate platforms with a few replicates per device, this is the first platform that has the required throughput to be used as an robust screening assay. Furthermore, it is usable in a general cell culture laboratory, as the microtiter format is compatible with almost all laboratory equipment, including multichannel pipettes and automated microscopes. Also, since flow is induced by passive leveling instead of pumps, contamination and handling issues are minimized, while scalability and throughput is ensured. The microvessels can be maintained over prolonged periods of time and a robust assay has been developed to quantify the permeability in real-time.

Compared to traditional 2D-based assays, this platform has a comparable throughput (n=96) while it has several advantages. First, 2D-based macromolecular diffusion assays are based on horizontally stacked membranes, which limits the possibility to image leakage in real-time. In contrast, the permeability assay presented here allows correlating real-time permeability with phenotypic screening, and the permeability can be determined multiple times over the course of days or weeks. This can reveal interesting differences, as for example morphologically identical microvessels show a different permeability (Supplementary Fig. 2). Also, immunocytofluorescent stainings can be easily combined with the permeability assay to get a more comprehensive insight into the mechanisms behind induced permeability, which adds a valuable tool to the high-content imaging toolbox. Another advantage over 2D-based assays is the possibility of patterning of gels and ECMs. By providing the cells a soft matrix, the gene expression and morphology comes closer to of that *in vivo*[9].

The robustness and throughput of this method is clearly illustrated in Fig. 3. In principle, 96 microvessels can be formed that have a significant barrier in 7 days. The different culture media clearly show a difference in barrier function of the microvessels. The serum concentration in each culture media is different. This might explain the observed differences, as serum contains factors that module the permeability. Under optimal culture conditions, our results show that the microvessels have a size-se-

lective permeability: 150 kDa TRITC-Dextran is confined to the lumen, while 20 kDa FITC-Dextran diffused into the interstitial space. The permeability value we observed are comparable to vasculature *in vivo*[37]. Furthermore, it is shown that microvessels *in vivo* have shown a size selective permeability[43]. Although a range of literature reports have created perfused vasculature in microfluidic culture platforms prior to this publication only very few have convincingly demonstrated impermeability to high molecular weight compounds[11]and none of them have shown this throughput and robustness over time.

Inducing perfusion by passive leveling results in a bidirectional, oscillating flow, and the microvessels is this platform are periodically exposed to significant levels of shear (5 dyne/cm^2) right after the rocker position has been changed. We did not observe alignment of the endothelial cells to the flow direction, which could be due the absence of continuous, unidirectional flow. *In vivo*, similar-sized venules are exposed shear levels between 1 to 5 dyne/cm^2. It is shown *in vitro* that exposure to unidirectional flow in combination with high levels of shear (7-10 dyne/cm^2)[44,45] decreases the permeability of endothelial monolayers. Nonetheless, our experiment show that the microvessels are still able to form a significant barrier function with bi-directional flow and lower shear. We aim to compare the effect between bidirectional and unidirectional flow with various levels and durations of shear stress on the permeability of the microvessels.

In our experiments, collagen type I was used as matrix for cells to adhere on. Interestingly, it is shown that collagen type I and IV promote angiogenesis and tube formation in other in vitro platforms, while laminins stabilize the endothelium[46]. However, the microvessels in this platform did not show any invasive behavior or angiogenic sprouting into the collagen. This suggests that the endothelial cells are in a more quiescent state than a proliferative, invasive state. However, we have shown that when stimulated with right combination of angiogenic factors on the basal side, the microvessels are able to form angiogenic sprouts into the collagen-I gel [47]. As this platform allows the integration of different ECMs or ECM-derived components (e.g.

laminins or different types of collagen), it will be a valuable tool to decipher the role of ECM and proteins in the stabilization and maturation of vasculature.

The inflammatory cytokines TNFα and IL1β both significantly increased the permeability of our microvessels, an effect that is extensively described *in vitro* [35,48-50] and *in vivo* [51,52]. INFγ exposure did not result in a significant change in permeability, which is also shown in impedance assays[35]. The response to VEGF is different from other *in vitro* assays. In traditional membrane based studies, VEGF linearly increases the permeability of the monolayer[38,49], but our results show a biphasic response to VEGF exposure. The barrier protective effect of 10 ng/mL VEGF is shown by one other study, were it is contributed to the induction of cAMP[53]. cAMP is linked to barrier protective properties and explains the reduction in permeability[54]. Future studies will include the characterization of the effect of multiple cytokines or the combination of cytokines with inhibitors to elucidate the most important pathways that induce or prevent a change in permeability in this model.

A standardized platform like the one presented here will contribute to the transition from static, membrane-based, 2D culture techniques to more physiological relevant 3D culture methods. This will increase the efficiency of pre-clinical testing and validation of new lead compounds. In future work, the flexibility of the platform can be further leveraged by including other relevant cell types found in the vascular microenvironment. This allows the study of for example the detachment of pericytes from the vasculature, which is an important hallmark in for example rarefaction[1]. A more physiologically relevant *in vitro* model of vasculature will help to elucidate the key mechanisms behind the onset and progression of these and other diseases.

Conclusion

We developed and optimized a robust, high-throughput permeability assay to assess the barrier integrity of three dimensional, perfusable microvessels in high numbers (up to 96 per plate) against a collagen-1 matrix. We have shown that the microvessels have a size selective permeability which can be correlated with *in vivo* data. The

permeability is influenced after exposure to cytokines which are involved in inflammation. The throughput and compatibility of the platform as well as the availability of tailored assays make the platform ready for adoption by end-users in vascular biology.

Acknowledgements

We thank Angiocrine for the kind gift of VeraVec HUVEC cells.

Author Contribution

VD, AH, H.L and. S.J.T performed or planned the experiments. V.D. and P.V. wrote the manuscript with input from all authors. P.V. and T.H. supervised all aspects of the work.

Sources of funding

V. van Duinen was partially financially supported by the VIRGO consortium, which is funded by the Netherlands Genomics Initiative and by the Dutch Government (FES0908). S.J.T., A.H., P.V., T.H. and H.L. received funding from the European Union's Horizon 2020 research and innovation programs SysMedPD (No. 668738), Adapted (No. 115975), European Union's FP7 program Campac (No. 602783) and Eurostars program HepaPlate (ESTAR16107); J. van Gils received funding from the Netherlands Heart Foundation (2013T127).

Disclosures

V. van Duinen, J.M van Gils and A.J. van Zonneveld declare no potential conflict of interest. A van den Heuvel and H.L Lanz are employees of Mimetas BV. S.J. Trietsch, P. Vulto and T. Hankemeier are shareholders in Mimetas BV.

References

1 Schrimpf, C., Teebken, O. E., Wilhelmi, M. & Duffield, J. S. The role of pericyte detachment in vascular rarefaction. *J Vasc Res* **51**, 247-258, doi:10.1159/000365149 (2014).

2 Iadecola, C. The pathobiology of vascular dementia. *Neuron* **80**, 844-866, doi:10.1016/j.neuron.2013.10.008 (2013).

3 Candelario-Jalil, E. *et al.* Matrix metalloproteinases are associated with increased blood-brain barrier opening in vascular cognitive impairment. *Stroke* **42**, 1345-1350, doi:10.1161/STROKEAHA.110.600825 (2011).

4 Rosenberg, G. A. Blood-Brain Barrier Permeability in Aging and Alzheimer's Disease. *J Prev Alzheimers Dis* **1**, 138-139, doi:10.14283/jpad.2014.25 (2014).

5 Kook, S. Y., Seok Hong, H., Moon, M. & Mook-Jung, I. Disruption of blood-brain barrier in Alzheimer disease pathogenesis. *Tissue Barriers* **1**, e23993, doi:10.4161/tisb.23993 (2013).

6 Huveneers, S., Daemen, M. J. & Hordijk, P. L. Between Rho(k) and a hard place: the relation between vessel wall stiffness, endothelial contractility, and cardiovascular disease. *Circ Res* **116**, 895-908, doi:10.1161/CIRCRESAHA.116.305720 (2015).

7 Rozenberg, I. *et al.* Histamine H1 receptor promotes atherosclerotic lesion formation by increasing vascular permeability for low-density lipoproteins. *Arterioscler Thromb Vasc Biol* **30**, 923-930, doi:10.1161/ATVBAHA.109.201079 (2010).

8 Camare, C., Pucelle, M., Negre-Salvayre, A. & Salvayre, R. Angiogenesis in the atherosclerotic plaque. *Redox Biol* **12**, 18-34, doi:10.1016/j.redox.2017.01.007 (2017).

9 Griffith, L. G. & Swartz, M. A. Capturing complex 3D tissue physiology in vitro. *Nature Reviews Molecular Cell Biology* **7**, 211-224 (2006).

10 Zheng, Y. *et al.* In vitro microvessels for the study of angiogenesis and thrombosis. *Proc Natl Acad Sci U S A* **109**, 9342-9347, doi:10.1073/pnas.1201240109 (2012).

11 Kim, J. *et al.* Engineering of a Biomimetic Pericyte-Covered 3D Microvascular Network. *PLoS One* **10**, e0133880, doi:10.1371/journal.pone.0133880 (2015).

12 Tourovskaia, A., Fauver, M., Kramer, G., Simonson, S. & Neumann, T. Tissue-engineered microenvironment systems for modeling human vasculature. *Exp Biol Med (Maywood)* **239**, 1264-1271, doi:10.1177/1535370214539228 (2014).

13 Bischel, L. L., Young, E. W., Mader, B. R. & Beebe, D. J. Tubeless microfluidic angiogenesis assay with three-dimensional endothelial-lined microvessels. *Biomaterials* **34**, 1471-1477, doi:10.1016/j.biomaterials.2012.11.005 (2013).

14 Schimek, K. *et al.* Integrating biological vasculature into a multi-organ-chip microsystem. *Lab Chip* **13**, 3588-3598, doi:10.1039/c3lc50217a (2013).

15 Hsu, Y. H., Moya, M. L., Hughes, C. C., George, S. C. & Lee, A. P. A microfluidic platform for generating large-scale nearly identical human microphysiological vascularized tissue arrays. *Lab Chip* **13**, 2990-2998, doi:10.1039/c3lc50424g (2013).

16 Lee, H., Kim, S., Chung, M., Kim, J. H. & Jeon, N. L. A bioengineered array of 3D microvessels for vascular permeability assay. *Microvasc Res* **91**, 90-98, doi:10.1016/j.mvr.2013.12.001 (2014).

17 Kim, S., Lee, H., Chung, M. & Jeon, N. L. Engineering of functional, perfusable 3D microvascular networks on a chip. *Lab Chip* **13**, 1489-1500, doi:10.1039/c3lc41320a (2013).

18 Junaid, A., Mashaghi, A., Hankemeier, T. & Vulto, P. An end-user perspective on Organ-on-a-Chip: Assays and usability aspects. *Current Opinion in Biomedical Engineering* **1**, 15-22, doi:10.1016/j.cobme.2017.02.002 (2017).

19 Berthier, E., Young, E. W. & Beebe, D. Engineers are from PDMS-land, Biologists are from Polystyrenia. *Lab Chip* **12**, 1224-1237, doi:10.1039/c2lc20982a (2012).

20 Shin, Y. *et al.* Microfluidic assay for simultaneous culture of multiple cell types on surfaces or within hydrogels. *Nature Protocols* **7**, 1247-1259 (2012).

21 Chrobak, K. M., Potter, D. R. & Tien, J. Formation of perfused, functional microvascular tubes in vitro. *Microvasc Res* **71**, 185-196, doi:10.1016/j.mvr.2006.02.005 (2006).

22 Wong, K. H., Chan, J. M., Kamm, R. D. & Tien, J. Microfluidic models of vascular functions. *Annu Rev Biomed Eng* **14**, 205-230, doi:10.1146/annurev-bioeng-071811-150052 (2012).

23 Haase, K. & Kamm, R. D. Advances in on-chip vascularization. *Regen Med* **12**, 285-302, doi:10.2217/rme-2016-0152 (2017).

24 Trietsch, S. J., Israels, G. D., Joore, J., Hankemeier, T. & Vulto, P. Microfluidic titer plate for stratified 3D cell culture. *Lab Chip* **13**, 3548-3554, doi:10.1039/c3lc50210d (2013).

25 Wevers, N. R. *et al.* High-throughput compound evaluation on 3D networks of neurons and glia in a microfluidic platform. *Sci Rep* **6**, 38856, doi:10.1038/srep38856 (2016).

26 Moreno, E. L. *et al.* Differentiation of neuroepithelial stem cells into functional dopaminergic neurons in 3D microfluidic cell culture. *Lab Chip* **15**, 2419-2428, doi:10.1039/c5lc00180c (2015).

27 Trietsch, S. J. *et al.* Membrane-free culture and real-time barrier integrity assessment of perfused intestinal epithelium tubes. *Nat Commun* **8**, 262, doi:10.1038/s41467-017-00259-3 (2017).

28 Jang, M., Neuzil, P., Volk, T., Manz, A. & Kleber, A. On-chip three-dimensional cell culture in phaseguides improves hepatocyte functions in vitro. *Biomicrofluidics* **9**, 034113, doi:10.1063/1.4922863 (2015).

29 Wen, H., Hao, J. & Li, S. K. Characterization of human sclera barrier properties for transscleral delivery of bevacizumab and ranibizumab. *J Pharm Sci* **102**, 892-903, doi:10.1002/jps.23387 (2013).

30 Schindelin, J. *et al.* Fiji: an open-source platform for biological-image analysis. *Nat Methods* **9**, 676-682, doi:10.1038/nmeth.2019 (2012).

31 Palm, K., Luthman, K., Ungell, A. L., Strandlund, G. & Artursson, P. Correlation of drug absorption with molecular surface properties. *J Pharm Sci* **85**, 32-39, doi:10.1021/js950285r (1996).

32 Ungell, A.-L. & Artursson, P. An Overview of Caco-2 and Alternatives for Prediction of Intestinal Drug Transport and Absorption. **40**, 133-159, doi:10.1002/9783527623860.ch7 (2008).

33 Kihara, T., Ito, J. & Miyake, J. Measurement of biomolecular diffusion in extracellular matrix condensed by fibroblasts using fluorescence correlation spectroscopy. *PLoS One* **8**, e82382, doi:10.1371/journal.pone.0082382 (2013).

34 Ramanujan, S. *et al.* Diffusion and convection in collagen gels: implications for transport in the tumor interstitium. *Biophys J* **83**, 1650-1660, doi:10.1016/S0006-3495(02)73933-7 (2002).

35 Kustermann, S. *et al.* A real-time impedance-based screening assay for drug-induced vascular leakage. *Toxicol Sci* **138**, 333-343, doi:10.1093/toxsci/kft336 (2014).

36 Yildirim, E. *et al.* Phaseguides as tunable passive microvalves for liquid routing in complex microfluidic networks. *Lab Chip* **14**, 3334-3340, doi:10.1039/c4lc00261j (2014).

37 Yuan, W., Lv, Y., Zeng, M. & Fu, B. M. Non-invasive measurement of solute permeability in cerebral microvessels of the rat. *Microvasc Res* **77**, 166-173, doi:10.1016/j.mvr.2008.08.004 (2009).

38 Lal, B. K., Varma, S., Pappas, P. J., Hobson, R. W., 2nd & Duran, W. N. VEGF increases permeability of the endothelial cell monolayer by activation of PKB/akt, endothelial nitric-oxide synthase, and MAP kinase pathways. *Microvasc Res* **62**, 252-262, doi:10.1006/mvre.2001.2338 (2001).

39 Fu, B. M. & Shen, S. Acute VEGF effect on solute permeability of mammalian microvessels in vivo. *Microvasc Res* **68**, 51-62, doi:10.1016/j.mvr.2004.03.004 (2004).

40 Pal, S. *et al.* Retinoic acid selectively inhibits the vascular permeabilizing effect of VPF/VEGF, an early step in the angiogenic cascade. *Microvasc Res* **60**, 112-120, doi:10.1006/mvre.2000.2246 (2000).

41 Lippmann, E. S., Al-Ahmad, A., Azarin, S. M., Palecek, S. P. & Shusta, E. V. A retinoic acid-enhanced, multicellular human blood-brain barrier model derived from stem cell sources. *Sci Rep* **4**, 4160, doi:10.1038/srep04160 (2014).

42 van Duinen, V., Trietsch, S. J., Joore, J., Vulto, P. & Hankemeier, T. Microfluidic 3D cell culture: from tools to tissue models. *Curr Opin Biotechnol* **35**, 118-126, doi:10.1016/j.copbio.2015.05.002 (2015).

43 Egawa, G. *et al.* Intravital analysis of vascular permeability in mice using two-photon microscopy. *Sci Rep* **3**, 1932, doi:10.1038/srep01932 (2013).

44 Cucullo, L., Hossain, M., Puvenna, V., Marchi, N. & Janigro, D. The role of shear stress in Blood-Brain Barrier endothelial physiology. *BMC Neurosci* **12**, 40, doi:10.1186/1471-2202-12-40 (2011).

45 Cucullo, L. *et al.* A new dynamic in vitro model for the multidimensional study of astrocyte–endothelial cell interactions at the blood–brain barrier. *Brain Research* **951**, 243-254, doi:10.1016/s0006-8993(02)03167-0 (2002).

46 Davis, G. E. & Senger, D. R. Endothelial extracellular matrix: biosynthesis, remodeling, and functions during vascular morphogenesis and neovessel stabilization. *Circ Res* **97**, 1093-1107, doi:10.1161/01.RES.0000191547.64391.e3 (2005).

47 Van Duinen, V., Trietsch, S. J., Van Zonneveld, A. J., Hankemeier, T. & P., V. in *20th International Conference on Miniaturized Systems for Chemistry and Life Sciences, MicroTAS.* (2016).

48 Friedl, J. *et al.* Induction of permeability across endothelial cell monolayers by tumor necrosis factor (TNF) occurs via a tissue factor-dependent mechanism: relationship between the procoagulant and permeability effects of TNF. *Blood* **100**, 1334-1339 (2002).

49 Sheikpranbabu, S. *et al.* Silver nanoparticles inhibit VEGF-and IL-1beta-induced vascular permeability via Src dependent pathway in porcine retinal endothelial cells. *J Nanobiotechnology* **7**, 8, doi:10.1186/1477-3155-7-8 (2009).

50 Nooteboom, A., Hendriks, T., Otteholler, I. & van der Linden, C. J. Permeability characteristics of human endothelial monolayers seeded on different extracellular matrix proteins. *Mediators Inflamm* **9**, 235-241, doi:10.1080/09629350020025755 (2000).

51 Bamforth, S. D., Lightman, S. & Greenwood, J. The effect of TNF-alpha and IL-6 on the permeability of the rat blood-retinal barrier in vivo. *Acta Neuropathol* **91**, 624-632 (1996).

52 Worrall, N. K. *et al.* TNF-alpha causes reversible in vivo systemic vascular barrier dysfunction via NO-dependent and -independent mechanisms. *Am J Physiol* **273**, H2565-2574 (1997).

53 Mirzapoiazova, T., Kolosova, I., Usatyuk, P. V., Natarajan, V. & Verin, A. D. Diverse effects of vascular endothelial growth factor on human pulmonary endothelial barrier and migration. *Am J Physiol Lung Cell Mol Physiol* **291**, L718-724, doi:10.1152/ajplung.00014.2006 (2006).

54 Waschke, J., Drenckhahn, D., Adamson, R. H., Barth, H. & Curry, F. E. cAMP protects endothelial barrier functions by preventing Rac-1 inhibition. *Am J Physiol Heart Circ Physiol* **287**, H2427-2433, doi:10.1152/ajpheart.00556.2004 (2004).

Supplementary figures

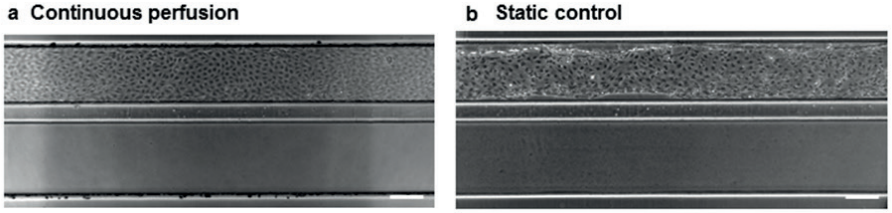

Supplementary Figure 1 | Culture of microvessels with and without perfusion after 7 days

(a) *Microvessels cultured for 7 days on rocker platform grow as a confluent monolayer against all surfaces. No contraction is observed and all cells are viable.* **(b)** *Without perfusion, microvessels shows severe contraction after 7 days of culture and non-viable cells are visible. Scale bars: 200 µm.*

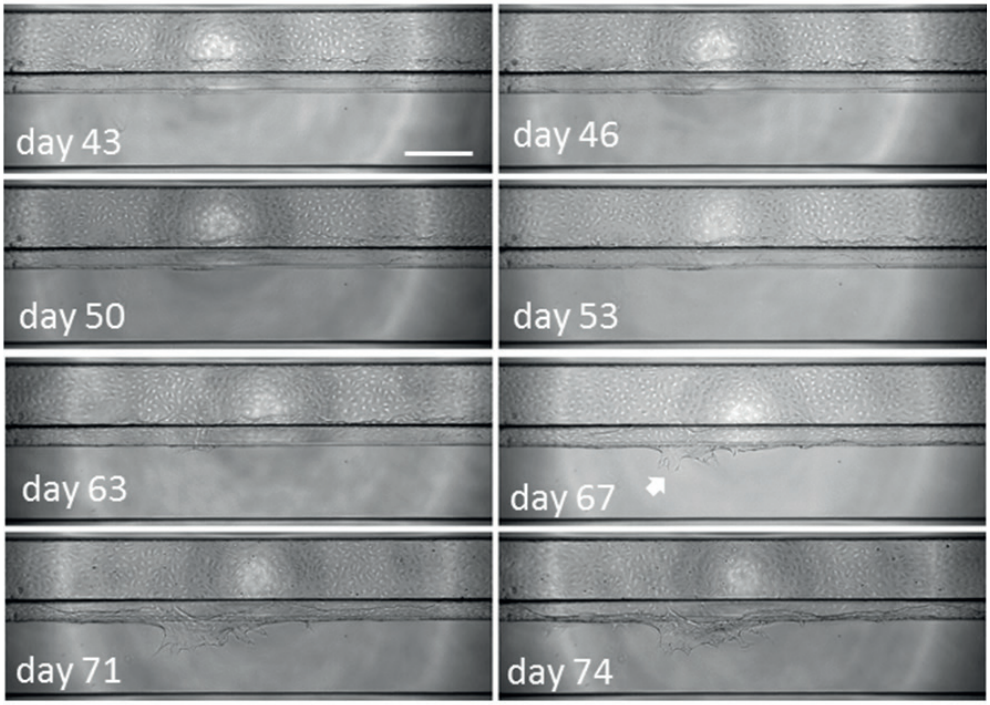

Supplementary Figure 2 | Prolonged culture of microvessels.

Microvessels show a stable morphology for up to around 60 days. At day 67, cells start to invade the collagen matrix and 2D outgrowth is visible (arrowhead). Scale bar: 400 µm.

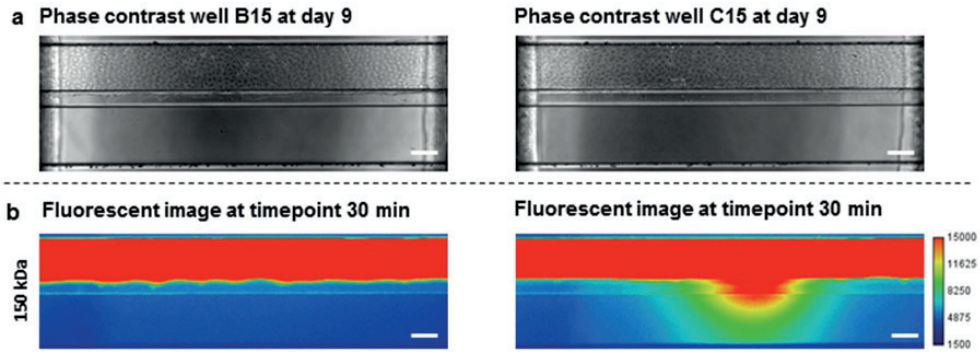

Supplementary Figure 3 | Morphological similar tubes show differences in permeability

(a) *Two microvessels after 9 days of culture on MV2 medium, which appear to be identical when imaged with phase contrast.* **(b)** *The same microvessels show clear differences in permeability when performing a permeability assay. While the left vessel is impermeable for 150 kDa, the right microvessel is permeable for 150 kDa dextran and a major point of permeability can be identified. Scale bars: 200 µm.*

CHAPTER

4

Perfused 3D angiogenic sprouting in a high-throughput in vitro platform

V van Duinen, D Zhu, C Ramakers, AJ van Zonneveld, P Vulto, T Hankemeier

Angiogenesis 22 (1), 157-165. (2018)

Abstact

Angiogenic sprouting, the growth of new blood vessels from pre-existing vessels, is orchestrated by cues from within the cellular microenvironment, such as biochemical gradients and perfusion. However, many of these cues are missing in current *in vitro* models of angiogenic sprouting. We here describe an *in vitro* platform that integrates both perfusion and the generation of stable biomolecular gradients and demonstrate its potential to study more physiologically relevant angiogenic sprouting and microvascular stabilization.

The platform consists of an array of 40 individually addressable microfluidic units that enable the culture of perfused microvessels against a three dimensional collagen-1 matrix. Upon the introduction of a gradient of pro-angiogenic factors, the ECs differentiated into tip cells that invaded the matrix. Continuous exposure resulted in continuous migration and the formation of lumen by stalk cells. A combination of vascular endothelial growth factor-165 (VEGF-165), phorbol 12-myristate 13-acetate (PMA) and sphingosine-1-Phospate (S1P) was the most optimal cocktail to trigger robust, directional angiogenesis with S1P being crucial for the guidance and repetitive sprout formation.

Prolonged exposure forces the angiogenic sprouts to anastemose through the collagen to the other channel. This resulted in remodeling of the angiogenic sprouts within the collagen: some angiogenic sprouts that did not connect retracted and degraded (pruning), while connect sprouts remained. Furthermore, perfusion with 150 kDa FITC-Dextran revealed that while the angiogenic sprouts were initially leaky, once they were connected they became leak tight. This demonstrating that once connection occurred, the sprouts matured and suggests that perfusion can act as an important survival and stabilization factor for the angiogenic microvessels.

The robustness of this platform in combination with the possibility to include a more physiological relevant three dimensional microenvironment, makes our platform uniquely suited to study angiogenesis *in vitro*.

Introduction

The loss of vascular integrity plays a rate-limiting role in the onset and progression of diseases such as arteriosclerosis, cancer and conditions such as chronic inflammation and ischemia[1,2]. Therefore, a detailed knowledge of the mechanisms of microvascular loss or the formation of novel vascular structures such as those generated by angiogenesis, is of major importance.

Endothelial cells (ECs) respond to pro-angiogenic stimuli by differentiating into characteristic phenotypes: tip, stalk and phalanx cells[3-6]. Each of these phenotypes have a specific function in the development and maturation of the newly formed vasculature, and need to be tightly coordinated and regulated in order to achieve functional, lumenized vascular networks. After formation of a pre-mature vascular network, perfusion of the newly formed capillary initiates the final phase of angiogenesis: stabilization of the vascular network that increase the adherence junctions, optimization by pruning of the non-functional sprouts, followed by pericyte attraction that maturate the vascular network[7-11]

In vitro models are essential to study the angiogenesis in a defined and well-controlled environment. Two dimensional *in vitro* models allow the study of fundamental EC behavior in high-throughput, such as migration and proliferation[12]. However, since these models lack a more physiologic, three-dimensional environment, the endothelial cells fail to show many of the typical hallmarks of endothelial cells during angiogenesis *in vivo*[13], such as lumen formation and differentiation into tip- and stalk cells. 3D cell culture models with EC growing within a matrix such as fibrin displays a more physiological relevance, as ECs are able to degrade the extracellular matrix, forming lumen and show anastomosis between adjacent sprouts[14,15]. However, as such 3D cell culture models have EC mixed with an extracellular matrix, the formed lumen are not accessible or perfusable. Furthermore, possibilities to apply a stable gradient of growth factors to direct the forming capillaries are limited.

Microfluidic devices have micrometer-sized channels that enable spatial control over cells and matrices and allow the incorporation of important biological parameters

such as flow[16] and spatial-temporal gradients[17], and is an important technique to facilitate 3D-cell culture models aimed to more faithfully mimic tissue architecture[18]. For instance, a number of microfluidic devices for microvascular modeling have been presented that allow lumen perfusion[19-30]. For an increasing number of research laboratories that study angiogenesis, microfluidic platforms are becoming the method of choice (table 1)[31]. However, most microfluidic assays are limited in terms of scalability and are hardly standardized[32]. Many microfluidic devices need to be manufactured manually before use, which introduces user-to-user variability[33]. Furthermore, many prototypes show limited throughput per assay ($n<8$)[18,20,34] and may depend on the use of a pump which further reduces the scalability of these platforms.

Here, we report a standardized, high-throughput culture platform to study angiogenesis. The platform consists of an array of 40 microfluidic devices, integrated underneath a 384-well plate. This format is compatible with standard (high content) imaging equipment. It enables the culture of individually addressable, perfusable microvessels against a patterned, three-dimensional matrix or hydrogel. To eliminate the need for pumps while increasing the robustness and scalability, passive leveling is used as a source of flow. Within this platform, reproducible gradients can be formed and maintained for multiple days. Since gradients and perfusion are two important cues during the initial sprouting and the stabilization phase in angiogenesis[3,35], the integration of these cues in our novel platform technology make our model uniquely suited to perform physiologically relevant studies on the formation and regression of the microvasculature *in vitro*.

Methods

Cell Culture

HUVEC-VeraVec™ human endothelial cells (Angiocrine Biosciences, hVera101) were cultured in T75 flasks (Nunc™ Easyflask, Sigma F7552) with endothelial Cell Growth Medium MV2 (Promocell, C-22022) and used at P3 till P9. Media was replaced three times a week. Cells tested negative for mycoplasma. MV2 endothelial cell Growth

Assay		Strength	Weakness	Ref
2D	Scratch	+ *Easy to perform* + *Easy to quantify*	– *Lacks soft substrate for the cells* – *Migration is in 2D*	[12]
	Tube formation	+ *Cells adhere to soft substrate* + *Self-organization into 3D-like cords* + *Reasonable throughput* + *Tools are available for quantification*	– *No distinct tip/stalk cell phenotype* – *Basement membrane extracts contain significant levels of growth factors and have a high batch-to-batch variability* – *Limited tube survival (<2 days)* – *High use of reagents compared to microfluidic assays* – *Lumens not accessible nor perfusable*	[13]
3D	Spheroid	+ *Cells grow in 3D in a soft supportive matrix* + *Endothelial cells differentiate into tip and stalk cells* + *Clear lumen formation* + *Fusion of sprouts is observed* + *Laser dissection allows capture of cells* + *Tools available to quantify the angiogenic sprouts*	– *No spatial control over gradients* – *Higher use of reagents compared to microfluidic assays* – *Spheroids are randomly distributed throughout gel or matrix* – *Lumens are not accessible nor perfusable*	[14, 15, 40]
	Microfluidic	+ *Biochemical gradients can be created and maintained* + *Lumen formation is closer to in vivo* + *Angiogenic sprouts can be perfused* + *Spatial control over multiple cells (e.g. fibroblasts, pericytes)*	– *Some devices require for pumps to supply flow and maintain gradients.* – *Handling and scalability issues due incompatibility with other equipment.* – *Some devices need to be manufactured by the end-user* – *Biocompatibility of the used materials* – *Lack of standardization* – *Limited possibilities to extract subset of cells*	[18-30, 32, 33]

Table 1 | Comparison of in vitro assays to study angiogenesis

Medium (Promocell, C-22022). All cell culture was performed in a humidified incubator at 37°C and 5% CO_2.

Microfluidic cell culture

3Lane microfluidic titerplates (MIMETAS OrganoPlates 4003-400B) were used for all microfluidic cell culture. Before gel seeding, every center well was filled with 50 µL hanks balanced salt solution (HBSS) to provide optical clarity and prevention of gel dehydration. Collagen type I (R&D systems, 3447-020-01) was used as 3D scaffold. A stock solution of 5 mg/mL rat tail collagen type I was neutralized with 10% 37 g/L $NaHCO_3$ (Sigma, S5761) and 10% 1 M HEPES buffer (Gibco, 15630-056) to obtain a concentration of 4 mg/mL. The neutralized collagen was kept on ice until use and used within 30 min. Using a repeater pipette, 2 µL of the neutralized collagen was added into the inlet of each gel channel. To polymerize the collagen, the device was incubated for 20 minutes at 37°C, 5% CO_2. After incubation, the device was removed from the incubator and kept sterile at room temperature right before cell loading. Endothelial cells were dissociated, pelleted and suspended in MV2 medium in a concentration of $2{\cdot}10^7$ cells/mL. 2 µL of the cell suspension was dispensed into the perfusion inlet and incubated for 45 min at 37°C, 5% CO_2. After the cells attached to the bottom of the perfusion channel, 50 µL of medium was added in the perfusion inlet and outlet wells and the plates were placed on an interval rocker platform for continuous perfusion. (Perfusion rocker, MIMETAS). The rocker was set at a 7-degree inclination and 8 minutes cycle time. Medium was refreshed three times a week.

Stimulation with angiogenic factors

Microvessels were first cultured for 3 days before any gradients of growth factors were applied. Growth factors were replaced every 2-3 days. Stock solutions were prepared as following: 50 ug/mL murine VEGF in MiliQ water (Preprotech, 450-32), 20 ng/mL bFGF in water (Peprotech, 100-18B), 1 mM Spingosine-1-Phosphate (Sigma, S9666) in 5% 1M HCl, 95% DMSO and 2 ug/mL PMA (Sigma, P1585) in 1% DMSO. Angiogenic factors were diluted in MV2 culture medium and used in the following

concentrations: 50 ng/mL for VEGF, 50 ng/mL for bFGF, 2 ng/mL for PMA and 500 nM for S1P.

Sprout permeability visualization

Angiogenic sprouts were stimulated with VEGF+bFGF+PMA+S1P for 9 days. At day 4 and day 9 after stimulation, 50 µL of a 150 kDa TRITC-Dextran (Sigma, 48946) solution (0.5 mg/mL in MV2 culture media) was added to the perfusion inlet well and time-lapse images were acquired at 1 minute intervals using the 10X objective.

Immunocytofluorescent staining

During all steps of the immunofluorescent staining, the device is placed under an angle to create flow, except during staining with primary antibody. All solutions were used in quantities of 50 µL per every inlet and outlet well, unless specified otherwise. Cells were fixed using freshly prepared 3.7% formaldehyde (Sigma 252549) in PBS. 50 µL of the fixative was added to both the perfusion inlet and outlet for 15 minutes at room temperature (RT), followed by a wash step with 4% FBS in PBS for 5 minutes. After fixation, the cells were permeabilized using 0.3% Triton-X (Sigma T8787) in PBS. After washing, the microvessels were blocked for 45 min using blocking solution (2% FBS, 0.1% Tween20 (Sigma P9169), 2% BSA (Sigma A2153) in PBS). The adherence junctions were visualized using a VE-Cadherin stain (Abcam, 33168, diluted 1:1000 in blocking solution, 30 µL pipetted in the perfusion inlet, 20 µL in the perfusion outlet), which was incubated for 1 hr at RT followed by 30 min incubation with Alexa Fluor 488 (ThermoFisher Scientific, A11008, 1:250 in blocking solution). To perfuse the chips with primary antibody, the device was placed on a rocker platform. After incubation with the secondary antibody, the device is washed once with washing solution, followed by nuclei staining (NucBlue Fixed cell staining, Life technologies, R37606), and the cytoskeletal marker F-actin, stained by ActinRed™ 555 ReadyProbes® (ThermoFisher Scientific, R37112) in PBS and imaged using a high content confocal microscope (Molecular Devices, ImageXpress™ Micro Confocal) at 10x magnification.

Sprouting quantification

The average sprouting length was quantified using FIJI v. 1.52 by manually determination of the distance between the microvessel and furthest sprouting tip cell within the gel. The sprouting length of PMA was obtained after 3 days, all other combinations after 4 days, and is represented as the mean of three replicates and two independent experiments. The sprout number, average diameter, circularity was obtained by imaging fixed microvessels that were stimulated for 6 days and stained with phalloidin/DAPI. Using a 10x objective, we aquired 180 z-steps with 1 µm spacing and obtained two adjacent sites. The orthogonal views extracted and analyzed in the middle of the gel region. Thresholding of the vessels was automated using Weka Segementation tool (v 3.2.27) and a watershed was applied to separate touching vessels. Particle analysis was performed to include particles between 10-10000 μm^2 with a circularity between 0.10-1.00.

a

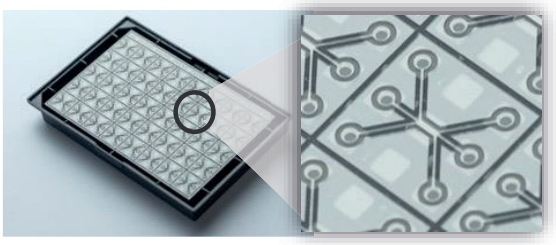

b

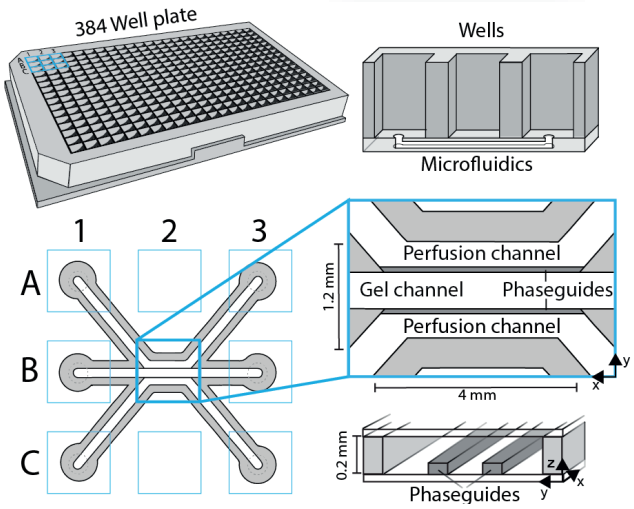
384 Well plate
Wells
Microfluidics
1
2
3
A
B
C
Perfusion channel
Gel channel
Phaseguides
Perfusion channel
1.2 mm
4 mm
0.2 mm
Phaseguides

c

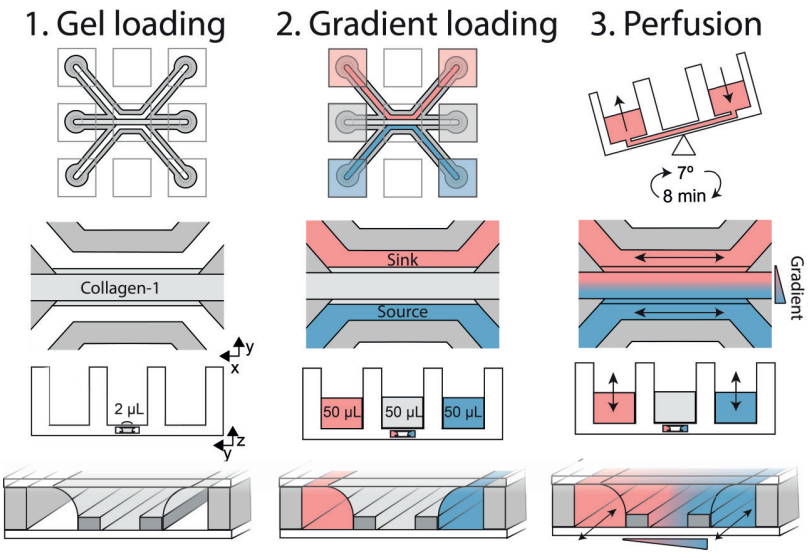
1. Gel loading
2. Gradient loading
3. Perfusion
7°
8 min
Collagen-1
Sink
Source
Gradient
2 µL
50 µL
50 µL
50 µL

d

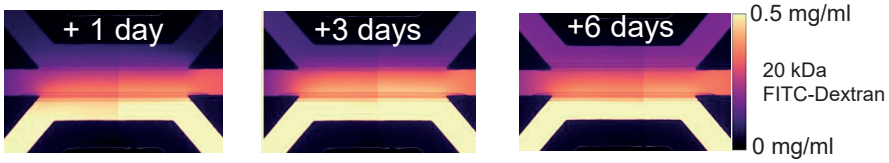
+ 1 day
+3 days
+6 days
0.5 mg/ml
20 kDa
FITC-Dextran
0 mg/ml

Results

Robust gradient formation in a 3D microenvironment

The microfluidic culture platform is based on a 384-well microtiter plate format. The glass bottom contains 40 microfluidic units (Fig. 1a), and each microfluidic unit is positioned underneath 9 wells (3x3). Every unit consists of 3 channels: the center channel that is used to pattern extracellular matrix ('gel channel') and two adjacent channels ('perfusion channels') (Fig. 1b). The channels are separated by PhaseGuides: small ridges that function as pressure barriers, which enabling patterning of cells and gel without the use of artificial membranes[36]. Every channel has one inlet and one outlet, which connect the channels with the wells in the microtiter plate.

Compartmentalization is achieved by patterning a hydrogel in the middle channel (Fig. 1c), and enables the formation of gradients by adding a source and sink in the opposite perfusion channels (step 2). Without continuous replenishment of the gradients source and sink in the microfluidic channels, gradients typically last only a few minutes (data not shown). To stabilize the gradient over time, the device was placed on a rocker platform to perfuse both perfusion channels continuously and simultaneously (step 3). As the volume inside the wells is typically orders of a magnitude higher than in the microfluidic channels (the wells typically contain volumes of 50 µl, compared to <1 µl in the microfluidic channels), the source and sink within the microfluidic channels are constant over prolonged periods of time. Thus a stable gradient could be maintained for multiple days (Fig. 1d) without the need to replenish. Although a gradient is still present after 6 days, the steepness is affected due to saturation of the sink. Therefore, growth factors and medium were replaced at 2

◄Figure 1 | Gradient generation in a 3D microenvironment

(a) *Bottom of the OrganoPlate®, a microfluidic culture platform based on a 384 well plate. The glass bottom includes 40 microfluidic devices.* **(b)** *The geometry of a single microfluidic device that is positioned underneath 9 wells (3x3). Every device consists of 3 channels: one 'gel' channel for gel patterning, and two adjacent channels, separated by phaseguides.* **(c)** *3-step method to generate gradients in patterned hydrogels.* **(d)** *Gradient visualization after 1, 3 and 6 days after addition of 20 kDa FITC-Dextran as a gradient source.*

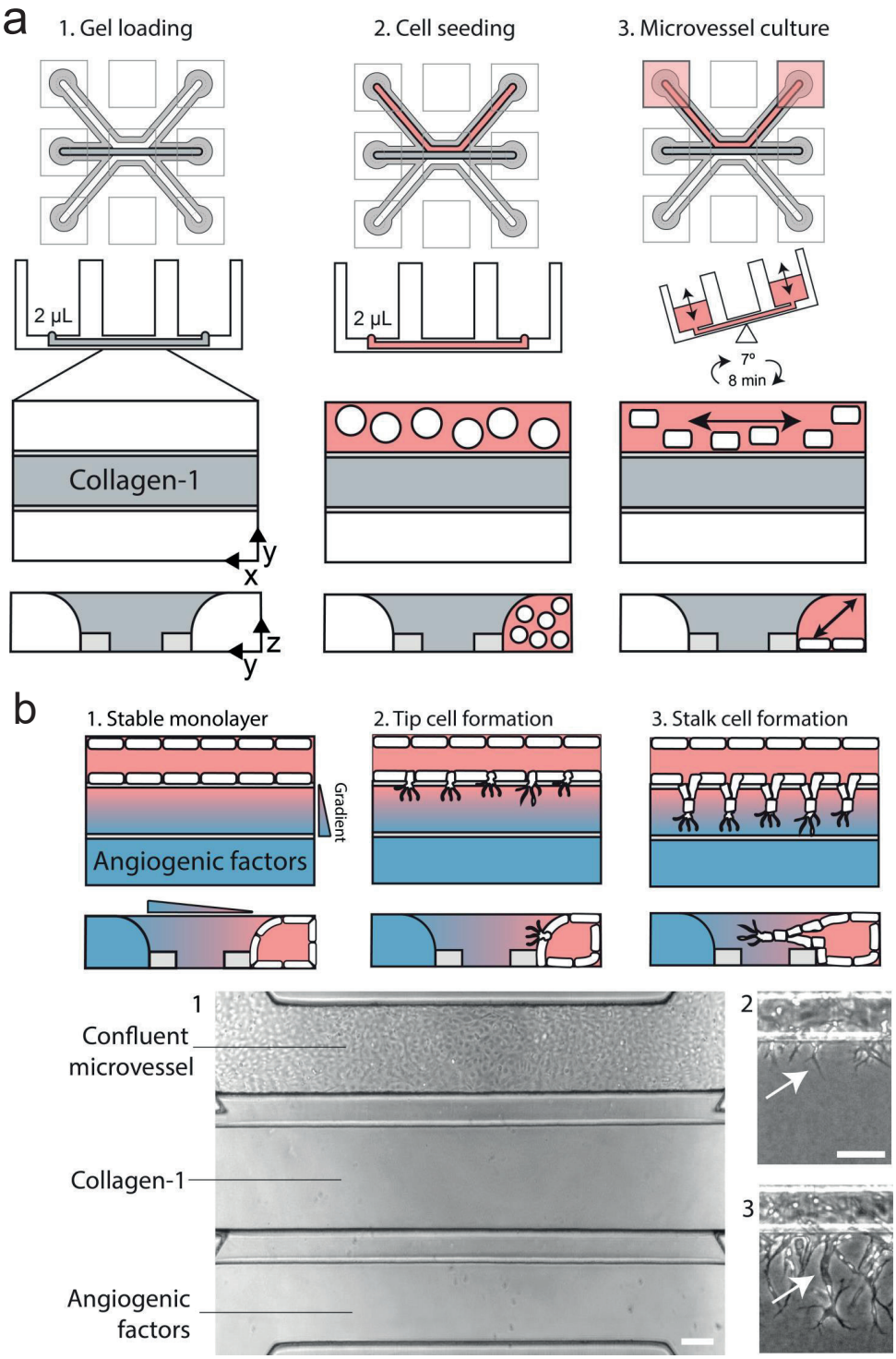
a
1. Gel loading
2. Cell seeding
3. Microvessel culture
2 µL
2 µL
7°
8 min
Collagen-1
y
x
z
y
b
1. Stable monolayer
2. Tip cell formation
3. Stalk cell formation
Gradient
Angiogenic factors
1
Confluent microvessel
Collagen-1
Angiogenic factors
2
3

to-3-day time intervals.

Importantly, the high hydraulic resistance of the hydrogel limits the influence of differences in hydrostatic pressure. This results in a reproducible and robust platform to generate gradients, despite the presence of small difference in volumes, for example due pipetting errors. Nonetheless, hydrostatic pressures still can influence the shape of the gradient, when the difference between the volumes is sufficiently large. This allows different types of gradient to be generated (e.g. linear or parabolic, supplementary Fig. 1).

Microvessels cultured against patterned collagen-1 gel

After gel loading and polymerization (Fig 2a, step 1), endothelial cell suspensions were added to the perfusion channels adjacent to the gel. After the cells adhered to the glass substrate (step 2) of the channel, perfusion was applied by placing the device on a rocker platform (step 3). Confluent microvessels were formed after 3 days of culture, and the apical side of the vessel (the lumen) can be accessed through the perfusion channel, while the gel forms the basal side of the tube[37].

Combination of angiogenic factors is required to induce sprouting

After reaching confluence in 3 days, the microvessels showed a stable morphology of a single monolayer against the gel (Fig 2b, step 1), despite the numerous (angiogenic) growth factors that are present in the media (such as vascular endothelial growth factor (VEGF) and basic fibroblast growth factor (bFGF). We included VEGF and S1P as they have been shown to induce angiogenic sprouting within a collagen-1 ma-

◄Figure 2 | Method the culture a microvessel within a microfluidic device

(a) *First, collagen-1 gel is patterned in the middle channel. After polymerization, an endothelial cell suspension was added in the top perfusion channel. By placing the device on a rocker platform, the channels are continuously perfused. After 72 hr, a confluent microvessel was formed.* **(b)** *Angiogenesis assay using a gradient of angiogenic factors. Angiogenic factors are added once a stable monolayer of ECs is formed against the gel (step 1). Addition of a gradient of angiogenic growth factors resulted in tip cells formation including filopodia at day 1 (step 2). Lumen formed by the stalk cells are visible at day 2 (step 3).*

trix[38-40] and included phorbol 12-myristate 13-acetate (PMA) as it has been found to promote lumen formation in absence of fibroblasts[15,41], and used in concentrations of 50 ng/ml for VEGF, 500 nM for S1P and 2 ng/ml for PMA. The angiogenic growth factor cocktail was added on the basal side of the vessels, and formed a gradient within the collagen-1 gel (Fig 2b, step 1). This induces the formation of tip- and stalk cells after respectively 1-2 days (Fig 2b, step 2-3).

Interestingly, adding either VEGF, S1P or PMA alone on the basal side did not result in angiogenic sprouting (Fig 3b and supplementary Fig 2). Addition of a gradient of VEGF+PMA+S1P together (Fig. 3c) resulted in angiogenesis including tip/stalk cell formation, presence of filopodia and lumen formation and directional growth towards the gradient. The sprouts fully traversed the gel after about 6 days and started to form a continuous monolayer against in the channel on the other side of the gel and in the basal perfusion channel. The angiogenic sprouts have a clear lumen formation (Fig 3d, panel i), appear circular in a cross-sectional view (Fig 3d, ii) and have clear VE-cadherin expression (Fig 3d, iii).

To identify the contribution of PMA and S1P to angiogenic sprouting, we directly compared VEGF+PMA with VEGF+S1P. The combination of VEGF+PMA triggered the formation of angiogenic sprouts into the gel, but the tip cells fail to develop their characteristic tip cell morphology including filopodia and the sprouts lack directionality after 6 days of sprouting (Fig. 3e and supplementary Fig. 3a+b). Furthermore, the sprouts appear to be non-homogenously distributed within the collagen gel. In contrast, VEGF+S1P shows sprouts that are also connected the sprouts to the main vessel, but are sprouts are equally distributed within the gel with a clear directionality towards the gradient. Although there are not significantly more sprouts (Fig 3g), the diameter of the lumen was significantly lower (Fig 3h). We quantified the circularity of the sprouts to estimate the directionality: a perpendicular sprout appears circular in a cross-sectional view with a value closer to 1, while a deviating sprouts appears flattened (closer to 0). This shows that VEGF+S1P sprouts have a significantly higher circularity and thus improved directionality towards the gradient compared to VEG-

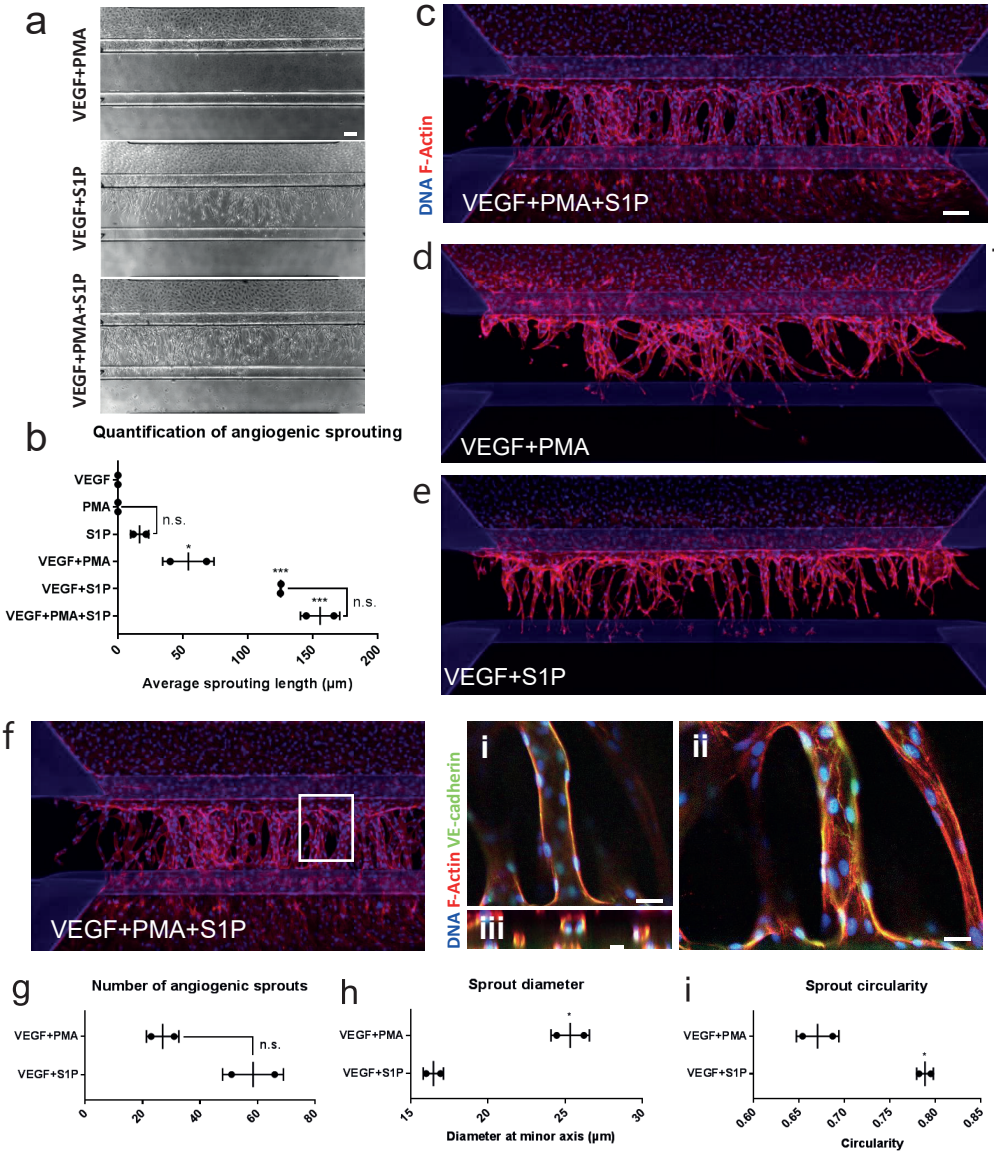

Figure 3 | Angiogenic sprouts after addition of angiogenic factors

(a) *Images of sprouting after 4 days of stimulation* **(b)** *Sprouting length in µm after stimulation for 3 (PMA) or 4 days (other).* **(c-e)** *Angiogenic sprouts after 6 days of stimulation with the indicated growth factors.* **(f)** *Close-up of middle (i) top (ii) and cross-scetion (iii) of VEGF+PMA+S1P stimulated sprouting.* **(g-i)** *Comparison between VEGF+PMA and VEGF+S1P in number of sprouts, diameter and circularity. All graphs present mean ± SD. Significance was calculated using one-way anova (b) or Student's t-test (g-i) and shown as n.s (non-significant), * (P < 0.05), ** (P < 0.01) or *** (P < 0.001). Scale bars: 100 µm*

F+PMA (Fig 3i). Taken together, these results clearly demonstrate that in a gradient driven, 3D cell culture environment, a combination of different cues is required to trigger angiogenesis, and S1P is a crucial factor in the distribution and guidance during angiogenic sprouting.

Anastomosis triggers remodeling and stabilization

Prolonged exposure to growth factors caused the angiogenic sprouts to anastomose, and connection is formed between the two perfusion channels. After anastomosis, we observed a significant reduction of sprouts (Fig 4a+b). Some angiogenic sprouts display the characteristic steps involved in pruning: first, the lumen collapses, followed by regression of the angiogenic sprouts towards the parental vessel (Fig 4a+b, arrows), while other angiogenic sprouts remained and increased their lumen diameter (Fig 4a+b arrowheads).

The formation of perfusable lumen within the sprouts is visualized by perfusion of the main vessel with 0.5 mg/mL 150 kDa TRITC-Dextran (Fig 4c+d). A surplus of 50 µL is added to the inlet well, which fills the parental vessels and flows into the angiogenic spouts. When angiogenic sprouts did not connect to the basal perfusion channel (Fig 4c), spots were visible within the collagen where dextran leaks out of the tip of the sprouts (panel ii, left, 0 minutes). This spots increased over time (right, 9 minutes). However, after anastomosis (Fig 4d), sprouts retained the dextran in their lumen, and shows subsequent filling of the bottom basal perfusion channel. This shows that sprouts stabilize and form a functional barrier after a connection has been formed.

Discussion

We report a robust, standardized microfluidic cell culture platform to study gradient-driven angiogenesis of a perfused microvessel in high-throughput. Each device contains 40 individually addressable microfluidic units and enable the culture of 40 identical microvessels. An important advantage of this assay is the defined geometry of the microfluidic channels, as this results in reproducible experimental cell culture conditions (position and density of the cells, amount of flow, position of the

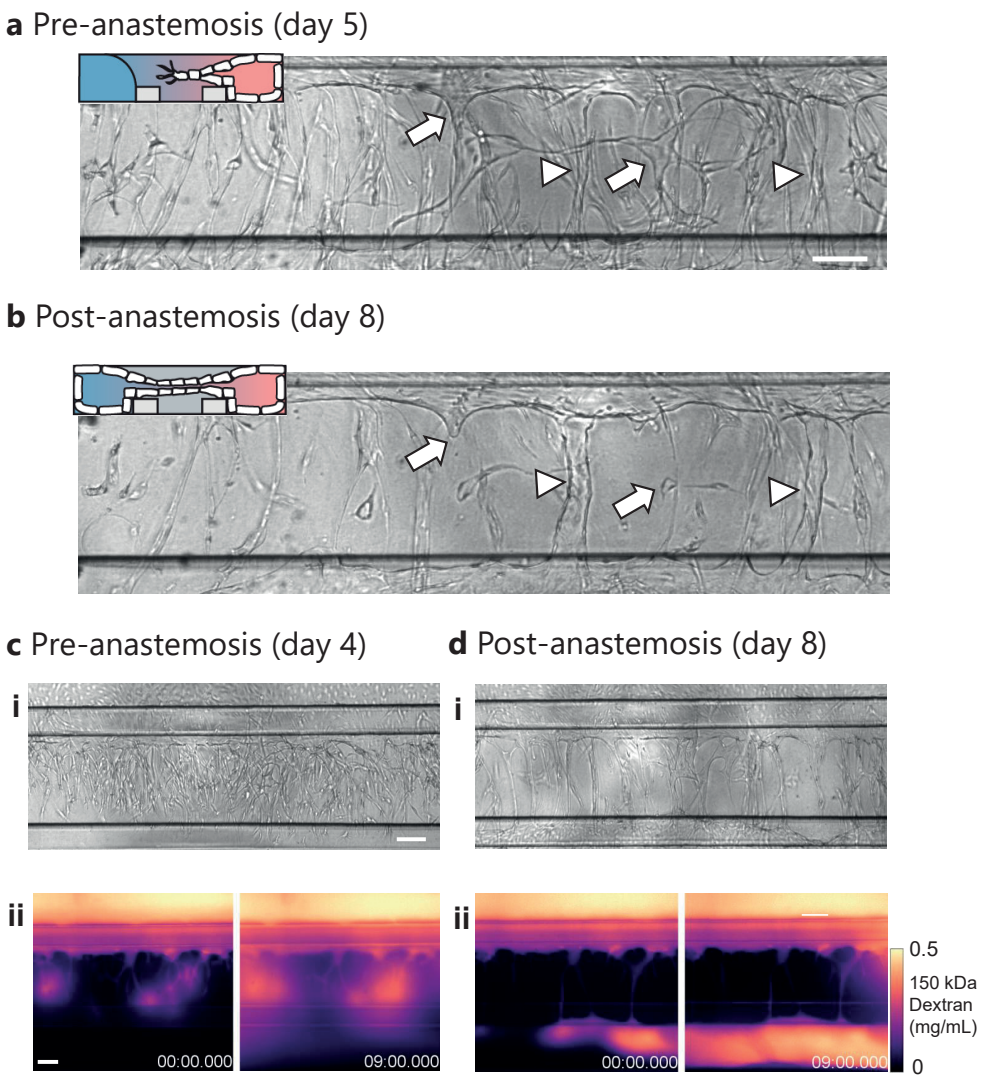

Figure 4 | Anastemosis with basal channel triggers pruning and maturation of angiogenic sprouts

(a) *Angiogenic sprouts 5 days after addition of VEGF+PMA+S1P.* **(b)** *Same, but at day 8. Arrows indicated regressed sprouts, arrowheads indicated remaining sprouts.* **(c)** *Angiogenic sprouts after 4 days were perfused with 0.5 mg/mL 150 kDa TRITC-Dextran. Panel ii show the pseudocolored fluorescent images after 0 and 9 minutes after addition. Time is indicated in minutes.* **(d)** *Same as in c, but after 8 days of stimulation. Scale bars: 100 µm.*

extracellular matrix and the shape of the gradient), and increases the robustness and scalability of our assay.

Perfusion in our device is induced by passive leveling using a rocker platform, and has as two crucial advantages. First, the flow simultaneously applied throughout all microfluidic units, which results in reproducible gradient formation. Second, as tubing and pumps are not required the throughput is greatly increased: the assay is scalable since multiple experiments can be performed by stacking of culture platforms on top of each other. Nonetheless, using a rocker platform to induce flow has also two trade-offs: first, the requirement of a rocker platform limited us to do time-lapse imaging only at discrete time points, as the vessels and gradient require continuous perfusion. Second is in physiological relevance: vasculature *in vivo* is exposed to continuous, unidirectional flow and is an important mechano-biological signal in during angiogenesis[42], while to flow in this assay occurs at discrete time points and is bi-directional. Thus, despite the evidence that flow affects the remodelling and maturation of the capillaries in our model, the exact contribution of flow in this assay is difficult to determine.

We showed that gradient-driven angiogenic sprouting through a extracellular matrix requires not just the presence of VEGF, but confirm that this requires a combination of angiogenic factors[43]. In our assay, VEGF+PMA showed a random distribution of the sprouts and an absence of filopodia on the tips cells, and the sprouts lacked the directionality. In contrast, a VEGF+S1P gradient showed formation of angiogenic sprouts, including tip cells with filopodia. Filopodia allow the tip cells to sense a biochemical gradient[4], and therefore explains the observed directionality of the angiogenic sprouts. This suggests that S1P plays an important role in the differentiation into functional tip cells and the observed repetitive formation of angiogenic sprouts. Such a repetitive formation of angiogenic sprouts can be explained by a reaction-diffusion mechanism between VEGF and Flt-1, the soluble form of VEGF receptor. Stalk cells are known to secrete Flt-1, which binds VEGF and prevents neighboring cells to become tip cells[44]. This is required for efficient angiogenic sprouting into the matrix[3],

with evenly distributed sprouts roughly every 100 µm, as predicted in silico[8,9]. It has been shown that S1P has a pro-angiogenic effects *in vitro* [38,39,45-47] and *in vivo*[38,48,49]. Our data suggests a pro-angiogenic synergy between S1P and VEGF, which is in agreement with the fact that inhibition of S1P also prevents VEGF-induced angiogenesis *in vivo*[50]. Interestingly, S1P is also known for its barrier stabilizing, anti-angiogenic properties and vascular maturation[51,52]. Therefore, we hypothesize that the effect of S1P is dependent on whether it is present on the apical side of ECs (lumen) or basal side, either mediated by differences in apical and basal expression of S1P receptors[53] or by dimerization with other receptors, like basally expressed VEGFR2[45]. A better understanding of the precise mechanisms of S1P signaling in angiogenesis will provide therapeutic strategies that specifically target the pro-angiogenic effects of S1P[48].

Prolonged exposure (>6 days) to a gradient of angiogenic stimuli resulted in sprouts that connect the two perfusion channels (anastomosis). This connection resolves the gradient, as there is a direct connection between the source and sink, and also results in the onset of flow through the sprouts. There remains controversy about the exact mechanism that leads to pruning. In vivo, this is either shear-mediated or due to changing receptor expression after a resolved (oxygen) gradient[10,54]. Once anastomosis occurred, we observed remodeling of the capillary bed, including pruning and regression of angiogenic sprouts within the collagen. Furthermore, some sprouts increased in lumen diameter, likely caused by the onset of perfusion[55]. By controlling shear levels and oxygen tension in this assay, we will be able to determine which of those effects is the crucial mechanism in pruning.

Perfusion of the sprouts with fluorescently labeled dextran showed that angiogenic sprouts that did anastomose are permeable near the tip/stalk cell region. In contrast, anastomosed sprouts remained the 150 kDa dextran solution within their lumen, suggesting that the connection between the two channels triggers (flow-mediated) maturation of the ECs in the sprouts, as they adopt their characteristic phalanx phenotype including mature cell-cell junctions[54,56]. Furthermore, once the angiogenic

sprouts connected, the medium can be switched back to the original culture medium with low levels or growth factors, while the integrity of the sprouts remained (supplementary movie 2+3), which suggests that perfusion is an important survival factor for angiogenic sprouts in absence of a high concentration of angiogenic factors like VEGF.

We expect that our platform will be widely adopted for a range of applications including both fundamental studies of the mechanisms of angiogenesis as well as for the identification of factors involved in microvascular destabilization or regression such as observed in for example diabetic retinopathy, nephropathy, macular degeneration, heart failure and tumour angiogenesis. The platform can be used to assess disease parameters on a high throughput scale and can be expanded to comprise other cell types such as stromal cells of the tissue or organ of interest.

Conclusion

We demonstrate a gradient-driven, three-dimensional angiogenesis assay in a standardized microfluidic platform. Angiogenic sprouting is induced from a perfused microvessel through a patterned collagen-1 gel. The combination of angiogenic factors was optimized to trigger angiogenic sprouting that faithfully reproduces all the angiogenic events that occur *in vivo*, such as the differentiation of the endothelial cells into tip-, stalk cells and phalanx cells and the formation of perfusable lumen. It was found that a combination of VEGF, S1P and PMA provided the optimal cocktail for 3D angiogenic sprouting. After the angiogenic sprouts anastomosed through the collagen to the other channel, remodeling and stabilization of the capillary bed was observed.

Conflict of Interest

V.vD., D.Z., C.R., and AJ.vZ. declare no potential conflict of interest. P.V. and T.H. are shareholders in Mimetas BV.

References

1 Carmeliet, P. Angiogenesis in life, disease and medicine. *Nature*. **438** (7070), 932-936, (2005).

2 Carmeliet, P. & Jain, R. K. Angiogenesis in cancer and other diseases. *Nature*. **407** (6801), 249-257, (2000).

3 Gerhardt, H. VEGF and endothelial guidance in angiogenic sprouting. *Organogenesis*. **4** (4), 241-246, (2014).

4 Gerhardt, H. *et al.* VEGF guides angiogenic sprouting utilizing endothelial tip cell filopodia. *J Cell Biol*. **161** (6), 1163-1177, (2003).

5 Phng, L. K. & Gerhardt, H. Angiogenesis: a team effort coordinated by notch. *Dev Cell*. **16** (2), 196-208, (2009).

6 Potente, M., Gerhardt, H. & Carmeliet, P. Basic and therapeutic aspects of angiogenesis. *Cell*. **146** (6), 873-887, (2011).

7 Pries, A. R., Hopfner, M., le Noble, F., Dewhirst, M. W. & Secomb, T. W. The shunt problem: control of functional shunting in normal and tumour vasculature. *Nat Rev Cancer*. **10** (8), 587-593, (2010).

8 Pries, A. R. & Secomb, T. W. Making microvascular networks work: angiogenesis, remodeling, and pruning. *Physiology (Bethesda)*. **29** (6), 446-455, (2014).

9 Secomb, T. W., Alberding, J. P., Hsu, R., Dewhirst, M. W. & Pries, A. R. Angiogenesis: an adaptive dynamic biological patterning problem. *PLoS Comput Biol*. **9** (3), e1002983, (2013).

10 Betz, C., Lenard, A., Belting, H. G. & Affolter, M. Cell behaviors and dynamics during angiogenesis. *Development*. **143** (13), 2249-2260, (2016).

11 Korn, C. & Augustin, H. G. Mechanisms of Vessel Pruning and Regression. *Dev Cell*. **34** (1), 5-17, (2015).

12 Liang, C. C., Park, A. Y. & Guan, J. L. In vitro scratch assay: a convenient and inexpensive method for analysis of cell migration in vitro. *Nat Protoc*. **2** (2), 329-333, (2007).

13 Staton, C. A., Reed, M. W. & Brown, N. J. A critical analysis of current in vitro and in vivo angiogenesis assays. *Int J Exp Pathol*. **90** (3), 195-221, (2009).

14 Nakatsu, M. N. *et al.* Angiogenic sprouting and capillary lumen formation modeled by human umbilical vein endothelial cells (HUVEC) in fibrin gels: the role of fibroblasts and Angiopoietin-1☆. *Microvascular Research*. **66** (2), 102-112, (2003).

15 Davis, G. E. *et al.* Control of vascular tube morphogenesis and maturation in 3D extracellular matrices by endothelial cells and pericytes. *Methods Mol Biol*. **1066** 17-28, (2013).

16 Chrobak, K. M., Potter, D. R. & Tien, J. Formation of perfused, functional microvascular tubes in vitro. *Microvasc Res*. **71** (3), 185-196, (2006).

17 Abhyankar, V. V. *et al.* A platform for assessing chemotactic migration within a spatiotemporally defined 3D microenvironment. *Lab Chip*. **8** (9), 1507-1515, (2008).

18 van Duinen, V., Trietsch, S. J., Joore, J., Vulto, P. & Hankemeier, T. Microfluidic 3D cell culture: from tools to tissue models. *Curr Opin Biotechnol.* **35** 118-126, (2015).

19 Kim, S., Chung, M. & Jeon, N. L. Three-dimensional biomimetic model to reconstitute sprouting lymphangiogenesis in vitro. *Biomaterials.* **78** 115-128, (2016).

20 Kim, C., Kasuya, J., Jeon, J., Chung, S. & Kamm, R. D. A quantitative microfluidic angiogenesis screen for studying anti-angiogenic therapeutic drugs. *Lab Chip.* **15** (1), 301-310, (2015).

21 Kim, J. *et al.* Engineering of a Biomimetic Pericyte-Covered 3D Microvascular Network. *PLoS One.* **10** (7), e0133880, (2015).

22 Park, J. *et al.* Three-dimensional brain-on-a-chip with an interstitial level of flow and its application as an in vitro model of Alzheimer's disease. *Lab Chip.* **15** (1), 141-150, (2015).

23 Jeon, J. S. *et al.* Generation of 3D functional microvascular networks with human mesenchymal stem cells in microfluidic systems. *Integr Biol (Camb).* **6** (5), 555-563, (2014).

24 Lee, K. H. *et al.* Integration of microfluidic chip with biomimetic hydrogel for 3D controlling and monitoring of cell alignment and migration. *J Biomed Mater Res A.* **102** (4), 1164-1172, (2014).

25 Kim, S., Lee, H., Chung, M. & Jeon, N. L. Engineering of functional, perfusable 3D microvascular networks on a chip. *Lab Chip.* **13** (8), 1489-1500, (2013).

26 Baker, B. M., Trappmann, B., Stapleton, S. C., Toro, E. & Chen, C. S. Microfluidics embedded within extracellular matrix to define vascular architectures and pattern diffusive gradients. *Lab Chip.* **13** (16), 3246-3252, (2013).

27 Buchanan, C. F., Verbridge, S. S., Vlachos, P. P. & Rylander, M. N. Flow shear stress regulates endothelial barrier function and expression of angiogenic factors in a 3D microfluidic tumor vascular model. *Cell Adh Migr.* **8** (5), 517-524, (2014).

28 Chan, J. M. *et al.* Engineering of in vitro 3D capillary beds by self-directed angiogenic sprouting. *PLoS One.* **7** (12), e50582, (2012).

29 Del Amo, C., Borau, C., Gutierrez, R., Asin, J. & Garcia-Aznar, J. M. Quantification of angiogenic sprouting under different growth factors in a microfluidic platform. *J Biomech.* **49** (8), 1340-1346, (2016).

30 Lee, H., Kim, S., Chung, M., Kim, J. H. & Jeon, N. L. A bioengineered array of 3D microvessels for vascular permeability assay. *Microvasc Res.* **91** 90-98, (2014).

31 Sackmann, E. K., Fulton, A. L. & Beebe, D. J. The present and future role of microfluidics in biomedical research. *Nature.* **507** (7491), 181-189, (2014).

32 Junaid, A., Mashaghi, A., Hankemeier, T. & Vulto, P. An end-user perspective on Organ-on-a-Chip: Assays and usability aspects. *Current Opinion in Biomedical Engineering.* **1** 15-22, (2017).

33 Berthier, E., Young, E. W. & Beebe, D. Engineers are from PDMS-land, Biologists are from Polystyrenia. *Lab Chip.* **12** (7), 1224-1237, (2012).

34 Haase, K. & Kamm, R. D. Advances in on-chip vascularization. *Regen Med.* **12**

(3), 285-302, (2017).

35 Blanco, R. & Gerhardt, H. VEGF and Notch in tip and stalk cell selection. *Cold Spring Harb Perspect Med.* **3** (1), a006569, (2013).

36 Trietsch, S. J., Israels, G. D., Joore, J., Hankemeier, T. & Vulto, P. Microfluidic titer plate for stratified 3D cell culture. *Lab Chip.* **13** (18), 3548-3554, (2013).

37 van Duinen, V. *et al.* 96 perfusable blood vessels to study vascular permeability in vitro. *Sci Rep.* **7** (1), 18071, (2017).

38 Argraves, K. M., Wilkerson, B. A. & Argraves, W. S. Sphingosine-1-phosphate signaling in vasculogenesis and angiogenesis. *World J Biol Chem.* **1** (10), 291-297, (2010).

39 Takuwa, Y. *et al.* Roles of sphingosine-1-phosphate signaling in angiogenesis. *World J Biol Chem.* **1** (10), 298-306, (2010).

40 Bayless, K. J., Kwak, H. I. & Su, S. C. Investigating endothelial invasion and sprouting behavior in three-dimensional collagen matrices. *Nat Protoc.* **4** (12), 1888-1898, (2009).

41 Taylor, C. J., Motamed, K. & Lilly, B. Protein kinase C and downstream signaling pathways in a three-dimensional model of phorbol ester-induced angiogenesis. *Angiogenesis.* **9** (2), 39-51, (2006).

42 Song, J. W. & Munn, L. L. Fluid forces control endothelial sprouting. *Proc Natl Acad Sci U S A.* **108** (37), 15342-15347, (2011).

43 Nguyen, D. H. *et al.* Biomimetic model to reconstitute angiogenic sprouting morphogenesis in vitro. *Proc Natl Acad Sci U S A.* **110** (17), 6712-6717, (2013).

44 Geudens, I. & Gerhardt, H. Coordinating cell behaviour during blood vessel formation. *Development.* **138** (21), 4569-4583, (2011).

45 Spiegel, S. & Milstien, S. Sphingosine-1-phosphate: an enigmatic signalling lipid. *Nat Rev Mol Cell Biol.* **4** (5), 397-407, (2003).

46 Yoon, C. M. *et al.* Sphingosine-1-phosphate promotes lymphangiogenesis by stimulating S1P1/Gi/PLC/Ca2+ signaling pathways. *Blood.* **112** (4), 1129-1138, (2008).

47 Oyama, O. *et al.* The lysophospholipid mediator sphingosine-1-phosphate promotes angiogenesis in vivo in ischaemic hindlimbs of mice. *Cardiovasc Res.* **78** (2), 301-307, (2008).

48 Kunkel, G. T., Maceyka, M., Milstien, S. & Spiegel, S. Targeting the sphingosine-1-phosphate axis in cancer, inflammation and beyond. *Nat Rev Drug Discov.* **12** (9), 688-702, (2013).

49 Natarajan, J. *et al.* Text mining of full-text journal articles combined with gene expression analysis reveals a relationship between sphingosine-1-phosphate and invasiveness of a glioblastoma cell line. *BMC Bioinformatics.* **7** 373, (2006).

50 LaMontagne, K. *et al.* Antagonism of sphingosine-1-phosphate receptors by FTY720 inhibits angiogenesis and tumor vascularization. *Cancer Res.* **66** (1), 221-231, (2006).

51 Jung, B. *et al.* Flow-regulated endothelial S1P receptor-1 signaling sustains vascular development. *Dev Cell.* **23** (3), 600-610, (2012).

52 Ben Shoham, A. *et al.* S1P1 inhibits sprouting angiogenesis during vascular development. *Development.* **139** (20), 3859-3869, (2012).

53 Bergelin, N., Lof, C., Balthasar, S., Kalhori, V. & Tornquist, K. S1P1 and VEGFR-2 form a signaling complex with extracellularly regulated kinase 1/2 and protein kinase C-alpha regulating ML-1 thyroid carcinoma cell migration. *Endocrinology.* **151** (7), 2994-3005, (2010).

54 Wacker, A. & Gerhardt, H. Endothelial development taking shape. *Curr Opin Cell Biol.* **23** (6), 676-685, (2011).

55 Lu, D. & Kassab, G. S. Role of shear stress and stretch in vascular mechanobiology. *J R Soc Interface.* **8** (63), 1379-1385, (2011).

56 Ribatti, D. & Crivellato, E. "Sprouting angiogenesis", a reappraisal. *Dev Biol.* **372** (2), 157-165, (2012).

Supplementary figures

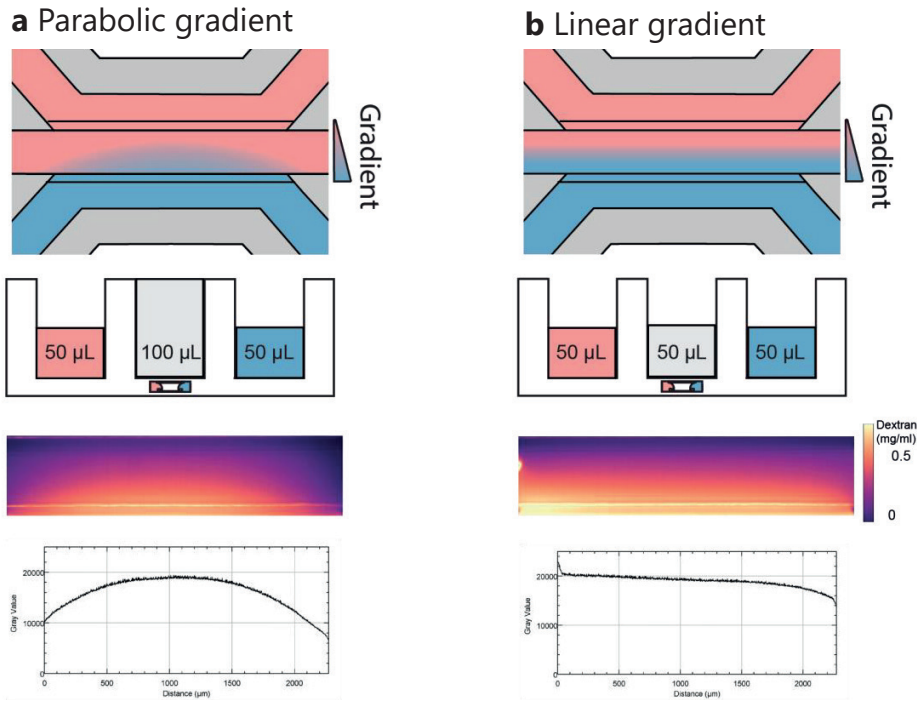

Supplementary Figure 1 | Shaping a gradient using hydrostatic pressure

(a) *Using double the volumes in the gel inlet and gel outlet compared to the perfusion inlets and outlets resulted in a parabolic gradient shape.* **(b)** *In contrast, equal volumes in all the wells result in a linear gradient shape. The gradient is visualized 4 hours after addition of 20 kDa FITC-Dextran. Fluorescence intensity is measured at the center of the gel, over the complete width of the gel and plotted accordingly.*

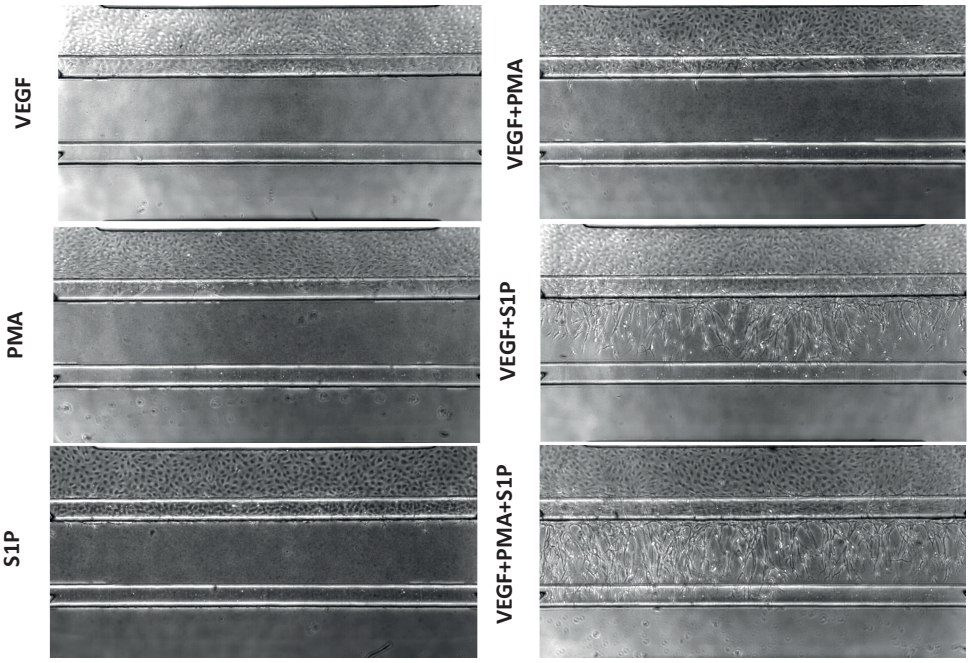

Supplementary figure 2 | Angiogenic sprout growth over time after stimulation with various angiogenic factors.

Microvessels were grown for 3 days and stimulated for 4 days using different angiogenic factors. Images acquired using a 4x objective and cropped to highlight the cells and collagen.

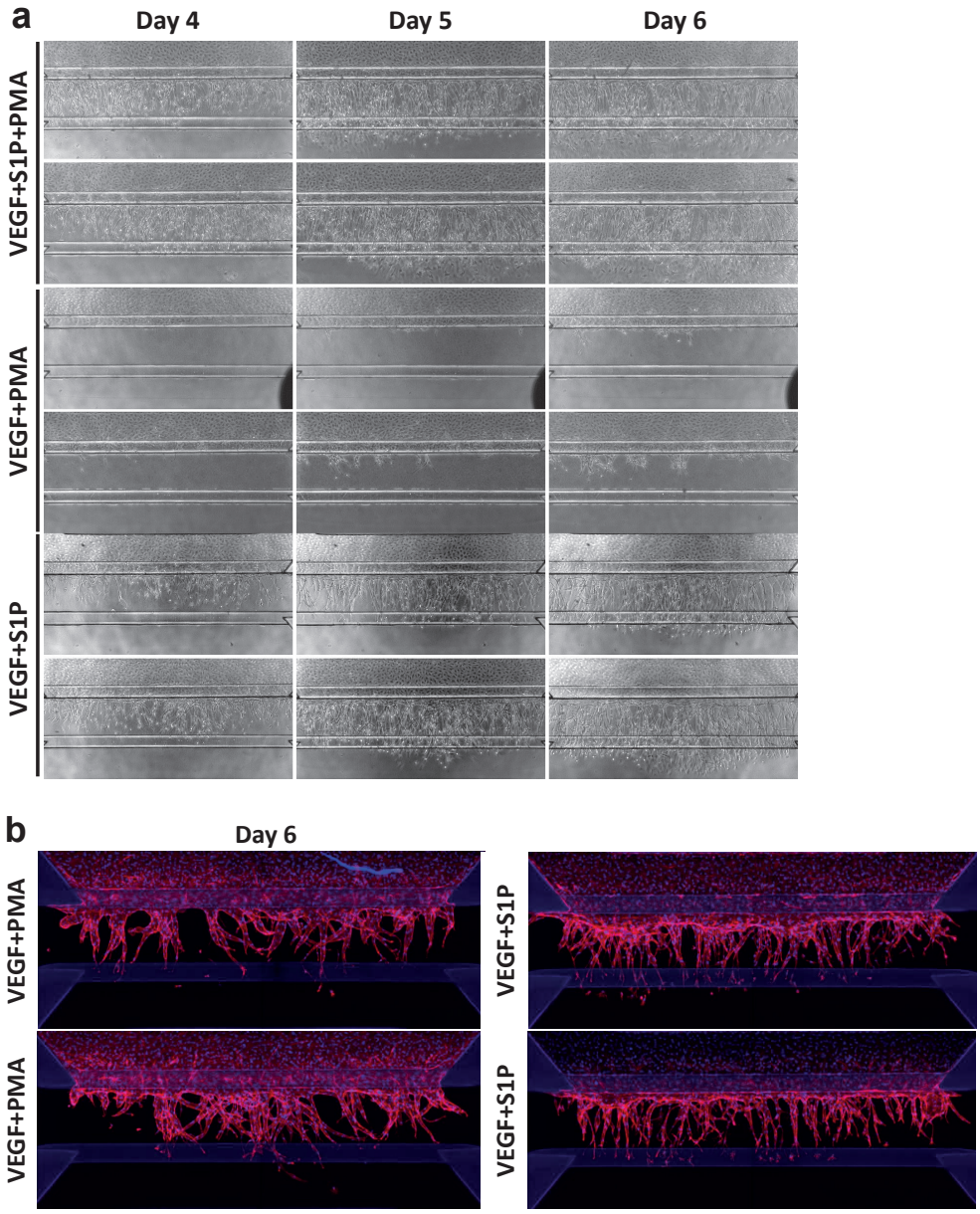

Supplementary figure 3 | Sprout morphology over time under culture different conditions.

(a) *Phase contrast images of sprouts of after 4,5 and 6 days of stimulation* **(b)** *Fixed microvessels after 6 days of stimulation with VEGF+PMA or VEGF+S1P and stained against F-actin (red) and nuclei (blue).*

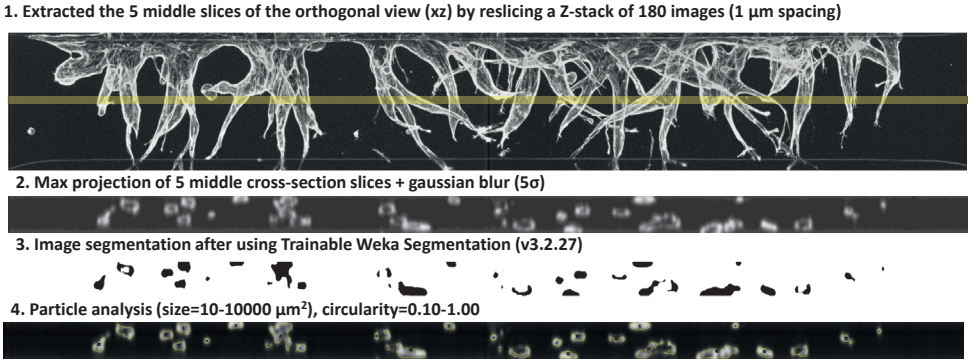

Supplementary figure 4 | Quantification method for sprout number, diameter and circularity

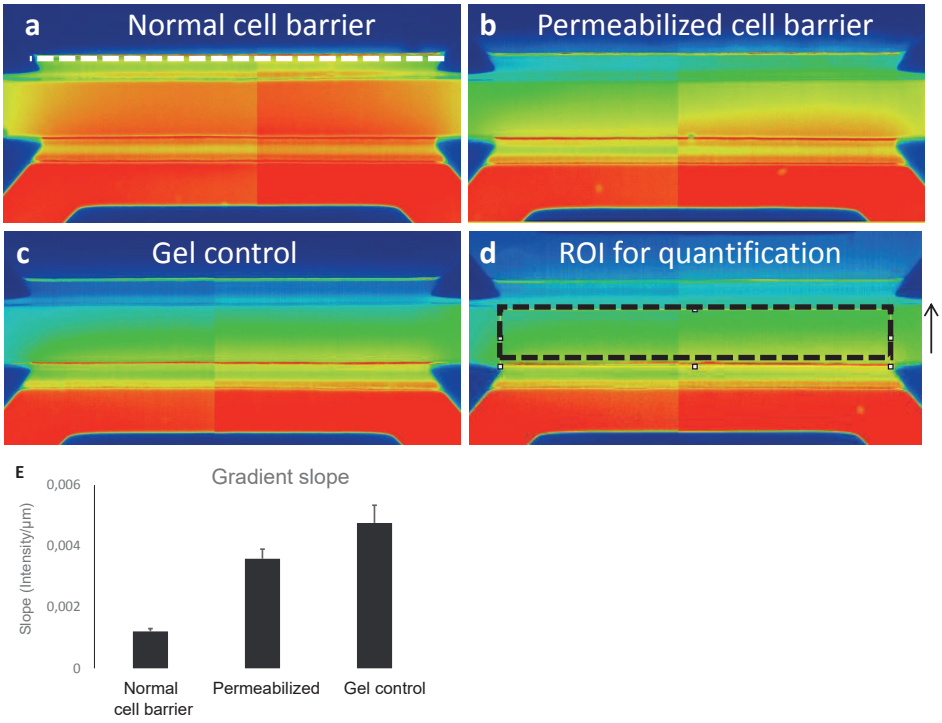

Supplementary Figure 5 | Influence of permeability of the gradient formation

(a) *Gradient profile without additional growth factors. Line indicates the position of the cell monolayer.* **(b)** *24 hr after permeabilization with VEGF+PMA+S1P shows that the gradient is restored and comparable to a gradient without cells (as demonstrated in* **(c-d)** *Region of interest used to quantify the intensity change in the y-direction (arrow)* **(e)** *Quantification of the slope of the gradient between different conditions (n=2) shows that the gradient in a system with permeable cell barriers is not significantly different compared to gel control (P=0.13). Bars represent mean±sd.*

CHAPTER

5

A standardized and scalable angiogenesis assay using iPSC-derived endothelial cells

V. van Duinen, W. Stam, V. Borgdorff, A. Reijerkerk, V. Orlova,
P. Vulto, T. Hankemeier and A.J. van Zonneveld

Journal of Visualized Experiments - In submission (2019)

Abstract

Pre-clinical drug research towards vascular diseases requires *in vitro* models of vasculature which are amendable to high-throughput screening. However, current *in vitro* screening models that have sufficient throughput only have limited physiological relevance, which hinders the translation of findings from *in vitro* to *in vivo*. On the other hand, microfluidic cell culture platforms have shown unparalleled physiological relevancy *in vitro*, but often lack the required throughput and scalability. Thus, there is a need for physiologically relevant *in vitro* models which can be integrated in the existing high-throughput screening infrastructure.

We demonstrate a robust platform to culture 40 3D microvessels under perfusion and against a collagen-1 scaffold. Upon the application of a gradient of angiogenic factors, important hallmarks of angiogenesis can be studied, including the differentiation into tip- and stalk cell and the formation of perfusable lumen. Perfusion with fluorescent tracer dyes enables the study of permeability during and after angiogenesis. Importantly, this assay is compatible with primary endothelial cells (ECs) as well as ECs derived from human induced pluripotent stem cells (iPSC-ECs). Finally, as the platform is suitable for high-content imaging, it is possible to automatically quantify the sprout permeability and sprout length.

In conclusion, the method presented here is suitable to study angiogenesis in a physiological relevant cellular microenvironment, including perfusion and gradients. The platform is compatible with automated microscopes, and has the required robustness and scalability to be integrated within the drug screening infrastructure. Both the platform as well as the endothelial cells differentiated from iPSC are commercially available, which enables the adoption across research groups and accelerates its implementation within drug research.

Introduction

It is now well recognized that angiogenesis, the growth of new blood vessels from pre-existing vasculature, plays a fundamental role in both health and disease[1]. For the discovery of new drugs targets of the microvasculature, research relies heavily on *in vitro* models, due to their unparalleled level of experimental control. However, it is still common practice to study endothelial cells (ECs) in culture systems that have limited physiological relevance[2]. To meet the demands of pre-clinical vascular drug research, improved *in vitro* models of vasculature are required that are amenable to high-throughput screening, with a scalable and robust cell source in a physiologically relevant cellular micro-environment.

Within the last decade significant progress has been made to increase the physiological relevance of *in vitro* models of vasculature. Instead of culturing endothelial cells on flat surfaces like tissue-culture plastics, endothelial cells can be embedded in three-dimensional scaffolds, such as fibrin and collagen gels[3]. Within these matrices, the endothelial cells show a more physiologically relevant phenotype associated with matrix degradation and lumen formation. However, these models only demonstrate a subset of the many processes that occur during angiogenic sprouting as important cues from the cellular microenvironment are still lacking.

Microfluidic cell culture platforms are uniquely suited to further increase the physiological relevance of *in vitro* models of vasculature. For example, endothelial cells can be exposed to shear stress, which is an important biomechanical stimulus in the homeostasis of vasculature. Also, the possibility to spatially control fluids within microfluidics allows the formation of biomolecular gradients[4-7]. Such gradients play an important role *in vivo* during the formation and patterning during angiogenesis.

However, while many microfluidic platforms show unparalleled physiological relevancy over traditional 2D and 3D cell culture methods, they often lack the required throughput and scalability[8]. Also, many of these platforms are not commercially available and require the end-users to microfabricate their devices prior to use[9]. This not only requires manufacturing apparatus and technical knowledge, it also limits

the level of quality control and negatively affects the reproducibility[10].

To date, primary human endothelial cells remain the most widely used cell source to model angiogenesis *in vitro*[11]. However, primary human cells have a number of limitations that hinder their routine application in screening approaches. First, there is a limited possibility to scale up and expand primary cell-derived cultures, like other primary cells, endothelial cells generally lose relevant properties when cultured *in vitro*[12,13]. Furthermore, such cells intrinsically suffer from genomic differences and batch-to-batch variations.

Endothelial cells derived from human induced pluripotent stem cells (iPSC) are a promising alternative: they resemble primary cells, but with a more stable genotype which is also amenable to precise genetic editing. Furthermore, as iPSCs are able to self-renew and thus can be expanded in nearly unlimited quantities which make iPSC-derived cells an attractive alternative to primary cells for usage within *in vitro* screening models[14].

Here we describe a method to culture endothelial cells as perfusable, 3D microvessels in a standardized, high-throughput microfluidic cell culture platform. Perfusion is applied by placing the device on a rocker platform. This ensures robust operation and increases the scalability of the platform. As the microvessels are continuously perfused and exposed to a gradient of angiogenic factors, angiogenic sprouting is studied in a more physiological relevant cellular microenvironment. Although the protocol is compatible with many different sources of (primary) endothelial cells[15,16], we focused on using commercially available human iPSC-derived ECs in order increase the standardization of this assay.

Protocol

Device preparation

1.1 Transfer the microfluidic 384-well plate to a sterile laminar-flow hood

1.2 Take of the lid and add 50 µL of water or PBS in every of the 40 observation wells (Fig 1b well 'B2') using a multichannel or repeater pipette.

Note: the protocol can be paused here. Leave the plate in the sterile culture cabinet at room temperature.

Prepare gel and coating

1.3 Prepare 2.5 mL of a 10 µg/mL fibronectin (FN) coating solution. Dilute 25 µL a 1 mg/mL fibronectin stock solution in 2.5 mL dulbecco's PBS (dPBS, calcium and magnesium free). Place in the waterbath at 37 ℃ till use.

1.4 Prepare a 100 µL collagen-1 solution: add 10 µL HEPES (1M) to 10 µL $NaHCO_3$ (37 g/L) and mix by pipetting. Place the tube on ice and add 80 µL collagen-1 (5 mg/mL) to yield a neutralized collagen-1 concentration of 4 mg/mL. Use a pipette to mix carefully and avoid the formation of bubbles.

1.5 Add 1.5 µL of collagen-1 solution (4 mg/mL) to every gel inlet (Fig 1b, well 'B1'). Make sure the droplet of gel should is placed in the middle of the well in order for the gel to enter the channel (see Fig 2a).

Note: Phaseguides prevent filling of the adjacent channels and enables gel patterning. Correct gel loading can be confirmed under a brightfield microscope, by flipping the plate upside down or observe the meniscus formation through the 'observation window' (well 'B2'). If the gel did not fill the channel completely, an additional droplet of 1 µL can be added.

1.6 Place the microfluidic plate in an incubator (37 ℃, 5% CO_2) for 10 minutes to polymerize the collagen-1.

Note: timing of the polymerization is crucial: due the low volumes used in mi-

crofluidics, evaporation can already be observed after 15 minutes of incubation, which results in gel collapse or shrinkage.

1.7 Take the plate out of the incubator and transfer to a sterile laminar-flow hood

1.8 Add 50 µL of the 10 µg/mL FN-coating to the inlet well of the top perfusion channel of every microfluidic unit (Fig 1b, well 'A1'). Press the pipette tip against the side of the well for correct filling of the well without trapping air bubbles (see Fig 2b). The channel should fill, and the liquid should pin on the outlet ('C1'), without filling the outlet well.

1.9 Put the plate in the incubator (37 ℃, 5% CO_2) for at least 2 days.

Note: the protocol can be paused here, as the collagen-1 gel together with the coating mixture is stable for at least 5 days in the incubator. If the coating mixture is refreshed, longer periods could be possible, but this has not been tested. Crucial is the level of FN-coating, as this prevents the dehydration of the collagen-1 gel.

Cell seeding/microvessel culture

1.10 Add 5 mL serum and 2.5 mL Pen/Strep (P/S) to 500 mL basal endothelial cell culture medium and filter sterilize using a bottle top filter with 0.22 µm pore size. This medium is now referred to as 'basal medium'.

1.11 Prepare vascular growth medium: Add 3 µL of 50 µg/mL vascular endothelial growth factor (VEGF) and 2 µL of a 20 µg/mL basic fibroblast growth factors (bFGF) to 5 mL basal medium + 1% serum + 0.5% P/S.

1.12 Thaw the iPSC-EC, transfer to a 15 mL tube and dilute in 10 mL basal medium.

1.13 Count the cells, a single vial contains 1 million cells with >90% viability.

1.14 Centrifuge at 100 RCF for 5 minutes

1.15 Aspirate supernatant without disturbing the cell pellet and resuspend in basal medium to a yield a concentration of 2×10^7 cells/mL.

1.16 Aspirate FN-coating solution (well 'A1')

1.17 Add 25 µL of basal medium in the inlet wells (Fig 1b, well 'A1').

1.18 Add a 1 µL droplet of cell suspension on every top perfusion inlet (Fig 1b, well 'C1'). The droplet should flatten in a few seconds (see Figure 3a+b for an illustration of this 'passive pumping' method).

Note: check under the microscope whether the seeding is homogeneous. If not, add another 1 µL in the outlet and wait till the droplet flattens.

1.19 Incubate the microfluidic well-plate for 1 h at 37 ℃, 5% CO_2. After this, the cells should have adhered. If not, wait another 30 minutes.

1.20 Remove the basal medium from the top perfusion outlet wells ('A1')

1.21 Add warm vessel culture medium in the top perfusion inlet and outlet (Fig 1b, well 'A1' and 'A3')

1.22 Place the plate on the rocker platform (set on 7° angle, 8 min rocking interval)

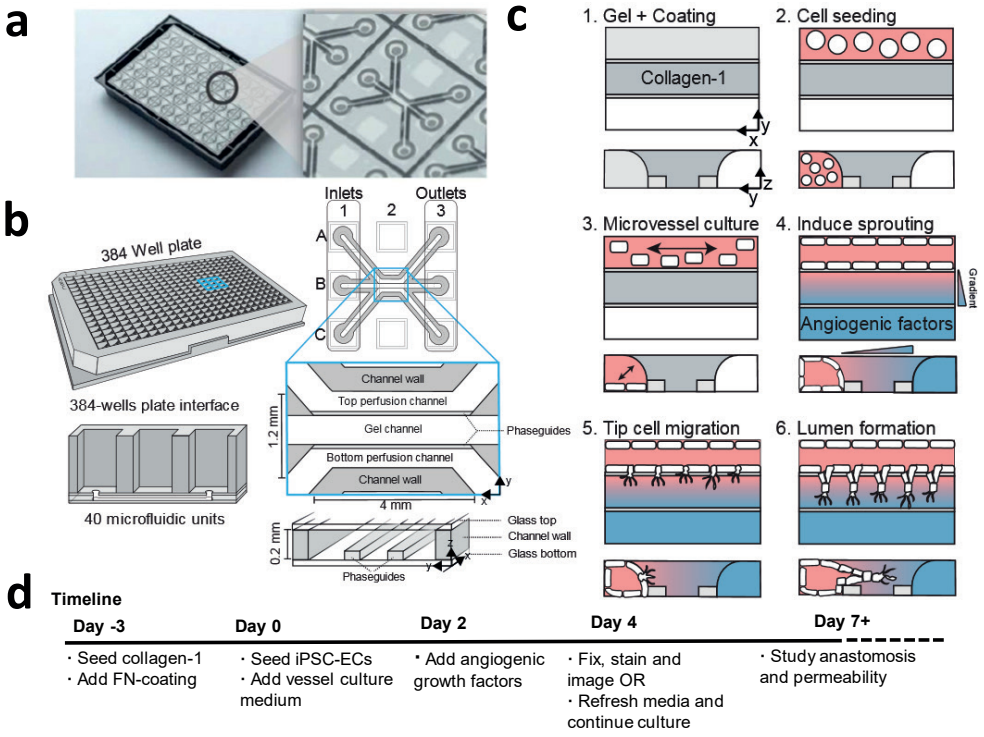

Figure 1 | Microfluidic cell culture protocol for iPSC-derived microvessels

(a) *The bottom of the microfluidic cell culture device is shown displaying the 40 microfluidic units that are integrated underneath the 384-well plate. Larger view displays one of the 40 microfluidic units* **(b)** *Each microfluidic unit is positioned underneath 9 wells with 3 wells that are used as inlets and 3 wells as outlet. The microfluidic channels are separated by ridges ('Phaseguides'), which enable the patterning of hydrogels in the central channel ('gel channel') while there is still contact with the adjacent channels ('perfusion channels').* **(c)** *Method to culture a perfused microvessel within the microfluidic device, which is used to study gradient driven angiogenic sprouting through a patterned collagen-1 matrix.* **(d)** *Timeline for studying angiogenic sprouting and/or anastomosis. Figure has been modified from*[15].

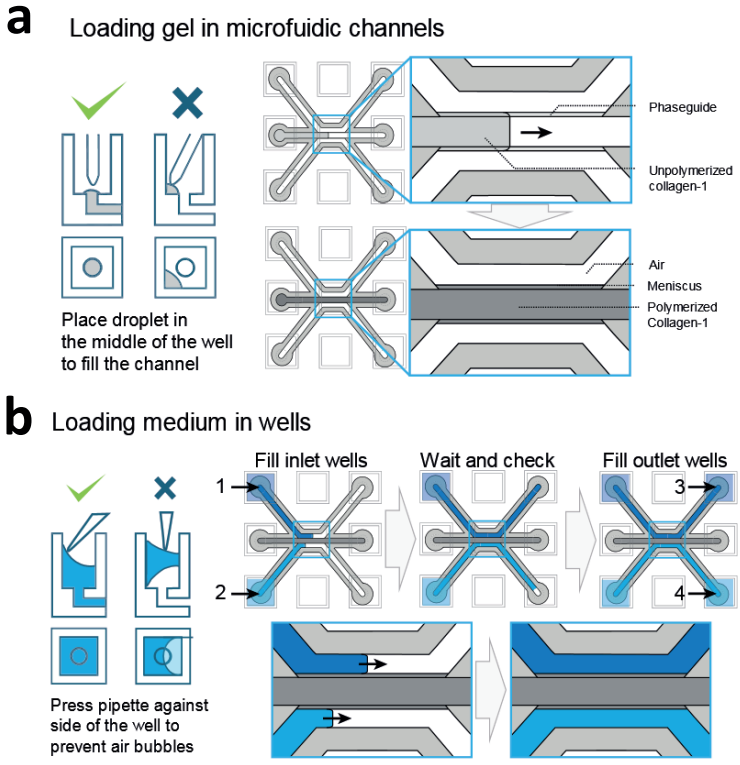

Figure 2 | Loading procedures for gel and medium

(a) *Examples of correct and incorrect gel deposition. Correct filing results in a patterned collagen-1 gel in the middle channel, which is subsequently polymerized* **(b)** *Examples of correct and incorrect filling of the wells. Wells are filled in order 1-4 to prevent air-bubble trapping within the microfluidic channels.*

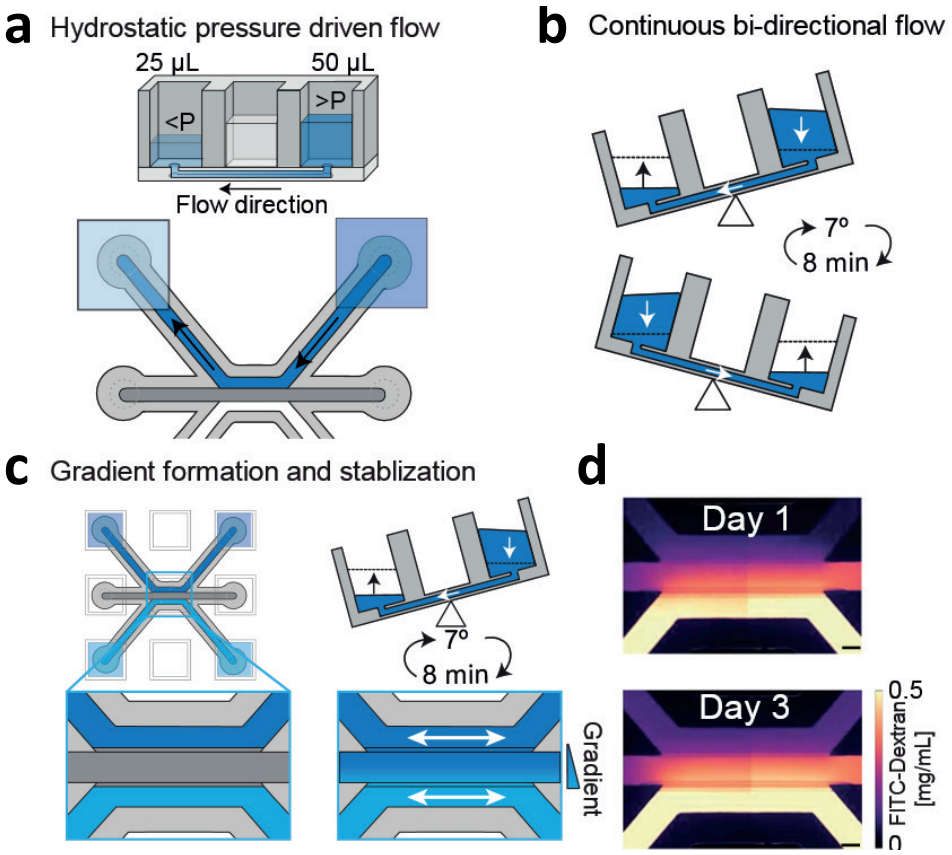

Figure 3 | Continuous hydrostatic pressure driven flow and gradient stabilization

(a) *Hydrostatic pressure differences between wells result in passive levelling and flow within the microfluidic channels* **(b)** *When the device is placed on a rocker platform set at 7° and 8 min cycle time results in continuous, bidirectional perfusion* **(c)** *Gradients are formed by introducing two different concentrations within the wells, which are continuously refreshed by passive leveling.* **(d)** *Gradient visualization using FITC-Dextran. Bi-directional flow stabilizes the gradient up till 3 days. Modified rom Scale bar = 200 µm. Figure has been modified from* [15].

in the incubator.

1.23 Image the plate using a brightfield microscope with automated stage at day 1 and 2 post-seeding to confirm cell viability.

1.24 After 2 days, a confluent monolayer should have formed against the collagen-1 scaffold.

Note: if the channels do not appear to be equally confluent, the microvessels can be cultured for an additional 24 hours.

Study angiogenic sprouting

1.25 Prepare 4.5 mL angiogenic sprouting medium by supplementing basal medium with 4.5 µL VEGF (1:1000, 50 µg/mL stock), 4.5 µL phorbol 12-myristate-13-acetate (PMA) (1:1000, 20 µg/mL stock) and 2.25 µL sphingosine-1-phosphate (S1P) (1:2000, 1 mM stock).

1.26 Prepare 8.5 mL vessel culture medium (basal medium supplemented with 30 ng/mL VEGF and 20 ng/mL bFGF)

1.27 Aspirate medium and add 50 µL fresh vessel culture medium in the top perfusion inlet and outlet wells and gel inlet and outlet wells (Well 'A1, A3, B1 and B3'),

1.28 Add 50 µL angiogenic sprout mixture to every bottom perfusion channel inlet and outlet well (Fig 1b, well 'C1' and 'C3').

1.29 Place the device back on the rocker platform to form a gradient of angiogenic growth factors.

1.30 And image after 1 day and 2 days using a brightfield microscope with automated stage.

1.31 The microvessels can be fixed, stained and imaged in order to quantify sprouting length and morphology (go to step 7).

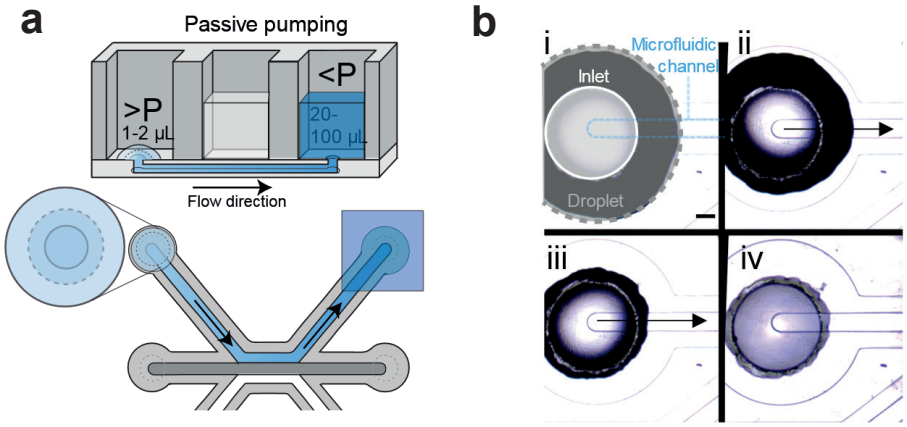

Figure 4| Passive pumping method for cell seeding

(a) *Passive pumping is driven by pressure differences which are caused by differences in surface tension. This results in a flow from the droplet (high internal pressure) towards the reservoir (low internal pressure)* **(b)** *Time lapse of a droplet (gray outline) that is placed on top of the inlet (white outline) of the microfluidic channel (blue outline). Right after addition (i, the droplet on top of the inlet shrinks (ii:, 1 sec after addition, iii: 2 sec after addition), which results in a flow towards the opposite outlet. This continuous till the droplets meniscus is pinned by the inlet. Scale bar = 400 µm.*

5

►Figure 5 | Robust 3D sprouting of iPSC-EC microvessels

(a) *Sprouting of iPSC-EC over time. Microvessels were grown for 48 hours (left) and then stimulated with an angiogenic cocktail containing 50 ng/mL VEGF, 500 nM S1P and 2 ng/mL PMA. 1 day after exposure, the first tip-cells are visible that invade the collagen-1 scaffold (middle. 2 days after exposure (right), the first lumen are visible (arrows) while the tip-cells have migrated further in the direction of the gradient.* **(b)** *Array of 15 microvessels that were stimulated with VEGF, S1P and PMA for 2 days and stained for F-actin (yellow) and Nuclei (blue). Scale bar = 200 µm* **(c)** *Stimulated microvessel (positive control)* **(d)** *Unstimulated microvessel (negative control)* **(e)** *Max projection of a single capillary within the gel* **(f)** *Same as e, but focused on middle.* **(g)** *orthogonal view of the vessel displayed above***.** *Scale bars (a-d 200 µm, e-g: 20 µm)*

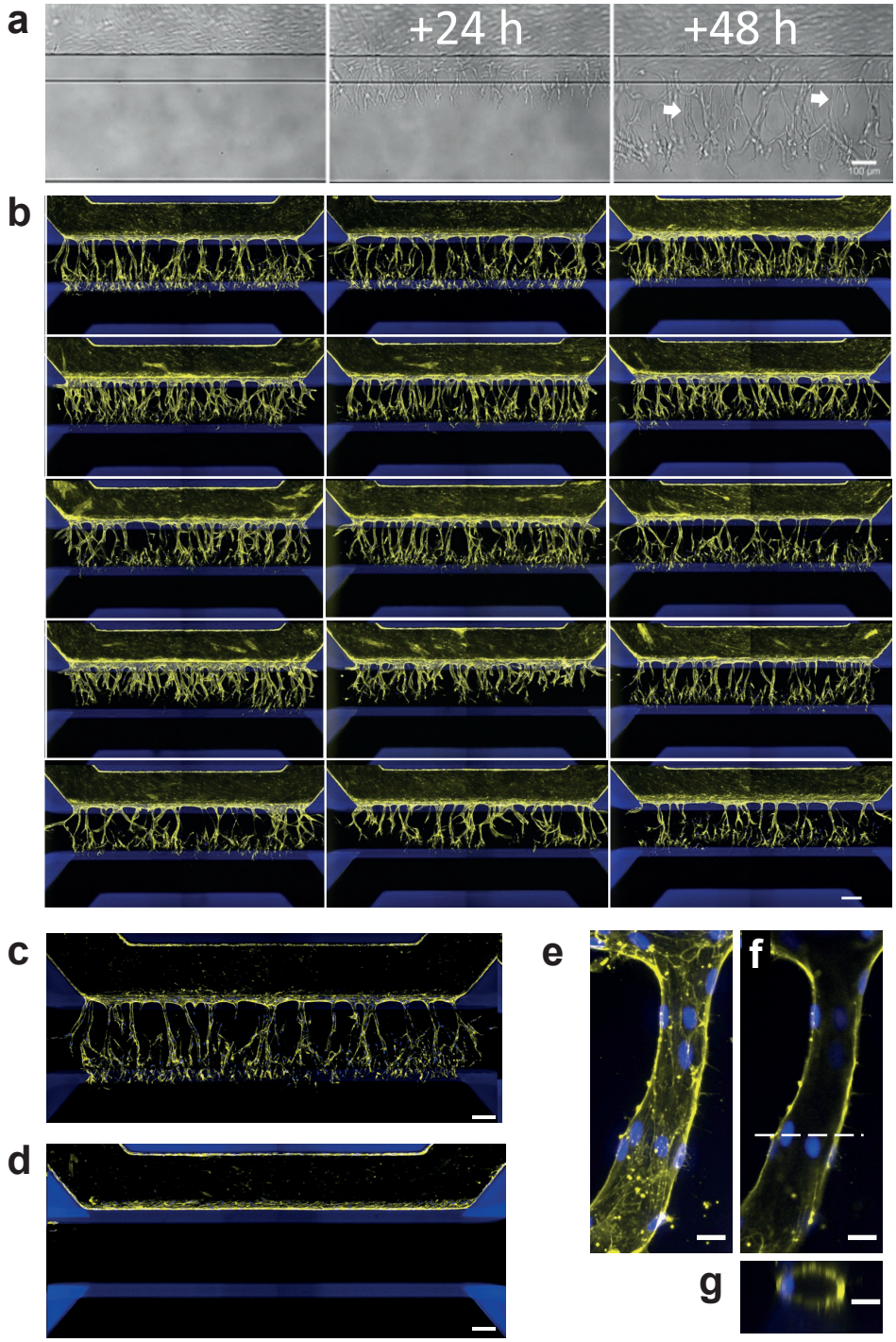
a
+24 h
+48 h
b
c
d
e
f
g

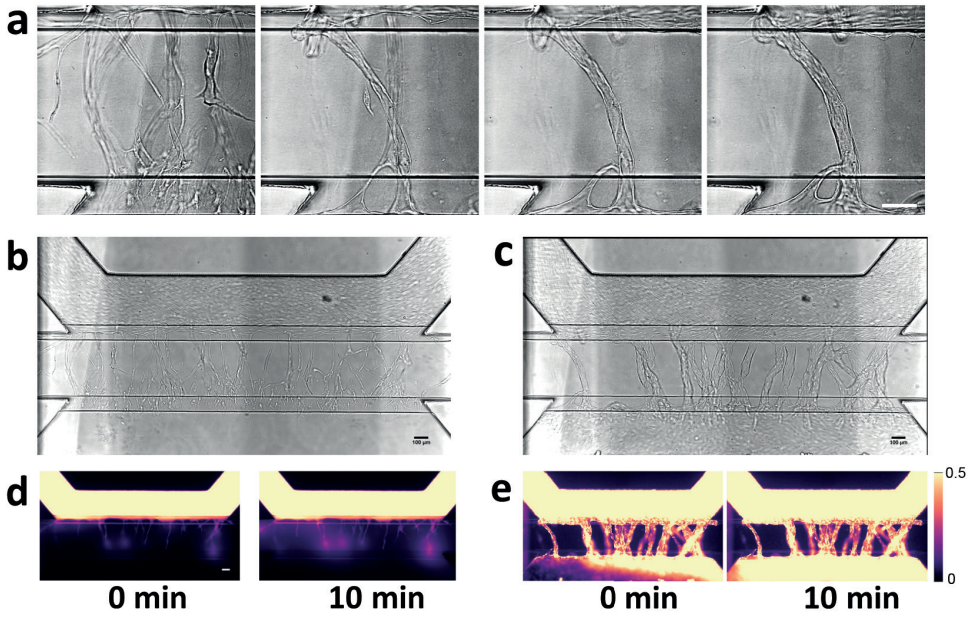

Figure 6 | Visualization of angiogenic sprout permeability before and after anastomosis

(a) *Anastomosis with basal channel triggers pruning and maturation of angiogenic sprouts. Closeup of capillary bed at 2, 4, 6 and 7 days after stimulation with angiogenic growth factors* **(b)** *Angiogenic sprouts after 2 days after addition of angiogenic growth factors. Angiogenic sprouts are formed within gel, but are not yet connected to the bottom perfusion channel* **(c)** *Perfusion of the microvessel with 0.5 mg/mL TRITC-albumin solution. Fluorescent images obtained at 0 and 10 min.* **(d-e)** *Same as in b+c, but after 7 days of stimulation. Sprouts are connected to the other side and formed a confluent microvessel in the basal perfusion channel. Scale bars: 100 µm*

Study anastomosis and sprout stabilization

1.32 Refresh both the angiogenic sprouting medium and vessel culture medium every 2-3 days

1.33 4 days after addition of angiogenic growth factors, the sprouts start to anastomose with the bottom channel, resulting in perfusion of the angiogenic sprouts. Permeability can be quantified at multiple time-points (see step 6)

Visualization of angiogenic sprout permeability

1.34 Add 1 µL of TRITC-albumin (0.5 mg/mL) to the top perfusion inlet and mix using a 50 µL pipette.

1.35 Transfer the plate to a fluorescent microscope with automated stage and incubator set at 37 ℃. .

1.36 Acquire a time-lapse for 10 minutes, with images taken every minute.

1.37 Remove the plate from the microscope and transfer the plate to a sterile laminar-flow hood.

1.38 Remove the TRITC-albumin by aspiration both the vessel culture medium and the angiogenic sprouting medium and replace both the vessel culture medium and angiogenic sprouting medium in the corresponding wells (see step 4.3-4.4).

1.39 Place the device back into the incubator to continue angiogenic sprouting.

Fixation, staining and imaging

1.40 Aspirate all culture media from all the wells.

Note: residual medium or liquids in the microfluidic channels does not influence the fixation: due its low volume (1-2 µL)

1.41 Add 25 µL of 4% paraformaldehyde (PFA) in PBS to all the perfusion inlet and outlet wells.

1.42 Incubate for 10 minutes at room temperature. Place the device under a slight angle to induce flow (e.g. by placing one side of the plate on a lid).

1.43 Aspirate the PFA from the wells.

1.44 Wash twice with 50 µL hanks balanced salt solution (HBSS) in all the perfusion inlets and outlets

1.45 Aspirate the HBSS from the wells.

1.46 Permeabilize by adding 50 µL 0.2% Triton-X100 to all the perfusion inlets and outlets

1.47 Aspirate the 0.2% Triton-X100 from the wells

1.48 Wash the perfusion channels twice by adding with 50 µL of HBSS to all perfusion inlets and outlet wells

1.49 Aspirate the HBSS from the wells.

1.50 Stain the nuclei using Hoechst (1:2000) and F-actin using Phalloidin (1:200) in HBSS. Prepare 2,2 mL for 40 units, and add 25 µL to every perfusion inlet and outlet well ('A1';'A3';'C1';C3'). Place the plate under a slight angle and incubate at room temperature for at least 30 minutes.

1.51 Wash twice with 50 µL of HBSS in all the perfusion inlets and outlets

1.52 Directly image using a fluorescent microscope with automated stage or store the plate protected from light at 4℃ for later use.

Results

The microfluidic 3D cell culture platform consists of 40 perfused microfluidic units (Fig 1a+b), which is used to study angiogenic sprouting of perfused microvessels against a patterned collagen-1 gel (Fig 1c). These microvessels are continuous perfused and exposed to a gradient of angiogenic growth factors (Fig 3a-d).

Seeding the iPSC-EC using the passive pumping method should result in homogenous seeding densities (Fig 4a+b). Culture under continuous perfusion resulted in confluent microvessels in 2 days, with the cells completely lining the circumference of the microfluidic channel and the formation of a confluent monolayer against the

patterned collagen-1 gel.

Exposure to a gradient of angiogenic factors resulted in directional angiogenic sprouting of the microvessels within the patterned collagen-1 gel (Fig 5a-g). Clear tip cell formation and invasion into the collagen-1 gel and was visible 24h after addition of the angiogenic gradient, while stalk cells including lumen formation was visible after 48h (Fig 5a). The angiogenic sprouts can be either studied 2 days after gradient exposure, or cultured for +5 days after gradient exposure to study anastomosis and sprout stabilization (see timeline, Fig 1d).

After fixation and staining, the capillary network can be clearly visualized more clearly using Phalloidin to stain F-actin and Hoechst 33342 to stain the nucleus (Fig 5b-c). These sprouts can be quantified (e.g. shape and length[15]). Without addition of growth factors, no invasion into the collagen-1 gel should be observed (Fig 5d). Confocal imaging was used to determine the sprout diameter and to confirm lumen formation(Fig 5e-g).

The sprouts continue to grow towards the direction of the gradient and reach the opposite perfusion channel after 3-4 days after addition of angiogenic growth factors. This results in remodeling of the vascular network, with a clear reduction in the number of angiogenic sprouts (Fig 6a). Lumen formation was assessed by perfusion of the vascular network with fluorescently labeled macromolecules (e.g. TRITC-albumin or FITC-dextran). Perfusing the microvessels with 0.5 mg/mL TRITC-albumin before and after anastomosis revealed a clear difference in sprout permeability after 10 min (Fig 6b-e), which suggests that the capillaries stabilize and mature after anastomosis.

Discussion and conclusion

This method describes the culture of 40 perfusable endothelial microvessels within a robust and scalable microfluidic platform. Compared to traditional 2D and 3D cell culture methods, this methods shows how a physiological relevant cellular microenvironment that includes gradients and continuous perfusion can be combined with

3D cell culture with adequate throughput for screening purposes.

One of the major advantages over comparable microfluidic assays is the that this method does not rely on pumps for perfusion, but uses a rocker platform to induce continuous perfusion in all microfluidic units simultaneously. This ensures that the assay is robust and scalable: plates can be stacked on a rocker platform. Importantly, all microfluidic units remain individually addressable, which allows this method to be implemented within drug screening including the generation of a dose-response curve. Furthermore, without a pump, imaging and medium replacement is far simpler with less risk of (cross)-contamination.

The lack of a pump is a limitation for continuous imaging, as this is restricted to sequential time intervals. Furthermore, the perfusion in this platform consist of bi-directional flow with low levels of shear stress, while vasculature *in vivo* is exposed to unidirectional flow with higher levels of shear stress. Though we do not observe negative effects of the bidirectional flow in the angiogenic sprouting, flow is an important biomechanical stimulus in vascular biology and preferably controlled. However, while there are commercially available pump setups, interfacing with the 384-well plate remains challenging, and pump setups severely hamper the scalability of this assay.

Another major advantage of this method is the commercial availability, while comparable microfluidic cell culture platforms need to be fabricated by the end-users. This availability facilitates the adoption of this assay among other academic and pharmaceutical research groups, leading to standardization. Also, unlike microfluidic prototypes, the 384-well plate interface ensures compatibility with the current lab equipment (e.g. aspirators, plate handlers and multichannel pipettes), facilitating the integration within the current screening infrastructure.

The most straight-forward future direction for this assay will be the integration of other cells types that play an important role during angiogenesis, such as pericytes and macrophages. To study for example the role of macrophages during anastomosis between sprouts or the adherence of pericytes after capillary formation. Also, it

is possible to culture various other cell types within or against a extracellular matrix (e.g. we have shown the culture of neurons and various epithelial structures such as proximal tubules and small intestines). Another interesting direction is the usage of synthetic hydrogels. Not only does this further increase the standardization of the assay, it also allows the tuning of for example the stiffness and cell-matrix interactions.

In conclusion, the method presented here is suitable to study angiogenesis in a physiological relevant cellular microenvironment, including perfusion and gradients. The platform is compatible with automated microscopes, and has the required robustness and scalability to be integrated within the drug screening infrastructure. Both the platform as well as the endothelial cells differentiated from iPSC are commercially available, which enables the adoption across research groups and accelerates its implementation within drug research.

Critical steps

Collagen 1 gel

The collagen 1 gel should completely fill the gel channel. During gel loading, this filling can be observed by inspecting the microfluidic channels either through the observation window or by flipping the plate upside down. While filling, the collagen gel should remain in the center channel, without flowing into the adjacent perfusion channels.

We found that the quality of the collagen-1 gel is crucial for proper assay performance. Collagen-1 batches with too high viscosity will lead to incomplete filling of the gel channel. After 10 minutes of polymerization at 37 degrees, the gel should be homogenous and clear. If collagen 1 is not stored properly (e.g. due to fluctuating temperatures in the fridge), the collagen will polymerize in- homogenously within the channels with clearly visible fiber formation. This can result in invasion of the ECs into the gel without addition of angiogenic factors, but without proper lumen development.

Cell seeding

When the cells are seeded, the fibronectin coating solution is only removed from the wells, leaving the microfluidic channels filled with coating solution. Aspiration of the coating from the microfluidic channels could cause gel disruption or gel aspiration.

The cell suspension need to replace/displace the FN-coating solution. This works best when the cell suspension is seeded using the passive pumping method, as directly pipetting the cell suspension into the channels show less reproducible seeding densities.

Angiogenic sprouting

But, as the microvessels form a stable monolayer against the gel, these small differences only result in different times needed for reaching confluency. Thus, the assay start point is determined by confluency rather than culture time. If necessary, the culturing time can be extended until a clear monolayer has been formed against the gel.

Adding or replacing medium

Immediately filling outlet wells without waiting for the media to flow from the inlet well through the microfluidic channels will trap air bubbles within the microfluidic channels. Thus, addition of medium should always be done in the order indicated in the protocol to prevent dehydration and trapping air bubbles (see Fig 2b). These air bubbles will restrict or even stop the flow, even when the device is placed on a rocker platform.

Air bubbles can also occur when medium has been removed from the wells: if the wells are empty, evaporation of liquid in the channel can occur in about half an hour. When medium is added again, the evaporated medium in the microfluidic channels will cause air bubbles to be trapped within the channels. These air bubbles within the microfluidic channels can be removed manually by placing a P20 pipette directly on either the inlet or outlet, and forcing medium through the microfluidics from the opposite well. Successful removal of the air bubbles results in a small but noticeable

decrease in volume in the other well.

Within the wells, air bubbles can be trapped by incorrect filling of the wells. Pressing the pipette tip against the side wall of the wells will increase the success of completely filling the well. If an air-bubble if trapped within the wells, these can be removed by gently inserting a sterile pipette tip till the glass bottom.

Acknowledgments

This work is in part supported by a research grants from the 'Meer Kennis met Minder Dieren' program (project number 114022501) of The Netherlands Organization for Health Research and Development (ZonMw) and the Dutch Heart Foundation CVON consortium grant RECONNECT.

Disclosures

P. Vulto and T. Hankemeier are shareholder of Mimetas BV. V. Borgdorff and A. Reijerkerk are employees of Ncardia BV. V. van Duinen, W. Stam and A.J. van Zonneveld have no disclosures.

Troubleshooting

Problem	Cause	Solution
ECM		
Collagen-1 does not enter or fill the channel completely	*Collagen-1 droplet is not placed on top of the inlet*	*Carefully place the droplet on top of the inlet from the gel channel*
	Volume of collagen-1 is too low	*Use 1.5 µL of the gel to fill the channel completely*
	Collagen-1 is too viscous	*Use another batch of collagen-1*
Collagen-1 flow into perfusion channels	*Collagen-1 is pipetted directly into the channels*	*Carefully place the droplet on top of the inlet from the gel channel*
Collagen-1 is not clear/fiber formation	*Collagen-1 is not stored properly*	*Store collagen-1 at 4 °C (do not freeze)*
	$NaHCO_3$ and HEPES are not mixed before adding collagen-1	*Carefully mix the $NaHCO_3$ and HEPES by pipetting before adding the collagen-1*
Cell seeding and sprouting		
Droplet does not shrink using passive pumping method	*Droplet adheres to side of the well*	*Aspirate droplet and add new droplet on top of the inlet*
		Make sure the outlet well if filled with at least 20 µL of medium
No sprouting is observed	*Growth factors not added or aliquots not stored properly*	*Prepare fresh angiogenic sprouting medium*
	Air bubble blocks perfusion/ gradient formation	*Remove air bubbles using a P20 or P200 pipette*
	Volume differences between wells	*Volumes in all wells need to be equal in order to form a linear gradient*
Cells not viable	*Plate not placed on rocker platform/rocker platform turned off*	*Make sure rocker platform is on and has the right cycle time/angle (8 min/7°)*
	No perfusion possible due presence of air bubbles	*Remove air bubbles using a P20 or P200 pipette*
No lumens are formed, cells migrate as single cells	*Angiogenic sprouting mixture was added before a monolayer was formed*	*Wait an additional 24h before adding the angiogenic growth factors*
Major variation in sprouting density	*Differences in cell densities after seeding*	*Check if cell density is homogenous and comparable between microfluidic units. Add another droplet of cell suspension if necessary.*

Table 1: troubleshooting common errors

References

1 Carmeliet, P. & Jain, R. K. Principles and mechanisms of vessel normalization for cancer and other angiogenic diseases. *Nat Rev Drug Discov.* **10** (6), 417-427, (2011).

2 Griffith, L. G. & Swartz, M. A. Capturing complex 3D tissue physiology in vitro. *Nature Reviews Molecular Cell Biology.* **7** (3), 211-224, (2006).

3 Davis, G. E. *et al.* Control of vascular tube morphogenesis and maturation in 3D extracellular matrices by endothelial cells and pericytes. *Methods Mol Biol.* **1066** 17-28, (2013).

4 Kim, S., Chung, M. & Jeon, N. L. Three-dimensional biomimetic model to reconstitute sprouting lymphangiogenesis in vitro. *Biomaterials.* **78** 115-128, (2016).

5 Kim, C., Kasuya, J., Jeon, J., Chung, S. & Kamm, R. D. A quantitative microfluidic angiogenesis screen for studying anti-angiogenic therapeutic drugs. *Lab Chip.* **15** (1), 301-310, (2015).

6 Kim, J. *et al.* Engineering of a Biomimetic Pericyte-Covered 3D Microvascular Network. *PLoS One.* **10** (7), e0133880, (2015).

7 Tourovskaia, A., Fauver, M., Kramer, G., Simonson, S. & Neumann, T. Tissue-engineered microenvironment systems for modeling human vasculature. *Exp Biol Med (Maywood).* **239** (9), 1264-1271, (2014).

8 Junaid, A., Mashaghi, A., Hankemeier, T. & Vulto, P. An end-user perspective on Organ-on-a-Chip: Assays and usability aspects. *Current Opinion in Biomedical Engineering.* **1** 15-22, (2017).

9 Pagano, G. *et al.* Optimizing design and fabrication of microfluidic devices for cell cultures: An effective approach to control cell microenvironment in three dimensions. *Biomicrofluidics.* **8** (4), 046503, (2014).

10 Berthier, E., Young, E. W. & Beebe, D. Engineers are from PDMS-land, Biologists are from Polystyrenia. *Lab Chip.* **12** (7), 1224-1237, (2012).

11 Nowak-Sliwinska, P. *et al.* Consensus guidelines for the use and interpretation of angiogenesis assays. *Angiogenesis.* 10.1007/s10456-018-9613-x, (2018).

12 Dejana, E., Hirschi, K. K. & Simons, M. The molecular basis of endothelial cell plasticity. *Nat Commun.* **8** 14361, (2017).

13 Geraghty, R. J. *et al.* Guidelines for the use of cell lines in biomedical research. *Br J Cancer.* **111** (6), 1021-1046, (2014).

14 Passier, R., Orlova, V. & Mummery, C. Complex Tissue and Disease Modeling using hiPSCs. *Cell Stem Cell.* **18** (3), 309-321, (2016).

15 van Duinen, V. *et al.* Perfused 3D angiogenic sprouting in a high-throughput in vitro platform. *Angiogenesis.* 10.1007/s10456-018-9647-0, (2018).

16 Wevers, N. R. *et al.* A perfused human blood-brain barrier on-a-chip for high-throughput assessment of barrier function and antibody transport. *Fluids Barriers CNS.* **15** (1), 23, (2018).

CHAPTER

6

Phenotypic anti-angiogenesis screening assay using iPSC-derived endothelial cells

V. van Duinen, W. Stam, V. Borgdorff, F. Famili, A. Reijerkerk, P. Vulto, T. Hankemeier and A.J. van Zonneveld

Manuscript in preparation

Abstract

For the discovery of new drug targets that target angiogenesis, drug research relies heavily on in vitro models, due their unparalleled level of experimental control. However, it is still common practice to study compounds that inhibit angiogenesis in assays that have limited physiological relevance. To meet the demands of pre-clinal vascular drug research, improved in vitro models of angiogenesis are required which are amendable to high-throughput screening, with a scalable and robust cell source in a physiologically relevant cellular micro-environment.

To validate the usage of hiPSC-ECs in our anti-angiogenic screening assay, we compared the angiogenic response of the hiPSC-derived endothelial cells with primary endothelial cells (HUVEC). We show that hiPSC-EC exhibit similar sprouting behavior as HUVECs, including tip cell formation, directional sprouting and lumen formation. Inhibition with Sunitinib, a clinically used VEGFR2 inhibitor, and 3PO, a transient glycolysis inhibitor both reduced the sprouting of both hiPS-ECs as well as primary HUVECs, suggesting that this sprouting in this assay is VEGF-driven with glycolysis as main energy source. Finally, quantification of the assay performance resulted in an acceptable Z′-factors for phenotype assays.

We have demonstrated that hiPSC-ECs are an attractive alternative to primary endothelial cells when used in a physiologically relevant *in vitro* anti-angiogenesis assay. The combination of a standardized microfluidic 3D cell culture platform with a scalable and more standardized cell source is a major step in the standardization of physiologically relevant *in vitro* angiogenesis assays, as it offers the required robustness, compatibility and scalability to be integrated within the drug screening infrastructure.

Introduction

It is now well recognized that angiogenesis, the growth of new blood vessels from pre-existing vasculature, plays a fundamental role in both health and disease[1]. However, for the discovery of new drug targets that target the formation of new vasculature, drug research relies heavily on in vitro models that have limited physiological relevance[2,3]. To meet the demands of pre-clinal vascular drug research, improved in vitro models of angiogenesis are required: assays that are amendable to high-throughput screening, with a scalable and robust cell source in a physiologically relevant cellular micro-environment[4,5].

Within the last decade, significant progress has been made to increase the physiological relevance of in vitro models of angiogenesis. For example, endothelial cells that are embedded in three-dimensional scaffolds such as fibrin and collagen gels show increased physiologically relevant behavior, such as tip- and stalk cell formation, matrix degradation and lumen formation[6,7]. However, important cues from the cellular microenvironment, such as gradients and perfusion are still lacking. As a result, these models only demonstrate a subset of the many processes that occur during angiogenic sprouting.

Microfluidic cell culture platforms can further increase the physiological relevancy in vitro, for example by incorporation of perfusion and control over biomolecular gradients[8-11]. However, while many microfluidic platforms show unparalleled physiological relevancy over traditional 2D and 3D cell culture methods, they often lack the required throughput and scalability[12]. Also, many of these platforms require the end-user to microfabricate their devices prior to use[13]. This not only requires manufacturing equipment and technical knowledge, it also limits the level of quality control and negatively affects the reproducibility and standardization[14].

To date, primary human endothelial cells (ECs) remain the most widely used cell source to model angiogenesis in vitro[4]. However, primary human cells have a number of limitations that hinder their routine application in drug screening. First, there is a limited possibility to scale up and expand primary endothelial cells, as they lose

relevant properties when cultured in vitro[15,16]. Furthermore, primary cells intrinsically have genomic differences and batch-to-batch variations. Endothelial cells derived from induced pluripotent stem cells (hiPSC) are a promising alternative: they resemble primary cells, but with a more stable genotype which is also amenable to precise gene editing. Furthermore, as hiPSCs are self-renewing, they can be expanded in nearly unlimited quantities, and can be patient-derived. All this makes in vitro assays based on cells derived from hiPSCs ideal for usage within in vitro screening models[17].

Here, we studied whether this platform can be used as a anti-angiogenic screening assay microvessels using hiPSC-ECs, and compare their angiogenic response with primary endothelial cells (HUVEC). We study the effect of the clinically available angiogenesis inhibitor Sunitinib, a tyrosine kinase inhibitor targeting the vascular endothelial growth factor receptor 2 (VEGFR2) and platelet-derived growth factor receptor beta (PDGFRβ) and 3-(3-pyridinyl)-1-(4-pyridinyl)-2-propen-1-one (3PO), a transient glycolysis inhibitor of 6-phosphofructo-2-kinase/fructose-2,6-bisphsphatase isozyme 3 (PFKFB3), which has been shown to reduce angiogenesis both *in vitro* as well as *in vivo*[18]. Finally, the signal window, Z' and assay variability window were calculated to quantify the assay performance.

Material and methods

Device preparation and cell culture in microfluidic channels

The protocol described in the previous chapter was used to culture hiPSC-ECs and HUVEC microvessels. Briefly, the ECs were thawed and resuspended in 5 mL basal medium, pelleted and suspended in basal medium in a concentration of $1{\cdot}10^7$ cells/mL Instead of using the passive pumping method described in step 3.5-3.6, the FN-coating was aspirated, and 1 µL of cell suspension was seeded in the top perfusion inlet and top perfusion outlet. The ECs were seeded and cultured for 2 days in medium supplemented with 30 ng/mL VEGF and 20 ng/mL bFGF to form confluent microvessels.

Sunitinib inhibition of Angiogenic sprouting

An angiogenic sprouting mixture was prepared by supplementing basal media with 50 ng/mL VEGF, 2 ng/mL PMA and 500 nM S1P. Sunitinib was prepared by diluting a 10 mM Sunitinib stock solution in DMSO in basal medium. This angiogenic sprout mixture with Sunitinib to was added to the bottom perfusion inlet well and outlet well (BI-BO) to induce angiogenic sprouting. Medium supplemented with 30 ng/mL VEGF and 20 ng/mL bFGF and Sunitinib was added to all other wells.

Fixation, staining and imaging

Same as protocol described in chapter 5a, step 6.1-6.8

Sprouting and assay performance quantification

The sprouting was quantified using a custom module developed in Molecular Devices MetaXpress software. Briefly, this module segments the max projection of the angiogenic sprouts into vessels and nuclei within the vessels in order to extract the total vessel area, the total vessel length and the y-position of the nuclei. We quantified the average migration distance by extracting the average Y-position of the 10 furthest nuclei in µm minus 400 µm (the average y-position of the monolayer against the gel) for the negative controls.

The assay performance parameters are defined as follows: m_t and s_t are the mean and standard deviation of the top (maximum) control signal, respectively. Similarly, m_b and s_b are the mean and standard deviation of the bottom (minimum) control signal, respectively. Then,

$$SW = \frac{m_t - m_b - 3(s_t + s_b)}{s_t},$$

$$Z' = \frac{m_t - m_b - 3(s_t + s_b)}{m_t - m_b} = 1 - \frac{3(s_t + s_b)}{m_t - m_b},$$

and

$$AVR = \frac{3(s_t + s_b)}{m_t - m_b},$$

where SW = signal window, Z′ = Z′ factor, and AVR = assay variability ratio.

Results

Sunitinib and 3PO inhibit HUVEC and hiPSC-EC sprouting

We validated the usage of hiPSC-ECs in our anti-angiogenesis model by directly comparing their response with HUVEC. Sunitinib and 3PO were used to inhibit angiogenic sprouting. This shows that the sprouting of hiPSC-EC is inhibited similar to primary HUVECs, both with Sunitinib (Figure 1a) and 3PO (Figure 1b).

Next, we quantified the Sunitinib inhibition of angiogenic sprouting of both HUVEC and hiPSC-ECs. Angiogenesis was induced using VEGF+S1P and PMA in combination with various concentrations (1, 3, 5, 10, 30, 50 and 100 nM) of Sunitinib. This shows

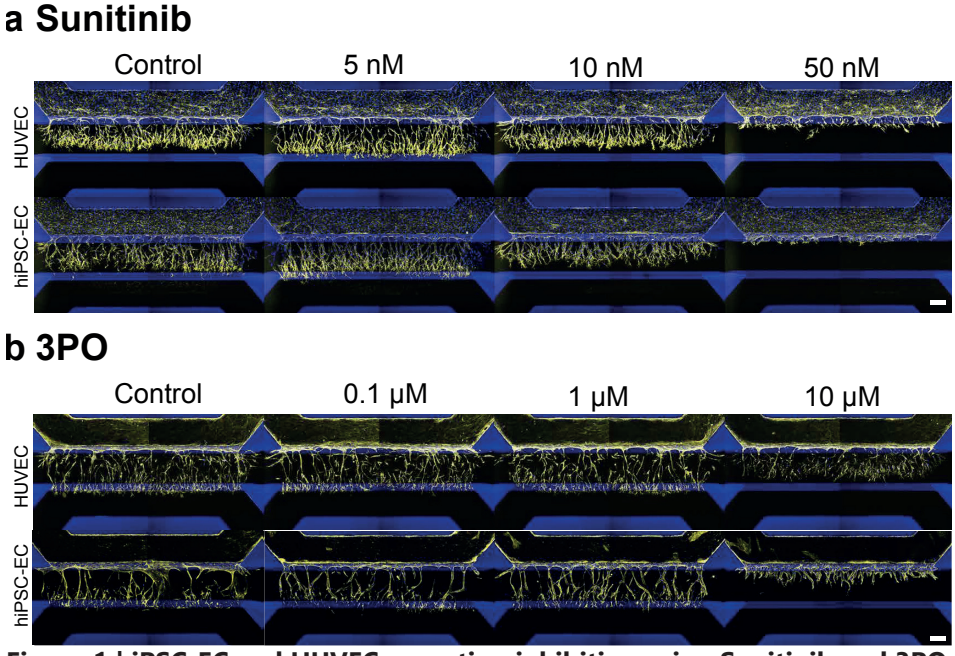

Figure 1 | iPSC-EC and HUVEC sprouting inhibition using Sunitinib and 3PO

Representative images of angiogenic sprouts of HUVEC and iPSC-EC. Sprouts were stimulated with angiogenic growth factactors for 48 hours in combination with various concentrations of Sunitinib **(a)** *or 3PO* **(b)**. *Stained for F-actin (yellow) and nucleus (blue). Scale bar = 200 µm.*

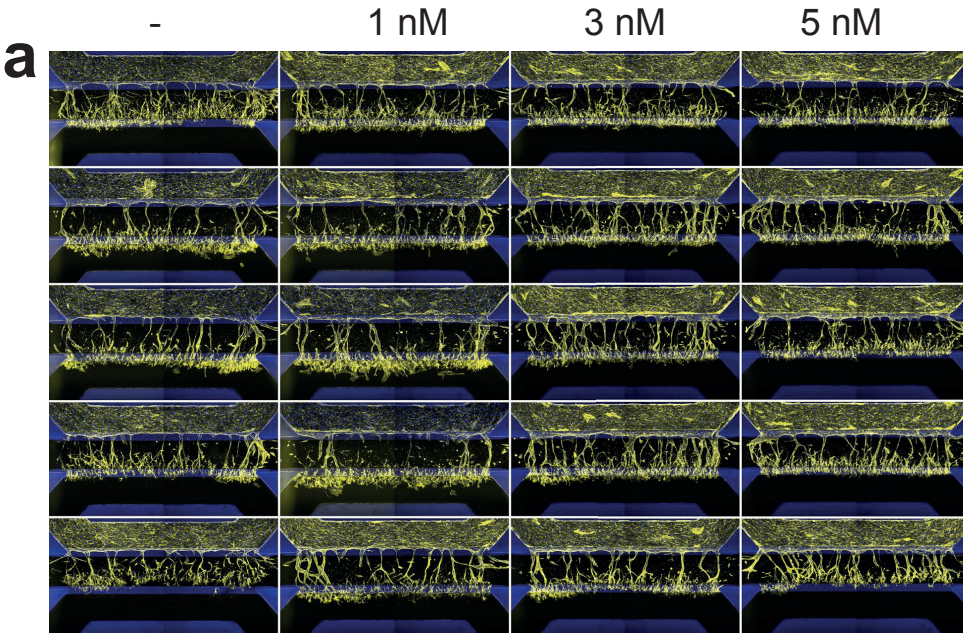

▲►Figure 2 | Inhibition of sprouting using Sunitinib of iPSC-EC

(a) *Representative images of angiogenic sprouts of iPSC-EC after 48 hours in combination with various concentrations of Sunitinib. Stained for F-actin (yellow) and nucleus (blue).* **(b)** *Vessels (blue) and nuclei (yellow) segmentation result with complete inhibition (left) and without inhibition (right)* **(c)** *Quantified sprout length, normalized to the positive control (n=2)* **(d-f)** *Assay window of hiPSC-ECs with or without Sunitinib inhibiton using total vessel area, sprout distance and total nuclei in vessels as parameter.* **(g)** *Assay performance characteristics of the quantified parameters, including the coefficient of variantion (CoV) of each parameter.*

that Sunitinib inhibits the sprouting of hiPSC-ECs at nanomolar levels and demonstrates the angiogenic sprouting in this assay is VEGF-driven (Figure 2) and comparable with sprouting of HUVECs.

We quantified sprouts between 1-50 µm in diameter in the TRITC channel and quantify the nuclei positions within the sprouts using the DAPI channel. We quantified the average migration distance by extracting the average Y-position of the 10 furthest nuclei (Figure 2b, yellow) in µm minus 400 µm (the average position of the monolayer against the gel) for the negative controls, and we quantified the area of vessel-like

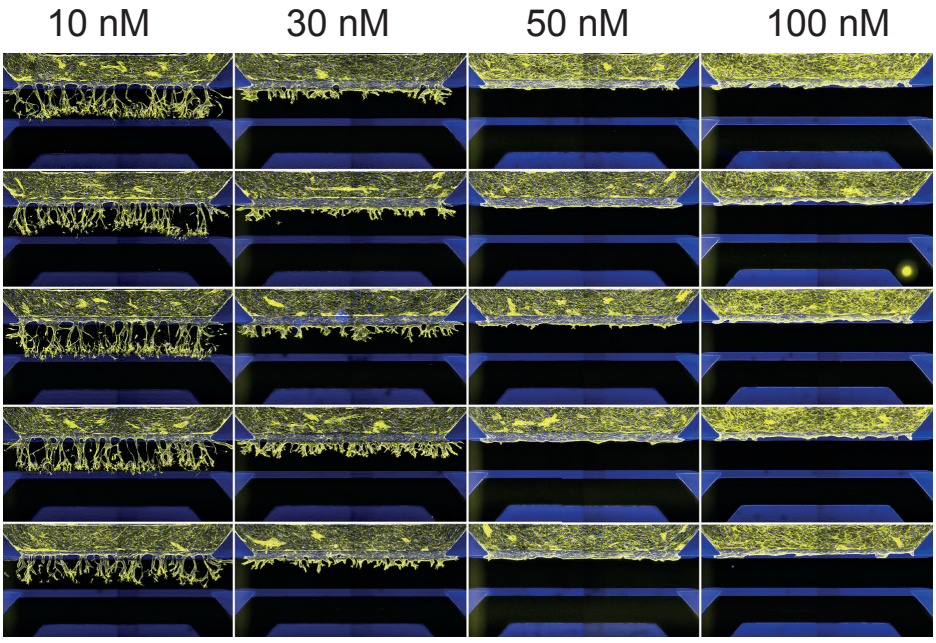

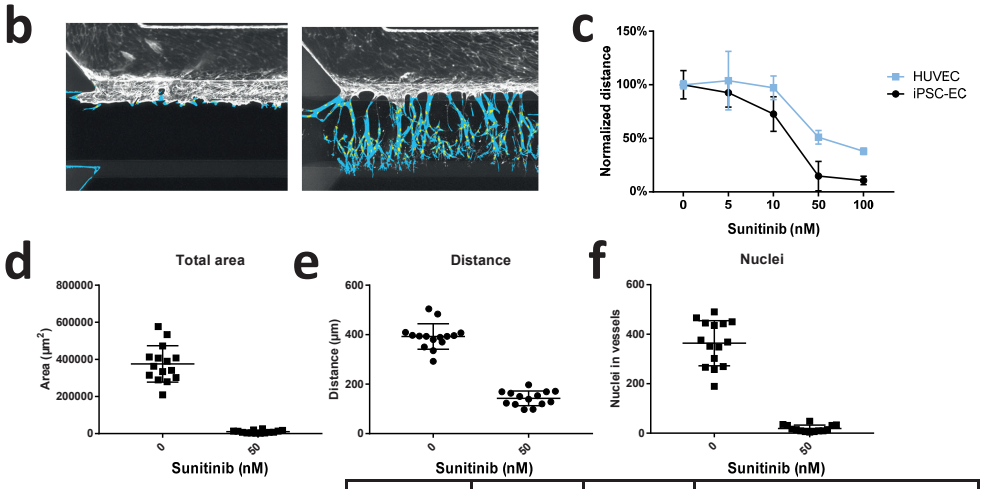

g

	Total area	Distance	Nuclei	Reference values
Signal Window	11,70	14,76	11,68	Acceptable: >1
Z'-factor	0,78	0,75	0,77	Acceptable: >0,5
Assay variability ratio	0,84	0,94	0,88	Recommended: < 0.6
CoV Max. signal 0 nM (%)	25	13	24	Acceptable: < 20
CoV Min. signal 50 nM (%)	70	20	71	Acceptable: < 20

structures (Figure 2b, light blue), and quantified both the inhibition of HUVECs and hiPSC-ECs (Figure 2c).

Finally, in order to quantify the assay performance when hiPSC-EC are used, different quantification parameters (sprouting distance, nuclei in vessels and total vessel area) were obtained. From every parameter, the assays signal window (SW), Z'-factor (Z') and assay variability window (AVR) were calculated. 0 nM of Sunitinib was chosen as maximum control signal, and 50 nM of Sunitinib as minimum control signal (Figure 2d-g).

Discussion

We described a phenotypic anti-angiogenesis screening assay of 40 perfusable microvessels using both HUVEC and hiPSC-derived endothelial cells, and shown that hiPSC-ECs are able to reproduce important aspects of angiogenic sprouting, including the differentiation into tip cells that display their characteristic filopodia and the trailing stalk cells form lumen. Furthermore, directional and repetitive sprouting is observed, which is an important indication that the cells are able to sense the imposed VEGF-gradient. We validated the use of ECs derived from hiPSCs in our assay by directly comparing their response to angiogenic inhibitors with primary ECs.

Sunitinib inhibited the sprouting of both HUVECs and hiPSC-ECs at nanomolar levels, which suggests that the angiogenic sprouting of hiPSC-ECs is mediated through VEGFR2 signaling. Interestingly, Sunitinib inhibited the hiPSC-EC sprout formation at concentrations ≥50 nM, while HUVECs showed single cell invasion into the collagen-1 matrix at concentrations ≥50 nM. Either the hiPSC-ECs are more sensitive to VEGF, or insensitive to other angiogenic factors that are present (e.g. PMA, S1P, bFGF). The concentrations of Sunitinib that completely inhibited the angiogenic sprouting is in he same range as the inhibiting plasma concentration in mice (50-100 mg/mL) and human (37,5 - 75 ng/ml; 94-188 nM)[19], not taking into account the differences free/unbound concentration of Sunitinib.

Our data shows that 3PO inhibits the angiogenic sprouting of hiPSC-ECs in the same

fashion as in HUVECs, which suggests that hiPSC-ECs, similar to primary ECs, undergo the same metabolic switch to use glycolysis as main energy source during angiogenic sprouting[18]. While the inhibition using both Sunitinib and 3PO appeared similar when hiPSC-ECs is compared to HUVECs, more data is required to quantify the assays performance of 3PO on HUVECs.

The total sprout area, nuclei in vessels and sprout length to quantify the angiogenic sprouting showed acceptable Z' for complex phenotype assays[20]. The quantification of sprout length had the lowest coefficient of variantion, which is probably since it is less sensitive small differences in sprout density. Although area quantification is an interesting phenotypic readout to study as this is describes the lumen development and proper functioning tip- and stalk cells[21], we observed significant differences in sprouting density. Probably, the differences in sprout density are caused by differences in initial seeding densities: proper sprout development requires proper DLL4-Notch signaling that are only expressed in confluent monolayers[22,23]. This suggests that the performance of the assays can be further increased by more homogenous seeding densities, for example using the previously described passive pumping method.

Maximum inhibition using 50 nM Sunitinib showed a shift of the monolayer compared to control. This suggests that other pathways that result in the growth and matrix degradation are still active and that the angiogenic sprouting cocktail can be further optimized. Preliminary results have shown that HUVECs and hiPSC-ECs are still able to form sprouts without PMA. As it is known that PMA activates a myriad of pathways that affect the proliferation and lumen formation[24], omitting this from the angiogenic sprouting mixture is likely to increase the assays sensitivity for VEGF and S1P while preventing the shift of the monolayer.

Conclusion

We have demonstrated that hiPSC-ECs are an attractive alternative to primary endothelial cells when used in a physiologically relevant *in vitro* anti-angiogenesis as-

say. The combination of a standardized microfluidic 3D cell culture platform with a scalable and more standardized cell source is a major step in the standardization of physiologically relevant *in vitro* angiogenesis assays, as it offers the required robustness, compatibility and scalability to be integrated within the drug screening infrastructure.

Acknowledgments

This work is in part supported by a research grants from the 'Meer Kennis met Minder Dieren' program (project number 114022501) of The Netherlands Organization for Health Research and Development (ZonMw) and the Dutch Heart Foundation CVON consortium grant RECONNECT.

Disclosures

P. Vulto and T. Hankemeier are shareholder of Mimetas BV. A. Reijerkerk is employee of Ncardia BV.

REFERENCES

1 Wong, B. W., Marsch, E., Treps, L., Baes, M. & Carmeliet, P. Endothelial cell metabolism in health and disease: impact of hypoxia. *EMBO J.* **36** (15), 2187-2203, (2017).

2 Horvath, P. *et al.* Screening out irrelevant cell-based models of disease. *Nat Rev Drug Discov.* **15** (11), 751-769, (2016).

3 Eglen, R. M. & Randle, D. H. Drug Discovery Goes Three-Dimensional: Goodbye to Flat High-Throughput Screening? *Assay Drug Dev Technol.* **13** (5), 262-265, (2015).

4 Nowak-Sliwinska, P. *et al.* Consensus guidelines for the use and interpretation of angiogenesis assays. *Angiogenesis.* 10.1007/s10456-018-9613-x, (2018).

5 Griffith, L. G. & Swartz, M. A. Capturing complex 3D tissue physiology in vitro. *Nature Reviews Molecular Cell Biology.* **7** (3), 211-224, (2006).

6 Davis, G. E. *et al.* Control of vascular tube morphogenesis and maturation in 3D extracellular matrices by endothelial cells and pericytes. *Methods Mol Biol.* **1066** 17-28, (2013).

7 Smith, A. O., Bowers, S. L., Stratman, A. N. & Davis, G. E. Hematopoietic stem cell cytokines and fibroblast growth factor-2 stimulate human endothelial cell-pericyte tube co-assembly in 3D fibrin matrices under serum-free defined conditions. *PLoS One.* **8** (12), e85147, (2013).

8 Kim, S., Chung, M. & Jeon, N. L. Three-dimensional biomimetic model to reconstitute sprouting lymphangiogenesis in vitro. *Biomaterials.* **78** 115-128, (2016).

9 Kim, C., Kasuya, J., Jeon, J., Chung, S. & Kamm, R. D. A quantitative microfluidic angiogenesis screen for studying anti-angiogenic therapeutic drugs. *Lab Chip.* **15** (1), 301-310, (2015).

10 Kim, J. *et al.* Engineering of a Biomimetic Pericyte-Covered 3D Microvascular Network. *PLoS One.* **10** (7), e0133880, (2015).

11 Tourovskaia, A., Fauver, M., Kramer, G., Simonson, S. & Neumann, T. Tissue-engineered microenvironment systems for modeling human vasculature. *Exp Biol Med (Maywood).* **239** (9), 1264-1271, (2014).

12 Junaid, A., Mashaghi, A., Hankemeier, T. & Vulto, P. An end-user perspective on Organ-on-a-Chip: Assays and usability aspects. *Current Opinion in Biomedical Engineering.* **1** 15-22, (2017).

13 Pagano, G. *et al.* Optimizing design and fabrication of microfluidic devices for cell cultures: An effective approach to control cell microenvironment in three dimensions. *Biomicrofluidics.* **8** (4), 046503, (2014).

14 Berthier, E., Young, E. W. & Beebe, D. Engineers are from PDMS-land, Biologists are from Polystyrenia. *Lab Chip.* **12** (7), 1224-1237, (2012).

15 Dejana, E., Hirschi, K. K. & Simons, M. The molecular basis of endothelial cell plasticity. *Nat Commun.* **8** 14361, (2017).

16 Geraghty, R. J. *et al.* Guidelines for the use of cell lines in biomedical research. *Br J Cancer.* **111** (6), 1021-1046, (2014).

17 Passier, R., Orlova, V. & Mummery, C. Complex Tissue and Disease Modeling

using hiPSCs. *Cell Stem Cell.* **18** (3), 309-321, (2016).

18 Schoors, S. *et al.* Partial and transient reduction of glycolysis by PFKFB3 blockade reduces pathological angiogenesis. *Cell Metab.* **19** (1), 37-48, (2014).

19 Mendel, D. B. *et al.* In vivo Antitumor Activity of SU11248, a Novel Tyrosine Kinase Inhibitor Targeting Vascular Endothelial Growth Factor and Platelet-derived Growth Factor Receptors. *Determination of a Pharmacokinetic/ Pharmacodynamic Relationship.* **9** (1), 327-337, (2003).

20 Iversen, P. W., Eastwood, B. J., Sittampalam, G. S. & Cox, K. L. A comparison of assay performance measures in screening assays: signal window, Z' factor, and assay variability ratio. *J Biomol Screen.* **11** (3), 247-252, (2006).

21 Arima, S. *et al.* Angiogenic morphogenesis driven by dynamic and heterogeneous collective endothelial cell movement. *Development.* **138** (21), 4763-4776, (2011).

22 Sharghi-Namini, S., Tan, E., Ong, L. L., Ge, R. & Asada, H. H. Dll4-containing exosomes induce capillary sprout retraction in a 3D microenvironment. *Sci Rep.* **4** 4031, (2014).

23 Bentley, K., Mariggi, G., Gerhardt, H. & Bates, P. A. Tipping the balance: robustness of tip cell selection, migration and fusion in angiogenesis. *PLoS Comput Biol.* **5** (10), e1000549, (2009).

24 Taylor, C. J., Motamed, K. & Lilly, B. Protein kinase C and downstream signaling pathways in a three-dimensional model of phorbol ester-induced angiogenesis. *Angiogenesis.* **9** (2), 39-51, (2006).

Supplementary figures

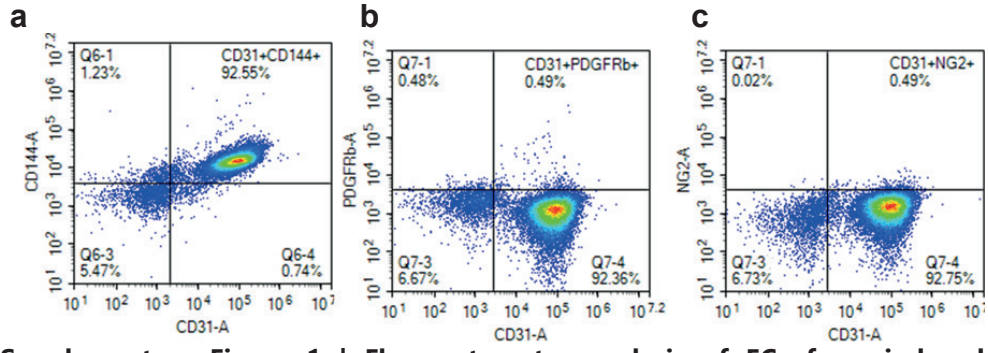

Supplementary Figure 1 | Flow cytometry analysis of ECs from induced pluripotent stem cells

Flow cytometry analysis comparing the expression of CD31 with the expression of CD144 **(a)** *PDGFRb* **(b)** *and NG2* **(c)** *2 days after differentation.*

CHAPTER 7

Discussion and conclusion

Microfluidics is increasingly recognized as an important tool to engineer cellular micro-environments *in vitro* and increase its physiological relevance[1-4]. This has led to an increasing interest in 3D cell culture models that make use of microfluidic techniques. We identified the three main drivers to move from traditional cell culture methods to microfluidic 3D cell culture: the ability to apply perfusion, the possibility to compartmentalize cells and hydrogels and the spatial control over signaling gradients **(chapter 2).** We concluded that vascular models benefit the most of these enhancements, and thus should be the ideal model to demonstrate and validate how microfluidics advances 3D cell culture.

This thesis focuses on the design of vascular models in robust, standardized assays with sufficient throughput and increased physiological relevance over 2D and 3D cell culture models. This not only meets the needs within drug research, but it will also help in the validation of these models and its possible application in clinical diagnosis.

Microfluidic 3D cell culture: from promise to paradigm

Many microfluidic cell culture models clearly demonstrate the unique advantages that microfluidics has over traditional culture methods[5-10]. However, although this increased our understanding of how microfluidic tools can be used to improve the physiological relevancy *in vitro*, routine adoption of microfluidic cell culture techniques is still limited. What are the current limitations that need to be addressed for microfluidic based approaches to become the gold standard in cell culture practice?

First, many of these microfluidic devices are designed from an engineering perspective[11,12], and while there are many available protocols with a detailed description of the manufacturing process of various microfluidic cell culture devices, these devices still need to be microfabricated by the end-user. This limits the availability of microfluidic cell culture platforms to a wider audience: not only does this require the end-user to have manufacturing equipment and sufficient technical knowledge, it also puts constraints on the used materials in terms of their manufacturability.

Furthermore, there is limited quality control of the end-product, which introduces variation and can negatively affect the reproducibility of the corresponding assays.

Second, while there is a wealth of microfluidic devices for 3D cell culture published in the academic literature, there is limited consensus which ones are most suitable. For example, to compartmentalize cells and hydrogels, some devices use geometrical structures like pillars or ridges[13,14], while others use casting or direct patterning[15,16]. Some devices rely on passive diffusion of cell culture media, while others implement pump setups. Such differences limit the comparability of the results obtained in different devices.

Finally, whether increased physiological relevance *in vitro* leads to better prediction of the clinical efficacy and safety is still an open question. Standardized microfluidic culture platforms with sufficient throughput will play a fundamental role in the systematic characterization of the most important parameters to culture a specific tissue or disease of interest.-

Validation of the predictive validity

Validation of *in vitro* models requires prior knowledge about the (patho)physiology in humans, and this knowledge should be translated to an *in vitro* assay. Ideally, an *in vitro* disease model is linked to a clear clinical question or scenario, and probably even more important, a clinical outcome. A disease model should reflect the appropriate disease context, including the right cell types that are known to be involved in a disease mechanism within an appropriate microenvironment. Such a cellular microenvironment should have the correct ECM composition, mechanical forces (matrix stiffness, shear forces), atmospheric condition (e.g. oxygen tension and pH) in order to study a disease mechanism as realistically as possible.

A validated set of assay conditions can help in identifying which microfluidic techniques increase the physiological relevance the most and thus are likely to increase the predictive value. For example, how important is perfusion and flow and does the directionality matter? Can biomarkers be identified that are uniquely expressed in

such engineered microenvironments that justify the added complexity? What parameters can be omitted in order to favor simplicity and scalability?

Validation of the predictive value of an assay could be determined using a set of molecules that have demonstrated clinical efficacy or toxicity. Another interesting approach is validation according to a human physiology assay checklist[17], which contains a set of validated (mechanistic) biomarkers per tissue or disease. Together with open-source assays and results, a set of design principles can be deducted to understand what assay condition result in the best recapitulation *in vitro*.

The crucial step is finding links between diseases and mechanistic pathways. One way is by determining the 'metabolic fingerprint' of a disease, using a quantitative description of all low-molecular-weight (<1 kDa) metabolites in a biological sample (e.g. blood plasma). Metabolites are the substrates and products of the cellular metabolism and drive essential cellular functions, such as energy production, signal transduction and apoptosis. Therefore, the cellular metabolome closely reflects the cellular phenotype. This allows the identification of biomarkers and mechanisms that are uniquely associated with a particular phenotype (e.g. health or disease). For example, it has been shown that endothelial cells undergo a metabolic shift during angiogenesis[18-21], which can be targeted to prevent angiogenic sprouting or normalize vascular function.

A multi-omics approach that integrates data from genomics, epigenomics, proteomics, transcriptomics and metabolomics will be required to determine the relationships between gene and protein expression and metabolite concentrations. This might be a required step to comprehend both the underlying disease mechanisms as well as understanding the disease model.

Perfusable microvessels *in vitro*

In **chapter 3**, we have demonstrated that passive levelling as a source of flow is sufficient to achieve selective permeability of microvessels *in vitro*: one of the important hallmarks of healthy, quiescent vasculature. We quantified this selective permeability

with the use of two tracer dyes: 20 kDa- and 150 kDa fluorescently labeled dextrans, and show that the microvessels in this platform exhibited a permeability to 20 kDa dextran but not to 150 kDa dextran, which mimics the functionality of vasculature *in vivo*. Also, a dose-dependent effect of VEGF, TNFα and several cytokines confirmed a physiologically relevant response. This demonstrates that the 96 perfused microvessels in this platform are suitable as a standardized platform to study microvessels with a physiological relevant behavior in a high-throughput fashion.

Interestingly, these results question the requirement for unidirectional flow in such permeability studies. We showed that unidirectional flow not required to achieve physiological relevant permeabilities, as perfusion in our assay is bi-directional and oscillatory. However, turbulent flow is absent due the laminar flow profiles that are inherently present due the low Reynolds number that is achieved in the channel dimensions used by us.

Nonetheless, the microvessels in this platform are periodically exposed to significant levels of shear (max. 5 dyne/cm^2), but only after the rocker position has been changed. In contrast, similar-sized venules *in vivo* are exposed shear levels between 1 to 5 dyne/cm^2. These results question the importance of high shear in vascular models in order to study permeability, as a low permeability can also be achieved just with exposure to laminar flow with low shear. We recommend to further investigate these findings in comparison to a setup which exposes the microvessels to a unidirectional flow.

From microvessels to 3D microvascular networks

Geometry and substrate stiffness play an important role in vascular biology, as bi-directional interactions between endothelial cells and the underlying extracellular matrix regulate adhesion and cellular responses. Cell interact with their ECM through cell adhesions structures, which result in cytoskeleton remodeling in response to binding sites and mechanical properties (e.g. stiffness, elasticity) of the ECM. It has been hypothesized that depending on the scaffold stiffness, different adhesion structures are present[22]. While the previously described permeability assay quantifies the permea-

bility of cells grown against a soft collagen-1 scaffold, the majority of the cells are in contact substrates with non-physiological stiffness. In contrast, cells would experience more physiological relevant mechanical forces when fully surrounded by ECM.

Thus, in order to create 3D vasculature that is surrounded by ECM, we studied how these single microvessels described earlier can be triggered to form angiogenic sprouts within the patterned collagen-1 gel.

In **chapter 4** that the microfluidic channels can be designed such that stable, reproducible and controllable biomolecular gradients can be generated. We used these gradients to study how microvessels form a 3D microvascular network within the patterned collagen-I gel. We optimized the angiogenic stimuli to trigger gradient-driven angiogenic sprouting and found that a gradient of vascular endothelial growth factor-165 (VEGF-165), phorbol 12-myristate 13-acetate (PMA) and sphingosine-1-Phospate (S1P) was the most optimal cocktail to trigger robust, directional angiogenesis, with S1P being crucial for the guidance and repetitive sprout formation.

Interestingly, continuous culture resulted in anastomosis with the bottom channel, with angiogenic sprouts traversing the collagen-I gel. This resulted in the optimization and reduction in the number of capillaries in the microvascular network. Perfusion of the sprouts with fluorescently labeled dextran showed that angiogenic sprouts that did not anastomose were permeable near the tip/stalk cell region. In contrast, anastomosed sprouts retained the 150 kDa dextran solution within their lumen, suggesting that the connection between the two channels triggers maturation of the ECs in the sprouts, as they adopt their characteristic phalanx phenotype including mature cell-cell junctions.

In reference to pre-existing models for studying 3D angiogenesis *in vitro*, our model allows routine experimentation at sufficient throughput. It allows to study the permeability in combination with angiogenesis, and can be used to understand how the vascular permeability changes between the sprouting and maturation phase of angiogenesis *in vitro*.

With the recognition that also perivascular cells play an important role during angiogenesis, from the onset to the final maturation phase, it will be interesting to study the effect of these cells in this model. For example, macrophages are known to affect the vascular patterning by guiding and connecting tip cells, and pericytes adhere and stabilize angiogenic sprouts. Both of these cell types can be embedded within the ECM.

For the integration of vascular smooth muscle cells and transcriptome analysis of the cells within these assays, the platform would benefit from a surrounding extracellular within the perfusion channel. Various methods have shown the possibility to form lumen within a patterned collagen-1 matrix (e.g. using rods[23]), but it remains to be investigated whether this method is feasible in this pre-manufactured platform without compromising on the scalability and ease-of-use.

Endothelial cell sources for in vitro drug research and drug screening

In the past, *in vitro* disease modeling and drug screening relied either on usage the cell derived from patient's samples or the usage of immortalized cell lines. However, both of these cell sources have their limitations: cells derived from patient samples have limited availability and scalability, and their phenotype is a result of both their genetic as well as their environmental background. On the other hand, cell lines often contain genetic and metabolic abnormalities which affect the translation of these findings to more phenotypically relevant model systems.

Part of the work in this thesis has been performed using the VeraVec-HUVECs. These cells have a lentiviral introduced E4ORF1 gene that enables long-term survival of these cells (cells can be maintained up till passage 12), without losing their endothelial phenotype[25]. This enables the expansion and cryopreservation of a single HUVEC clone, which makes these cells amenable for drug screening purposes. Importantly, the pro-survival effect of E4ORF1 is due to constitutive phosphorylation of Akt and autocrine activation of FGF-R1 by increased expressions of FGF-2[25]. Still, these cells remain responsive to VEGF-A and are able to undergo tubulogenesis and sprouting

in vitro and *in vivo*.

However, while this lentiviral E4ORF1 modification solves the issues of scalability and availability, the primary nature of these cells still exhibit donor to donor variation which could have an impact the results in large screening assays which require multiple donors to yield enough cells. Furthermore, this lentiviral modification can only be done on obtainable cells, which limits the possibility to build for example mimic human brain vasculature that incorporate human astrocytes and perivascular cells.

Cell differentiated from patients-derived iPSC overcomes the issues of availability and scalability while also enabling the generation of cell types which are otherwise difficult to obtain (e.g. neurons and cardiomyocytes[26]). Furthermore, as iPSCs are self-renewing, they can be expanded in nearly unlimited quantities. This makes that *in vitro* assays based on cells derived from iPSCs are ideal for usage within *in vitro* screening models.

In **chapter 5**, we showed that iPSC differentiated into endothelial cells (iPSC-ECs) have comparable characteristics as primary endothelial cells. Upon stimulation with an angiogenic cocktail we observed angiogenic sprouting that is comparable to the sprouting of primary endothelial cells (HUVEC), including the formation of tip-, stalk and phalanx cells.

Furthermore, after anastomosis the non-connected angiogenic sprouts regressed towards the monolayer. In contrast, the connected sprouts decreased their permeability but showed an increased lumen diameter over time. Not only is this similar to what was observed with HUVECs previously, this also demonstrates that these important mechanisms that occur during angiogenesis are preserved in iPSC-ECs.

We further investigated the possible usage of this model as a phenotypic anti-angiogenesis model in **chapter 6**. We used the clinically available angiogenesis inhibitor Sunitinib and observed that these cells respond to an inhibitory concentration that is comparable to primary HUVECs, and show that also iPSC-ECs require VEGF signaling in their response to angiogenic stimuli. This indicates that these cells can be used

in an angiogenic sprouting assay. Furthermore, the concentration of Sunitinib that completely inhibited the angiogenic sprouting in this assay (>50 nM) is in the same range as the inhibiting plasma concentration in mice (50-100 mg/mL, 125-251 nM) and humans (37,5 - 75 ng/ml; 94-188 nM)[27], not taking into account the possible differences between free and unbound concentration of Sunitinib between *in vitro* and *in vivo*.

One of the current issues is that it is unclear to what extent iPSCs differ from true pluripotent stem cells (e.g. embryonic stem cells)[28]. While some studies have shown that iPSCs retain some of the gene expression and epigenetic modifications (e.g. DNA methylation) of the somatic cell origin[29], a meta-analysis showed no consistent difference in chromatin structure and gene expression between ESCs and iPSC[30]. However, such a memory effect could affect phenotype of the cells differentiated from iPSC[31], as it has been shown that cardiomyocytes differentiated from iPSC have a more immature, fetal-like phenotype[32], which might also be true for other cell types that are differentiated from iPSCs.

The question is whether this immature phenotype is a consequence of the protocols used for differentiation, or is this an effect of the limited physiological relevancy that is offered to these cells *in vitro*? Do iPSC-derived cells require cues in their cellular microenvironment to achieve a more mature phenotype *in vitro* (e.g. 3D microenvironment, interaction with perivascular cells and/or exposure to flow)?

Together, we have demonstrated the feasibility of using a complex phenotypic assay within a high-throughput screening setting when a scalable and physiological relevant cell source is used. With the possibility to produce iPSC-ECs in large quantities, these cells will be a valuable addition to study angiogenesis in a standardized platform using a standardized cell source. Increased understanding and optimization in the iPSC-differentiation will enable the development of tissue specific which would both increase the physiological relevance of various other organ models systems *in vitro* and is likely to have a major impact in the drug research *in vitro*.

Future directions

Recently, several other promising biological and technical have been developed that have the potential to radically change how drug research is performed using *in vitro*. For example, 3D printing allows printing of cells and biocompatible scaffolds in unique spatial configurations, and precise genome editing could have a major impact in the cells that are used *in vitro*, especially in the combination with the discovery that stem cells are able to form complex, multicellular structures (organoids). How can each of these advancements contribute to drug research and what would be the role of microfluidic cell culture in this?

Vascularization of organoid cultures *in vitro*

The identification of tissue specific stem cells has led to the development of organoids: clusters of multiple cell types that can be grown *in vitro* that mimic tissue functionality *in vivo*. Such tissue specific stem cells were first identified in self-renewing organs, and thus enabled the formation of organoids of for example liver[33,34], small intestine[35-37], brain[38] and kidney[39] organoids.

These multicellular structures are formed out of a single induced, embryonic or adult stem cell[40,41], and show that stem cells have an intrinsic capacity to differentiate into multicellular structures that consist of various differentiated cell types. This results in a tissue architecture that more closely resembles that of naïve tissues.

However, the current limitation in the culture of organoids *in vitro* is the lack of perfused vasculature, which restricts the organoid size *in vitro* to a few millimeters. While it is possible to implant organoids *in vivo* to supply the organoid with the hosts vasculature[42], this limits the throughput that is required in drug-discovery and does not offer the fine control over the cellular microenvironment that is possibly associated with *in vitro* assays.

The integration of organoids into microfluidic cell culture platforms has the potential to control or steer the vascularization of organoids. Interestingly, recently It has been shown that iPSCs are able to differentiate into a mixture of endothelial cells and

pericytes, which resulted in vascular networks with associated pericytes *in vitro*[43]. But, similar to other organoid cultures, this vasculature was not perfused, which limited their growth and survival *in vitro*.

Understanding how and when vasculature interacts during the development of organoids will enable the formation of vascularized organoids. This could extend their live span *in vitro*, and increase the physiological relevancy of organoids. Such insight will accelerate the field of tissue regeneration and the development of bioengineered organs.

Precise genome editing for disease modeling *in vitro*

Currently, drug discovery *in vitro* is accelerated by recent developments in precise genome editing, which allows modifications to endogenous genes. Tags to be added to the native protein in a strategy called 'endogenous tagging', which is useful to develop assays can be developed that monitor gene products at endogenous levels. This is advantageous over overexpressing cell lines or reporter gene lines, which express gene products at non-physiological quantities.

Furthermore, applying genome editing to iPSCs will enable the development of libraries of gene knockouts and knock-ins, the introduction of specific deletions or insertions and the ability to induce or repress transcription. This can be for example used to study mechanisms and pathways.

Patient-derived iPSC have been successfully used to model hematological, neurological, cardiac and cardiovascular diseases *in vitro*. For example, iPSC-derived cardiomyocytes have been used to study cardiac arrhythmias, such as inherited long QT-interval syndrome[44], and neuronal disorders, such as Huntington's disease[45] and RETT syndrome[46]. Precise genome editing of patient-derived iPSC-cells could also be used to generate lines that reflect inherited vascular disorders[47], such as hereditary hemorrhagic telangiectasia (HHT) or cerebral cavernous malformations (CCM). Being able to study the disease mechanisms *in vitro* will help to stratify patients and predict clinical outcome.

Focusing on vasculature, it would be interesting which genes drive the heterogeneity of vasculature within different tissues: depending of the tissue, the (micro)vasculature has different barrier properties, angiogenic potential, and metabolic rate depending on the organ. However, many of this heterogeneity is lost when cultured *in vitro* after 72 hours[48], which suggests that besides the correct genotype, a physiological relevant cellular microenvironment is required to maintain the correct vascular phenotype.

It has been shown endothelial cells express clusters of transcription factors, angiocrine growth factors, adhesion molecules, and chemokines in unique combinations in each organ[49,50]. Microfluidic cell culture techniques can play a important role in providing the right spatial-temporal control over signals that drive endothelial cells differentiation. Recreating organ-specific vascular beds will advance the vascularization of organoids and tissues *in vitro*.

3D printing of cell culture models

Recent advances show the possibility to 3D print biocompatible and biodegradable scaffolds, hydrogels and cells. Such 3D printed cell culture models allow the realization of novel, unique geometries and structures that are not possible using conventional manufacturing and microfabrication techniques. For example, 3D printing can be used to generate complex, 3D microvascular networks that include bifurcations, different diameters and spatially defined perivascular cells[51-54].

As 3D printing can be used to directly print cells and scaffolds into a desired spatial configuration, it enables rapid prototyping and offers more flexibility in the spatial definition of multiple cells types. This makes 3D printed *in vitro* models are a promising alternative to pre-manufactured microfluidic cell culture platforms in terms of flexibility, as pre-fabricated microfluidic platforms have restraints in terms of materials, design and geometry.

However, similar to microfluidic cell culture models, 3D printed *in vitro* models need to balance complexity and compatibility if used as a drug screening platform. Early

examples of 3D printed *in vitro* models often lack the interfacing and possibility to perform experiments in parallel[55], and lack a standardized interface, quality control and large scale manufacturing. These issues need to be addressed before 3D printed *in vitro* models can be used in drug screening[12].

Also, the question arises how much complexity is necessary in an *in vitro* assay? As cells are able to modify and form complex tissues architectures themselves when the right cues are provided, is it necessary to force cells into a specific spatial configuration? Or can we rely on an approximate spatial distribution using (pre-manufactured) microfluidic channels and use the morphogenic capacity of cells in order to have mature, functional, native-like tissue *in vitro*. Substantial development and research are required before it will be clear how and where 3D printed assays will fit in drug screening pipeline.

Conclusion

The field of microfluidic cell culture has changed tremendously in the last 5 years. Initially microfluidic cell culture was focused on throughput with the development of microfluidic chips that use a massive parallel approach[56,57], often in combination with integrated sensors and actuators and cells cultured in 2D[58]. But, with the increased awareness that microfluidic techniques are uniquely suited to improve the physiological relevance of 3D cell cultures, the current efforts are focused on increasing the complexity *in vitro*[4,59-62].

This thesis was focused on how to improve 3D models of vasculature *in vitro*, and:

1. The identification of the advantages of microfluidic cell culture and how this is uniquely suited to study vasculature *in vitro*.
2. Methods to study the permeability of perfused macro- and microvasculature in standardized platforms that include physiological relevant cellular microenvironments.
3. Development of a high-throughput platform that combines gradients and perfusion within a 3D cellular microenvironment, which enables the study of angiogenic sprouting and vascular remodeling *in vitro*.
4. Demonstrated that iPSC-derived endothelial cells are suitable to study angiogenic sprouting *in vitro*.

The early exploration phase of microfluidics showed how microfluidic can improve the physiological relevance of 3D cell culture, which justifies the increased complexity over traditional cell culture assays. The next step is the validation of the physiological relevancy of these assays and the definition of relevant end-points that can be translated into clinical practice before microfluidics-based 3D cell culture assays will become the new gold-standard in cell culture practice. This requires microfluidic cell culture platforms that are accessible by a wide audience with sufficient throughput to rigorously test in order to optimize the assay conditions and comparability of results between different research groups.

The work in this thesis contributed to the development of microfluidic cell culture models that balance usability and complexity with physiological relevance, which I see as a crucial step in the acceptance of microfluidic cell culture models and in order to become a new standard in vascular drug research.

References

1 Sackmann, E. K., Fulton, A. L. & Beebe, D. J. The present and future role of microfluidics in biomedical research. *Nature*. **507** (7491), 181-189, (2014).

2 Yum, K., Hong, S. G., Healy, K. E. & Lee, L. P. Physiologically relevant organs on chips. *Biotechnol J.* **9** (1), 16-27, (2014).

3 Bhatia, S. N. & Ingber, D. E. Microfluidic organs-on-chips. *Nat Biotechnol*. **32** (8), 760-772, (2014).

4 Sung, K. E. & Beebe, D. J. Microfluidic 3D models of cancer. *Adv Drug Deliv Rev*. **79-80** 68-78, (2014).

5 Kim, J. *et al.* Engineering of a Biomimetic Pericyte-Covered 3D Microvascular Network. *PLoS One*. **10** (7), e0133880, (2015).

6 Bichsel, C. A., Hall, S. R., Schmid, R. A., Guenat, O. T. & Geiser, T. Primary Human Lung Pericytes Support and Stabilize In Vitro Perfusable Microvessels. *Tissue Eng Part A*. **21** (15-16), 2166-2176, (2015).

7 Jeon, J. S. *et al.* Generation of 3D functional microvascular networks with human mesenchymal stem cells in microfluidic systems. *Integr Biol (Camb)*. **6** (5), 555-563, (2014).

8 Tourovskaia, A., Fauver, M., Kramer, G., Simonson, S. & Neumann, T. Tissue-engineered microenvironment systems for modeling human vasculature. *Experimental biology and medicine (Maywood, N.J.)*. **239** (9), 1264-1271, (2014).

9 Kim, S., Lee, H., Chung, M. & Jeon, N. L. Engineering of functional, perfusable 3D microvascular networks on a chip. *Lab Chip*. **13** (8), 1489-1500, (2013).

10 Nguyen, D. H. *et al.* Biomimetic model to reconstitute angiogenic sprouting morphogenesis in vitro. *Proc Natl Acad Sci U S A*. **110** (17), 6712-6717, (2013).

11 Berthier, E., Young, E. W. & Beebe, D. Engineers are from PDMS-land, Biologists are from Polystyrenia. *Lab Chip*. **12** (7), 1224-1237, (2012).

12 Junaid, A., Mashaghi, A., Hankemeier, T. & Vulto, P. An end-user perspective on Organ-on-a-Chip: Assays and usability aspects. *Current Opinion in Biomedical Engineering*. **1** 15-22, (2017).

13 Chung, S., Sudo, R., Vickerman, V., Zervantonakis, I. K. & Kamm, R. D. Microfluidic platforms for studies of angiogenesis, cell migration, and cell–cell interactions. *Annals of Biomedical Engineering*. **38** (3), 1164-1177, (2010).

14 Yeon, J. H., Ryu, H. R., Chung, M., Hu, Q. P. & Jeon, N. L. In vitro formation and characterization of a perfusable three-dimensional tubular capillary network in microfluidic devices. *Lab Chip*. **12** (16), 2815-2822, (2012).

15 Zheng, Y. *et al.* In vitro microvessels for the study of angiogenesis and thrombosis. *Proc Natl Acad Sci U S A*. **109** (24), 9342-9347, (2012).

16 Chrobak, K. M., Potter, D. R. & Tien, J. Formation of perfused, functional microvascular tubes in vitro. *Microvasc Res*. **71** (3), 185-196, (2006).

17 Horvath, P. *et al.* Screening out irrelevant cell-based models of disease. *Nature Reviews Drug Discovery*. **15** (11), 751-769, (2016).

18 Yu, P. *et al.* FGF-dependent metabolic control of vascular development. *Nature.* **545** (7653), 224-228, (2017).

19 Schoors, S. *et al.* Fatty acid carbon is essential for dNTP synthesis in endothelial cells. *Nature.* **520** (7546), 192-197, (2015).

20 Schoors, S. *et al.* Partial and transient reduction of glycolysis by PFKFB3 blockade reduces pathological angiogenesis. *Cell Metab.* **19** (1), 37-48, (2014).

21 Goveia, J., Stapor, P. & Carmeliet, P. Principles of targeting endothelial cell metabolism to treat angiogenesis and endothelial cell dysfunction in disease. *EMBO Mol Med.* **6** (9), 1105-1120, (2014).

22 Harunaga, J. S. & Yamada, K. M. Cell-matrix adhesions in 3D. *Matrix Biol.* **30** (7-8), 363-368, (2011).

23 Jimenez-Torres, J. A., Peery, S. L., Sung, K. E. & Beebe, D. J. LumeNEXT: A Practical Method to Pattern Luminal Structures in ECM Gels. *Adv Healthc Mater.* **5** (2), 198-204, (2016).

24 Bischel, L. L., Lee, S. H. & Beebe, D. J. A practical method for patterning lumens through ECM hydrogels via viscous finger patterning. *J Lab Autom.* **17** (2), 96-103, (2012).

25 Seandel, M. *et al.* Generation of a functional and durable vascular niche by the adenoviral E4ORF1 gene. *Proc Natl Acad Sci U S A.* **105** (49), 19288-19293, (2008).

26 van den Berg, C. W., Elliott, D. A., Braam, S. R., Mummery, C. L. & Davis, R. P. Differentiation of Human Pluripotent Stem Cells to Cardiomyocytes Under Defined Conditions. *Methods Mol Biol.* **1353** 163-180, (2016).

27 Mendel, D. B. *et al.* In vivo Antitumor Activity of SU11248, a Novel Tyrosine Kinase Inhibitor Targeting Vascular Endothelial Growth Factor and Platelet-derived Growth Factor Receptors. *Determination of a Pharmacokinetic/Pharmacodynamic Relationship.* **9** (1), 327-337, (2003).

28 Ohnuki, M. & Takahashi, K. Present and future challenges of induced pluripotent stem cells. *Philos Trans R Soc Lond B Biol Sci.* **370** (1680), 20140367, (2015).

29 Kim, K. *et al.* Epigenetic memory in induced pluripotent stem cells. *Nature.* **467** (7313), 285-290, (2010).

30 Liu, Y. *et al.*, The gene expression profiles of induced pluripotent stem cells (iPSCs) generated by a non-integrating method are more similar to embryonic stem cells than those of iPSCs generated by an integrating method. *Genetics and molecular biology*, **35** (3), 693-700, (2012).

31 Koyanagi-Aoi, M. *et al.* Differentiation-defective phenotypes revealed by large-scale analyses of human pluripotent stem cells. *Proceedings of the National Academy of Sciences.* **110** (51), 20569-20574, (2013).

32 Sala, L., Bellin, M. & Mummery, C. L. Integrating cardiomyocytes from human pluripotent stem cells in safety pharmacology: has the time come? *Br J Pharmacol.* 10.1111/bph.13577, (2016).

33 Huch, M. *et al.* In vitro expansion of single Lgr5+ liver stem cells induced by Wnt-driven regeneration. *Nature.* **494** (7436), 247-250, (2013).

34 Yamada, M. *et al.* Controlled formation of heterotypic hepatic micro-organoids in anisotropic hydrogel microfibers for long-term preservation of liv-

er-specific functions. *Biomaterials.* **33** (33), 8304-8315, (2012).

35 Sato, T. & Clevers, H. Growing self-organizing mini-guts from a single intestinal stem cell: mechanism and applications. *Science.* **340** (6137), 1190-1194, (2013).

36 Barker, N. *et al.* Lgr5(+ve) stem cells drive self-renewal in the stomach and build long-lived gastric units in vitro. *Cell Stem Cell.* **6** (1), 25-36, (2010).

37 Sato, T. *et al.* Long-term expansion of epithelial organoids from human colon, adenoma, adenocarcinoma, and Barrett's epithelium. *Gastroenterology.* **141** (5), 1762-1772, (2011).

38 Lancaster, M. A. *et al.* Cerebral organoids model human brain development and microcephaly. *Nature.* **501** (7467), 373-379, (2013).

39 Takasato, M., Er, P. X., Chiu, H. S. & Little, M. H. Generation of kidney organoids from human pluripotent stem cells. *Nat Protoc.* **11** (9), 1681-1692, (2016).

40 Astashkina, A. & Grainger, D. W. Critical analysis of 3-D organoid in vitro cell culture models for high-throughput drug candidate toxicity assessments. *Adv Drug Deliv Rev.* **69-70** 1-18, (2014).

41 Ranga, A., Gjorevski, N. & Lutolf, M. P. Drug discovery through stem cell-based organoid models. *Adv Drug Deliv Rev.* **69-70** 19-28, (2014).

42 Mansour, A. A. *et al.* An in vivo model of functional and vascularized human brain organoids. *Nat Biotechnol.* **36** (5), 432-441, (2018).

43 Wimmer, R. A. *et al.* Human blood vessel organoids as a model of diabetic vasculopathy. *Nature.* 10.1038/s41586-018-0858-8, (2019).

44 Itzhaki, I. *et al.* Modelling the long QT syndrome with induced pluripotent stem cells. *Nature.* **471** (7337), 225-229, (2011).

45 Park, I. H. *et al.* Disease-specific induced pluripotent stem cells. *Cell.* **134** (5), 877-886, (2008).

46 Marchetto, M. C. *et al.* A model for neural development and treatment of Rett syndrome using human induced pluripotent stem cells. *Cell.* **143** (4), 527-539, (2010).

47 Zhu, Z., Gonzalez, F. & Huangfu, D. The iCRISPR platform for rapid genome editing in human pluripotent stem cells. *Methods Enzymol.* **546** 215-250, (2014).

48 Langenkamp, E. & Molema, G. Microvascular endothelial cell heterogeneity: general concepts and pharmacological consequences for anti-angiogenic therapy of cancer. *Cell and Tissue Research.* **335** (1), 205-222, (2008).

49 Rafii, S., Butler, J. M. & Ding, B. S. Angiocrine functions of organ-specific endothelial cells. *Nature.* **529** (7586), 316-325, (2016).

50 Nolan, D. J. *et al.* Molecular signatures of tissue-specific microvascular endothelial cell heterogeneity in organ maintenance and regeneration. *Dev Cell.* **26** (2), 204-219, (2013).

51 Wang, X. Y. *et al.* Engineering interconnected 3D vascular networks in hydrogels using molded sodium alginate lattice as the sacrificial template. *Lab Chip.* **14** (15), 2709-2716, (2014).

52 Gross, B. C., Erkal, J. L., Lockwood, S. Y., Chen, C. & Spence, D. M. Evaluation of 3D printing and its potential impact on biotechnology and the chemical sciences. *Anal Chem.* **86** (7), 3240-3253, (2014).

53 Song, H. H., Park, K. M. & Gerecht, S. Hydrogels to model 3D in vitro microenvironment of tumor vascularization. *Adv Drug Deliv Rev.* **79-80** 19-29, (2014).

54 Miller, J. S. *et al.* Rapid casting of patterned vascular networks for perfusable engineered three-dimensional tissues. *Nat Mater.* **11** (9), 768-774, (2012).

55 Lin, N. Y. C. *et al.* Renal reabsorption in 3D vascularized proximal tubule models. *Proc Natl Acad Sci U S A.* **116** (12), 5399-5404, (2019).

56 Yildirim, E. *et al.* Phaseguides as tunable passive microvalves for liquid routing in complex microfluidic networks. *Lab Chip.* **14** (17), 3334-3340, (2014).

57 Thorsen, T., Maerkl, S. J. & Quake, S. R. Microfluidic large-scale integration. *Science.* **298** (5593), 580-584, (2002).

58 Gomez-Sjoberg, R., Leyrat, A. A., Pirone, D. M., Chen, C. S. & Quake, S. R. Versatile, fully automated, microfluidic cell culture system. *Anal Chem.* **79** (22), 8557-8563, (2007).

59 Griffith, L. G. & Swartz, M. A. Capturing complex 3D tissue physiology in vitro. *Nature Reviews Molecular Cell Biology.* **7** (3), 211-224, (2006).

60 Montanez-Sauri, S. I., Sung, K. E., Berthier, E. & Beebe, D. J. Enabling screening in 3D microenvironments: probing matrix and stromal effects on the morphology and proliferation of T47D breast carcinoma cells. *Integr Biol (Camb).* **5** (3), 631-640, (2013).

61 Sung, K. E. *et al.* Control of 3-dimensional collagen matrix polymerization for reproducible human mammary fibroblast cell culture in microfluidic devices. *Biomaterials.* **30** (27), 4833-4841, (2009).

62 Abhyankar, V. V. *et al.* A platform for assessing chemotactic migration within a spatiotemporally defined 3D microenvironment. *Lab Chip.* **8** (9), 1507-1515, (2008).

CHAPTER

8

Addendum

Curriculum vitae

Vincent van Duinen was born on June 24th 1988 in Amsterdam. After graduating from the pre-university education in Delft, he started studying Biopharmaceutical Sciences at Leiden University in 2007. His bachelor's degree was finished in 2010 with in internship at the division of Analytical Biosciences, under the supervision of Jan-Willem Schoonen. During this internship, he produced his first microfluidic chips in order to achieve liquid-liquid electroextraction.

He started a masters in Biopharmaceutical sciences in 2010 with a 9 months internship under the supervision of Peter Lindenburg and Jan-Willem Schoonen. During this internship, he developed a novel continuous-flow microelectroextraction flow cell that allows for electric field enhanced extraction of low-abundant metabolites. This work is part of a publication in Analytical Chemistry.

Realizing that microfluidics would be a powerful tool to improve cell culture, another 6 months internship was performed at the microtechnology, medicine and biology lab at the department of biomedical engineering at the University of Wisconsin. During this internship. Under supervision of Kyung Sung and David Beebe, Vincent combined 3D cell culture with microfluidic chips, with the goal of developing an in vitro model to monitor the invasion of breast cancer cells.

After obtaining his master degree in 2013, he was invited by Thomas Hankemeier and Paul Vulto to start a PhD at the division of Analytical Biosciences. The project was focused on the development of novel microfluidic cell culture models in a standardized platform. Together with MIMETAS, Vincent developed high-throughput in vitro assays, with a strong focus on vasculature in collaboration with the group of Anton-Jan van Zonneveld.

Currently, Vincent is working at the Leiden University Medical Center. Together with Mimetas and Ncardia, he aims to develop a next generation capillary-on-a-chip model to study the mechanism of small blood vessel loss in diseases such as heart failure and diabetes.

List of Publications

1. Schoonen J. W., **van Duinen, V**., Oedit, A., Vulto, P., Hankemeier, T. and Lindenburg, P. W.
   Continuous-flow microelectroextraction for enrichment of low abundant compounds.
   Analytical chemistry, *86*(16), 8048-8056. (2014).

2. **van Duinen, V**., Trietsch, S. J., Joore, J., Vulto, P., & Hankemeier, T.
   Microfluidic 3D cell culture: from tools to tissue models.
   Current opinion in biotechnology, *35*, 118-126. (2015)

3. **van Duinen, V.**, Van Den Heuvel, A., Trietsch, S. J., Lanz, H. L., Van Gils, J. M., Van Zonneveld, A. J. and Hankemeier, T.
   96 perfusable blood vessels to study vascular permeability in vitro.
   Scientific reports, *7*(1), 18071. (2017)

4. **van Duinen, V.**, Zhu, D., Ramakers, C., van Zonneveld, A. J., Vulto, P. and Hankemeier, T.
   Perfused 3D angiogenic sprouting in a high-throughput in vitro platform.
   Angiogenesis, *22*(1), 157-165. (2018)

5. Marianne K. Vormann, Linda Gijzen, Simon Hutter, Lisette Boot, Arnaud Nicolas, Angelique van den Heuvel, Jelle Vriend, Chee Ping Ng, Tom T. G. Nieskens, **Vincent van Duinen**, Bjorn de Wagenaar, Rosalinde Masereeuw, Laura Suter-Dick, Sebastiaan J. Trietsch, Martijn Wilmer, Jos Joore, Paul Vulto, Henriette L. Lanz,
   Nephrotoxicity and kidney transport assessment on 3D perfused proximal tubules.
   The American Association of Pharmaceutical Scientists journal, *20*(5), 90. (2018)

6. B. Yetkin-Arik, I. M. C. Vogels, N. Neyazi, **V. van Duinen**, R. H. Houtkooper, C. J. F. van Noorden, I. Klaassen & R. O. Schlingemann.
   Endothelial tip cells in vitro are less glycolytic and have a more flexible response to metabolic stress than non-tip cells.
   Scientific Reports 9(1), 10414 (2019)

Nederlandse samenvatting

Ontwikkeling van nieuwe medicijnen

Het lijkt een eenvoudige vraag: wat kost het ontwikkelen van een nieuw geneesmiddel? Er is niemand die het echt weet, maar de schatting lopen uiteen van grofweg 0.5 tot 2.5 miljard euro. Een van de verklaringen dat de prijs zo hoog is komt door de enorme ontwikkelingskosten en lage kans op succes. Na het moment dat er in mensen getest is, heeft slechts een klein deel de medicijnen de eindstreep gehaald. Zo geeft fabrikant Roche aan dat slechts 2% van de potentiële geneesmiddelen uiteindelijk goedgekeurd wordt. Anders onderzoek laat zien dat problemen met de werkzaamheid of bijwerkingen vaak de belangrijkste redenen zijn om de ontwikkeling van een medicijn te staken.

De zoektocht naar nieuwe medicijnen begint vaak met menselijke cellen die worden gekweekt in het lab. Zo kan op een controleerde wijze worden onderzocht wat er misgaat bij bepaalde ziektes en onderzocht worden hoe dit vervolgens aangepakt moet worden. Vervolgens worden de meest veelbelovende kandidaat-medicijnen getest in proefdieren voordat de stap naar de mens wordt gemaakt. Helaas blijkt keer op keer bij de vertaalslag van cellen in het lab naar proefdieren dat de complexiteit van ziektes onvoldoende kan worden nagebootst in een bakje met cellen. En zelfs als er bij proefdieren gunstige resultaten gezien worden kan later in de mens toch nog blijken dat het medicijn niet werkzaam is of dat er onvoorziene bijwerkingen zijn.

Waarom is de vertaalslag van menselijke cellen naar proefdieren (inclusief de mens) zo lastig? Zijn de processen in de menselijke cellen zo anders dan in een muis? Of zijn ziektes te complex om in een bakje met cellen na te kunnen bootsen? Waarschijnlijk ligt de waarheid ergens in het midden, maar feit is dat er nog veel te verbeteren valt op de manier waarop we onderzoek doen naar cellen.

Van cel tot mini-orgaan

In het lab worden veel cellen nog steeds gekweekt op een plat plastic oppervlak. Dit is

goedkoop, handig en schaalbaar. Helaas verliezen cellen zo veel eigenschappen die ze oorspronkelijk hadden omdat ze uit hun natuurlijke omgeving worden gehaald. De bloedvaten zijn bijvoorbeeld in elk orgaan anders, maar zodra de cellen van deze bloedvaten geïsoleerd en opgekweekt worden zijn de na een aantal dagen niet meer van elkaar te onderscheiden. Zulke verschillen zorgen ervoor dat veelbelovende resultaten die behaald worden in lab soms niet vertaalbaar zijn naar de muis of mens.

Nu kunnen veel van deze eigenschappen weer worden hersteld als de cellen de juiste omgeving wordt aangeboden. Cellen die gekweekt worden in een zachte, driedimensionale (3D) gel kunnen zo uitgroeien tot complexere structuren, zoals buisjes en klompjes. Op deze manier beginnen bijvoorbeeld levercellen weer de juiste afbraakenzymen aan te maken, en kunnen cellen uit bloedvaten weer complete vatennetwerken opbouwen die beter overeenkomen met hoe ze in het menselijk lichaam eruitzien

Waarom niet iedereen in 3D kweekt

Het ligt in lijn der verwachting dat resultaten op deze complexere 3D celmodellen een betere voorspellende waarde hebben doordat de processen die een rol spelen bij ziektes beter worden nagebootst. Toch wordt er voor veel onderzoek nog steeds gebruik gemaakt van simplistischere 2D celmodellen, omdat 3D celkweek nadelen heeft die zowel technisch als biologisch van aard zijn.

Voor grootschalig onderzoek moeten er vele combinaties van condities en medicijnen worden getest voordat iets gevonden kan worden dat werkt. Doordat 3D kweekmethodes ingewikkelder zijn en er dure biologische materialen nodig zijn, is het duurder en arbeidsintensiever dan 2D celkweek. Ook is nog lang niet voor alle celtypes onderzocht is hoe groot de voordelen zijn van het kweken in 3D en is nog de vraag of dit opweegt dit op tegen deze hogere kosten en complexiteit. Verder zijn er in 3D meer variabelen waarmee rekening gehouden moet worden ten opzichte van het kweken in 2D. Zo speelt de compositie van die 3D omgeving een belangrijke rol in hoe cellen zich gedragen. Verder kunnen in deze 3D omgeving

afvalstoffen zich ophopen en dringen zuurstof en voedingstoffen moeilijker door tot in de kern waardoor sommige celstructuren in 3D niet groter worden dan een paar millimeter. Ook moeten de cellen continu worden opgebroken omdat dode cellen zich ophopen.

3D celkweek verbeteren

Bij conventionele 3D celkweek worden cellen gemengd in een gel. Hierdoor is er geen controle is over waar de cellen precies terecht komen. Door middel van microfluidica, kanaaltjes kleiner dan een millimeter, kunnen vloeistoffen op een gecontroleerde manier gepositioneerd worden. Hierdoor kunnen de gel en cellen los van elkaar geïntroduceerd en gepositioneerd worden, waardoor de celkweek beter lijkt op de organen die ze moeten nabootsen.

Het voordeel is nu ook dat nu signaalmoleculen op een bepaalde locatie en tijd toegevoegd kunnen worden, waardoor er concentratiegradiënten aangelegd kunnen worden. Zulke gradiënten spelen in het lichaam een belangrijke rol, aangezien dit helpt cellen te oriënteren en zich tot complexere structuren te organiseren. Verder kunnen de kanaaltjes in microfluidica gebruikt worden om vloeistofstromen aan te leggen, waardoor er efficiënt transport van afval- en voedingsstoffen plaatsvindt. Ten slotte zorgt de stroming van vloeistof voor mechanische stimulatie van cellen, die daar vervolgens weer op kunnen reageren.

De voordelen van microfluidica om cellen te kweken is niet onopgemerkt gebleven. Zo is er veel onderzoek gedaan naar de invloed van vloeistofstromen op cellen, en zijn verschillende typen sensoren geïntegreerd in de kanalen om hiermee real-time informatie uit te kunnen lezen over de toestand van de cellen. Echter, een nadeel is dat veel van dit onderzoek is dat dit wordt gedaan op zelf gefabriceerde prototypen. Hierdoor is er in het veld van microfluidische celkweek een gebrek aan standaardisatie en schaalbaarheid. Verder worden er vaak materialen gebruikt die goedkoop zijn en makkelijk te bewerken, maar een negatieve invloed kunnen hebben op de functionaliteit van de cellen.

Bloedvaten in microfluidica: een goede combinatie

De focus van het onderzoek in dit proefschrift is het namaken van bloedvaten. De reden hiervoor is dat microfluidica veel toe kan voegen op de manier waarop bloedvaten gekweekt kunnen worden. Zoals beschreven in hoofdstuk 2 spelen vloeistofstromen en gradiënten een belangrijke rol bij het tot stand komen en gezond houden van bloedvaten. Verder is een functioneel bloedvaten netwerk cruciaal om de relevantie van in het lab gekweekte mini-orgaantjes te vergroten. Door het toevoegen van bloedvaten kunnen deze mini-orgaantjes namelijk beter van voedingsstoffen worden voorzien, en kunnen belangrijke interacties tussen weefsels en bloedvaten beter bestudeerd worden.

De vraag waar dit proefschrift antwoord op probeert te geven, is: hoe kunnen we bepaalde complexiteit toevoegen om in het lab gekweekte bloedvaten relevanter te maken, zonder dat dit ten koste gaat van de schaalbaarheid en mogelijkheid tot grootschalige screening van medicijnen? Wat zijn de belangrijkste parameters die toegevoegd kunnen worden om functionele bloedvaten te kweken, en wat voor nieuwe mogelijkheden levert het kweken van bloedvaten in microfluidica op?

In dit onderzoek is gebruik gemaakt van een platform dat is gebaseerd op een 384-well microtiter plaat met daaronder geïntegreerde microfluidische kanalen (zie hoofdstuk 4, afbeelding 1). Afhankelijk van de configuratie van de kanalen zijn er 40 tot 96 losse units beschikbaar, die elk onafhankelijk van elkaar gebruikt kunnen worden. Omdat het 384-well formaat een standaard is binnen de industrie, is hiermee comptabiliteit met bestaande appratuur, zoals microscopen en pipetten, gewaarborgd.

In hoofdstuk 3 wordt een methode beschreven om endotheelcellen, de cellen die de binnenkant van een bloedvat bekleden, kunnen kweken in de microfluidische kanalen. Vervolgens kijken we of we dit kunnen gebruiken om de een belangrijke functie van bloedvaten kunnen bestuderen: de eigenschap om bloed binnen te houden, maar zijn wel in staat om voedingstoffen door te laten.

Voor het opkweken van deze endotheelcellen in het microfluidische platform

concluderen dat we gebruik moeten maken van een bewegend platform om op deze manier een vloeistofstroom aan te brengen. Hierdoor vindt er zwaartekracht gedreven perfusie plaats in twee richtingen die identiek is over het gehele platform. Deze perfusie is cruciaal om voldoende voedingsstoffen bij de bloedvaten te krijgen: zonder perfusie overleven de cellen slechts enkele uren. Een belangrijk feit is dat we geen nadelig effect vonden van het opkweken bloedvaten onder deze vorm van perfusie, wat het kweken van deze vaatjes een stuk eenvoudiger en simpeler maakt.

Verder hebben we aangetoond dat we door deze methode de bloedvaten maanden in leven konden houden en dat we de belangrijkste functionaliteit van bloedvaten, het transporteren en selectief doorlaten van stoffen, na kunnen bootsen. Bij normale condities zijn de bloedvaten lekdicht, maar na het blootstellen aan stoffen die een rol spelen bij ontstekingen gingen de bloedvaten lekken zoals ze ook in het lichaam doen.

Capillairen, de kleinste bloedvaten

De bloedvaten in de microkanaaltjes hebben een doorsnede die overeenkomt die van de kleine aderen. Nog kleiner zijn de capillairen: deze hebben een doorsnede van slechts enkele micrometer (ongeveer de doorsnede van een enkele rode bloedcel). Capillairen worden in het lichaam gevormd als een bloedvat wordt blootgesteld aan een combinatie van groeifactoren, een proces dat angiogenese wordt genoemd. Dit vindt bijvoorbeeld plaats tijdens het helen van een wond, het aanmaken van spierweefsel of tijdens de groei van tumoren.

Onder normale omstandigheden is angiogenese is een gecontroleerd proces, dat continue plaatsvindt en afhankelijk is van de behoefte en conditie van het weefsel. Wanneer deze balans is verstoord kan dit tot verlies of juist tot een ongecontroleerde groei van de kleine haarvaatjes leiden. Het verlies van de kleine haarvaten speelt een belangrijke rol bij hart- en nierfalen. De ongecontroleerde groei van capillairen speelt een belangrijke rol bij kanker, omdat dit deze nieuwe capillairen de tumorcellen zo van meer voedingstoffen te kunnen worden voorzien en dit ze in staat stelt zich te

kunnen verspreiden.

Door de mechanismes achter angiogenese beter te begrijpen kunnen er nieuwe aangrijpingspunten worden gevonden om de groei van tumoren te remmen of om hart- en vaatziekten eerder te kunnen behandelen.

In hoofdstuk 4 demonstreren we dat we met een ontwerp van drie kanalen stabiele gradiënten kunnen maken. Wanneer er bloedvaten bloot worden gesteld aan een gradiënt van verschillende groeifactoren zien we dat, afhankelijk van de combinatie, gerichte migratie en formatie van capillairen. Deze capillairen zijn volledig omgeven door collageen gel, en vormen een hol vaatje dat in connectie staat met het oorspronkelijke, grotere bloedvat.

Interessant is dat als deze capillairen langer gekweekt worden en er een connectie tussen beide vloeistofkanelen komt, er een reorganisatie plaatsvindt van het bloedvaten netwerk. Dit zorgt ervoor dat de capillairen verder ontwikkelen: waar eerst grote moleculen nog uit de capillairen konden lekken, blijven deze nu binnenin de haarvaten. Dit mechanisme wordt gedreven door het opheffen van het gradiënt en het tot stand komen van perfusie door de nieuwgevormde capillairen.

Het gebruik van stamcellen in ziektemodellen

Belangrijk bij ziektemodellen is oorsprong en type van de cellen zelf. Vroeger konden alleen oneindig delende tumorcellen gebruikt worden in celmodellen, omdat dit de enige cellen waren die buiten het lichaam in leven gehouden konden worden. Hoewel deze cellen in grote hoeveelheden opgekweekt kunnen worden, hebben ze als belangrijk nadeel dat veel tumorcellen zich anders gedragen dan het weefsel of orgaan dat ze voor moeten stellen. Hierdoor hebben ze een beperkte voorspellende waarde hebben voor ziektes anders dan kanker.

Primaire cellen zijn tegenwoordig de standaard in het preklinische onderzoek: dit zijn gezonde, functionele cellen afkomstig uit een levend organisme. Ze zijn relevanter dan tumorcellen, omdat ze zich natuurlijker gedragen maar kunnen maar beperkt in leven gehouden worden buiten het lichaam. Verder zijn ze maar in een beperkte

hoeveelheid te verkrijgen, en kunnen er grote verschillen zijn per individuele donor. Dit maakt het onpraktisch om primaire cellen te gebruiken voor grote screeningstudies.

Tegenwoordig is het mogelijk is om stamcellen te maken uit bloed, urine en huidweefsel (geïnduceerde pluripotente stamcellen, kortweg iPSC). Onder invloed van de juiste factoren en signaalmoleculen kunnen deze stamcellen vervolgens worden omgevormd tot allerlei verschillende celtypes en weefsels uit organen, zoals neuronen, hartspiercellen, nierweefsel en bloedvaten. Omdat stamcellen zich oneindig vaak kunnen delen, kunnen er zeer grote hoeveelheden cellen gemaakt worden en is er dus ook minder afhankelijkheid van verschillende donoren.

Helaas bestaat nog veel onduidelijkheid over de eigenschappen van deze cellen. Wat is de invloed van het terug vormen tot stamcel? Hoeveel 'herinneringen' hebben deze stamcellen? En als deze stamcellen vervolgens weer uitgroeien tot andere type weefsels, lijken ze alleen op het celtype dat ze voor moeten stellen, of zijn ze daadwerkelijk gezond en functioneel?

Desalniettemin maakt deze ontdekking veel nieuw onderzoek mogelijk. Omdat deze cellen de genetische informatie dragen van de donor, zijn deze cellen uiterst geschikt om het effect van genetische aandoeningen beter te begrijpen. In het kader van het onderzoek uit dit proefschrift zou bijvoorbeeld gebruik gemaakt kunnen worden van cellen van patiënten met aangeboren vaatafwijkingen. Door cellen uit deze patiënten te isoleren kunnen er persoonlijke celmodellen gemaakt worden, waardoor therapie op maat mogelijk zou kunnen maken.

In hoofdstuk 5 laten we zien dat wat betreft de angiogenese er veel overeenkomsten zijn tussen endotheelcellen gekweekt uit iPSC en met primaire cellen die uit een navelstreng. Dit suggereert dat veel belangrijke eigenschappen die een endotheelcel een endotheelcel maken dus nog steeds behouden blijven.

Ook hier zien we opnieuw dat de connectie tussen beide vloeistofkanelen weer een reorganisatie geeft van het vasculaire netwerk en de bijbehorende afname in de lekkage van grote moleculen, net als bij de primaire endotheelcellen. Ook zien we

een duidelijke toename van de diameter wanneer de capillairen langer gekweekt worden. Dit wordt waarschijnlijk veroorzaak wordt door het ontbreken van cellen die normaal gesproken om de capillairen heen liggen: pericyten.

Ons toekomstig onderzoek zal zich focussen op het integreren van deze pericyten, om zo inzicht te krijgen in de communicatie tussen pericyten en endotheelcellen. We moeten verder wat de overeenkomsten en de verschillen zijn tussen uit stamcellen gedifferentieerde endotheelcellen en primaire endotheelcellen, omdat dit de sleutel kan zijn tot het opkweken van organen buiten het lichaam met behulp van lichaamseigen stamcellen.

Het remmen of voorkomen van angiogenese is een interessante strategie om de groei van tumoren te kunnen remmen. In hoofdstuk 6 laten we zien hoe het platform gebruikt kan worden om remmers van angiogenese te testen en zo nieuwe aangrijpingspunten te vinden voor medicijnen. We laten zien dat een klinisch toegepaste angiogenese-remmer, Sunitinib, zowel op primaire endotheelcellen als op IPSC-endotheelcellen een sterke remming van angiogenese geeft in dit systeem.

Ook hebben we laten zien dat het beïnvloeden van het suiker metabolisme een sterk remmend effect geeft op zowel primaire als op iPSC endotheelcellen. Dit suggereert dat onder deze condities, het suikermetabolisme van iPSC endotheelcellen vergelijkbaar is met primaire cellen.

Tenslotte laten we zien dat we de remming op een geautomatiseerde manier kunnen meten. Doordat dit platform de vereiste schaalbaarheid bezit in combinatie met micro-omgeving voor de cellen die de menselijke situatie beter nabootst, moet dit model uiteindelijk beter inzicht geven en een beter voorspelende waarde hebben dan traditionele modellen van angiogenese.

Toekomstvisie

Als laatste wordt er in hoofdstuk 7 een perspectief gegeven in hoe het functioneren van de celmodellen gevalideerd kan worden door het stofwisseling van de cellen te bestuderen. Omdat het metabolisme een breed overzicht geeft van alle processen

die in een cel plaatsvinden, is dit een veelbelovende techniek om inzicht te krijgen in het functioneren van het model.

Onderzocht moet worden is hoeverre de bloedvaten in dit systeem lijken om de bloedvaten in het lichaam, en welke (groep van) stoffen die vrijkomen bij de stofwisseling hiervoor geschikt zijn. Bijvoorbeeld, stikstofoxiden en prostacycline spelen een cruciale rol in de gezonde vaatwand, en de expressie hiervan is moeilijk te meten wanneer er gebruik gemaakt wordt van traditionele kweekmethodes. Nu is de vraag of de realistischere kweekomgeving die we gebruiken in onze methodes dit wel mogelijk maakt.

Verder worden de technische mogelijkheden van 3D printen belicht, wat snellere en complexere celmodellen mogelijk kan maken. Ten slotte wordt de impact van nieuwe genoomtechnieken besproken die het mogelijk maken om specifieke ziektemodellen te gaan maken door gericht genetische variaties aan te brengen. Dit is een krachtige techniek die zeker in combinatie met de iPSC techniek vele nieuwe inzichten gaat opleveren.

Dankwoord

Thomas, de vrijheid die je me hebt gegeven om dit onderzoek te kunnen doen was geweldig, en de mooie discussies en nieuwe inzichten die je me hebt gegeven onmisbaar. Paul, in het begin nog zoekende naar wat we nu precies wilde met de microfluidica, maar fantastisch om te zien hoe ver Mimetas is gekomen. Ik ben trots dat ik daaraan heb kunnen bijdragen, en hopelijk groeit Mimetas nog veel verder.

Anton-Jan, zonder je kennis en kunde over de (vasculaire) biologie was ik nooit zo ver gekomen, je enthousiasme en je steun in mijn onderzoek waren mij erg waardevol.

Alle collega's van de universiteit, vooral de laatste jaren was het een komen en gaan. Hoewel mijn positie niet altijd even duidelijk was heb ik me altijd heel welkom gevoeld en ik zal hopelijk in de toekomst nog steeds regelmatig langs komen.

Dan alle collega's bij Mimetas: mooi om met jullie vanuit de universiteit mee te verhuizen en aan iets nieuws te bouwen vanuit (bijna) niets. Ook fijn was alle nieuwe (koffiezet)apparatuur. En hoewel ik misschien een buitenbeentje was die zijn eigen gang leek te gaan, voelde ik me helemaal opgenomen in het team.

Wendy, hoewel je soms wel eens twijfelt aan de microfluidica en alle resultaten die daaruit voortkomen, maken jouw kritische vragen, je toewijding aan het onderzoek en je humor je een geweldige collega om mee samen te werken. Bedankt voor alle hulp.

Alle studenten die geholpen bij het onderzoek in dit proefschrift, in het bijzonder Anshel, Dani, Suze en Christian. Bedankt voor al jullie hulp! Ondanks dat jullie een begeleider hadden die probeerde op twee locaties tegelijkertijd te zijn, hoop ik dat jullie nog altijd met veel plezier terugdenken aan jullie stages.

Mijn ouders, zonder jullie was deze 'scriptie' er überhaupt nooit gekomen en bedankt voor jullie steun en oprechte interesse tijdens mijn afstuderen.

En ten slotte natuurlijk Marloes: je bent enorm belangrijk geweest tijdens deze tijd en zonder jou had ik er waarschijnlijk nog veel langer over gedaan.